



**INTERNATIONAL UNIVERSITY LIAISON INDONESIA (IULI)**

**BACHELOR'S THESIS**

---

**EFFECT OF WING LOCATION ON THE AERODYNAMIC PROFILE OF A  
SUPERSONIC AIRCRAFT USING ANSYS FLUENT**

---

By

**Kevin Rahangiar**

11202101010

Presented to the Faculty of Engineering and Life Sciences  
In Partial Fulfilment Of the Requirements for the Degree of

**SARJANA TEKNIK**

In

**AVIATION ENGINEERING**

**FACULTY OF ENGINEERING AND LIFE SCIENCES**

**BSD City 15345**

**Indonesia**

**February 2025**

## APPROVAL PAGE

### EFFECT OF WING LOCATION ON THE AERODYNAMIC PROFILE OF A SUPERSONIC AIRCRAFT USING ANSYS FLUENT

KEVIN RAHANGIAR

11202101010

Presented to the Faculty of Engineering

In Partial Fulfillment of the Requirements for the Degree of

SARJANA TEKNIK

In

AVIATION ENGINEERING

FACULTY OF ENGINEERING AND LIFE SCIENCES

Dr. Eng. Ressa Octavianty

Thesis Advisor

\_\_\_\_\_ Date (MM/DD/YYYY)

Triwanto Simanjuntak, PhD

Thesis Co-Advisor

\_\_\_\_\_ Date (MM/DD/YYYY)

Dipl.-Ing. Sentot Wahjoe Georitno, M.Si.

Dean of Faculty of Engineering and Life Sciences

\_\_\_\_\_ Date (MM/DD/YYYY)

## EXAMINERS APPROVAL PAGE

M. Ilham Adhynugraha, PhD

Examiner 1

\_\_\_\_\_  
Date (MM/DD/YYYY)

Dr. Eng. Odi Akhyarsi

Examiner 2

\_\_\_\_\_  
Date (MM/DD/YYYY)

## STATEMENT BY THE AUTHOR

I hereby declare that this submission is my own work and to the best of my knowledge, it contains no material previously published or written by another person, nor material which to a substantial extent has been accepted for the award of any other degree or diploma at any educational institution, except where due acknowledgment is made in the thesis.



Kevin Rahangiar

Student

02/18/2025

Date (MM/DD/YYYY)

## ABSTRACT

Effect of Wing Location on the Aerodynamic Profile of a Supersonic Aircraft  
Using ANSYS Fluent

by

Kevin Rahangiar

Dr. Eng. Ressa Octavianty, Advisor

Triwanto Simanjuntak, PhD, Co-Advisor

This bachelors thesis investigates the effects of wing placement on the aerodynamic profile of a supersonic transport (SST) aircraft, focusing on lift coefficient ( $C_L$ ), drag coefficient ( $C_D$ ), and moment coefficient ( $C_M$ ). Using OpenVSP and ANSYS Fluent, three wing configurations were analyzed: the original position (20 meters from the nose), an intermediate position (35 meters), and a fully aft position (50 meters). The diamond airfoil, selected through comparative analysis, was used as the wing profile. Simulations were conducted under supersonic conditions at Mach 1.2 and Mach 2.0 with a fixed angle of attack of 5 degrees. The results indicate that the 20-meter wing location achieved the highest lift-to-drag ratio ( $\frac{L}{D}$ ) and stable moment coefficient, making it the most efficient configuration. The aft configurations at 35 meters and 50 meters exhibited higher wave drag, reduced lift efficiency, and negative pitching moments, posing potential stability issues. Comparisons between OpenVSP and ANSYS Fluent showed consistent trends, validating the approach despite discrepancies in absolute moment coefficient values. This study highlights the critical role of wing placement in supersonic aerodynamic performance, providing valuable insights for future SST design considerations.

Keyword: *Supersonic Transport, Wing Location, Supersonic, Airfoil, CFD*

## ACKNOWLEDGEMENTS

I would like to express my deepest gratitude to those who have supported and guided me throughout the process of completing this thesis.

First and foremost, I am immensely thankful to Dr. Eng. Ressa Octavianty, my advisor, and Triwanto Simanjuntak, PhD, my co-advisor, for their invaluable guidance, encouragement, and constructive feedback. Their expertise and insights have been instrumental in shaping the direction and quality of this research.

I extend my sincere appreciation to the Faculty of Engineering at the International University Liaison Indonesia for providing the resources and a supportive academic environment necessary for the successful completion of this study.

I would also like to express my gratitude to my examiners, M. Ilham Adhynugraha, PhD, and Dr. Eng. Odi Akhyarsi, for their time, valuable insights, and constructive feedback. Their evaluation and suggestions have helped refine this research and enhance its academic quality.

I am also grateful to my fellow students and colleagues for their encouragement and collaborative discussions, which enriched my understanding of the subject matter. Thanks to your company, encouragement, and shared experiences, we have bonded like siblings, especially during these challenging times as we adjust to a new environment. Your camaraderie has been a source of strength and motivation throughout this journey.

A special thank you goes to Rosita, our beloved cat whom we adopted from the streets. Her playful spirit and comforting presence have been a constant source of joy and relaxation during the most stressful moments of this process. She truly remind us to find happiness in the simplest things.

Finally, I would like to thank my family for their unwavering love, patience, and support throughout my academic endeavors. Your belief in me has been the foundation of my achievements.

This thesis is dedicated to all those who have contributed to its realization. Thank you for being part of this journey.

# Contents

<b>Approval Page</b>	<b>i</b>
<b>EXAMINERS APPROVAL PAGE</b>	<b>ii</b>
<b>Statement by The Author</b>	<b>iii</b>
<b>Abstract</b>	<b>iv</b>
<b>Acknowledgements</b>	<b>v</b>
<b>Contents</b>	<b>vi</b>
<b>List of Figures</b>	<b>x</b>
<b>List of Tables</b>	<b>xii</b>
<b>1 Introduction</b>	<b>1</b>
1.1 Background . . . . .	1
1.2 Problem Statement . . . . .	4
1.3 Research Objectives . . . . .	5
1.4 Research Scope and Limitation . . . . .	5
1.5 Significance of the Study . . . . .	6
<b>2 Literature Review</b>	<b>8</b>
2.1 Airfoil Fundamentals . . . . .	8
2.1.1 Introduction to Airfoil . . . . .	8
2.1.2 Airfoil Definition . . . . .	9
2.2 Aerodynamics Principles . . . . .	9

2.2.1	Aerodynamics Forces and Moments . . . . .	9
2.3	Airfoil Design . . . . .	12
2.3.1	Airfoil Geometry . . . . .	12
2.3.2	Airfoil Nomenclature . . . . .	13
2.4	Evolution of Airfoil Design . . . . .	15
2.4.1	Subsonic Airfoil Design . . . . .	15
2.4.2	Transonic Airfoil Design . . . . .	15
2.4.3	Supersonic Airfoil Design . . . . .	16
2.5	Supersonic Aerodynamics . . . . .	18
2.5.1	The Physics of Supersonic Flight . . . . .	18
2.5.2	Key Aerodynamic Challenges in Supersonic Transport . . . . .	18
2.5.3	Introduction to Oblique Shocks and Expansion Wave . . . . .	19
2.5.4	Design Strategies for Managing Supersonic Aerodynamics . . . . .	22
2.6	Wing Placement in Supersonic Aircraft . . . . .	22
2.6.1	Historical and Modern Wing Designs for SST . . . . .	23
2.6.2	Effects of Wing Placement on Lift, Drag, and Stability . . . . .	23
2.7	Supersonic Airfoil Characteristics . . . . .	24
2.7.1	Thin Airfoils and Drag Reduction . . . . .	24
Supersonic Drag Components . . . . .	25	
Drag Breakdown . . . . .	25	
Drag Formulation . . . . .	26	
Wave Drag Due to Volume . . . . .	26	
Summary . . . . .	27	
2.8	Custom Airfoils vs. NACA Airfoils . . . . .	27
2.8.1	Benefits of Custom Airfoil Design . . . . .	27
2.8.2	Tools for Custom Airfoil and Wing Design and Analysis . . . . .	28
<b>3</b>	<b>Research Methodology</b>	<b>29</b>
3.1	Research Flowchart . . . . .	29
3.2	Benchmarking Study . . . . .	30
3.3	Airfoil and Wing Geometry Modeling . . . . .	30
3.3.1	Introduction to OpenVSP . . . . .	30
3.3.2	Initial Airfoil Configuration . . . . .	31

3.3.3	SST Aircraft Modeling . . . . .	33
3.3.4	Workflow in OpenVSP . . . . .	35
	Airfoil Selection and Testing Phase . . . . .	35
	SST Aircraft Modeling and Analysis Phase . . . . .	37
3.4	Computational Fluid Dynamics Simulation . . . . .	40
3.4.1	Introduction to ANSYS Fluent . . . . .	40
3.4.2	Workflow in ANSYS Fluent . . . . .	40
3.4.3	Validation of Simulation Process Results . . . . .	49
	Comparison with OpenVSP Results . . . . .	49
	Benchmarking Against Reference Studies . . . . .	49
3.4.4	Computational Hardware and Software Setup . . . . .	51
	Minimum Hardware Requirements . . . . .	51
<b>4</b>	<b>Results and Discussions</b>	<b>52</b>
4.1	Airfoil Selection and Preliminary Analysis . . . . .	52
4.1.1	Airfoil Candidates and Comparison . . . . .	52
	NACA 2412 . . . . .	52
	NACA 0005 . . . . .	53
	Hexagonal Airfoil . . . . .	53
	Diamond Airfoil . . . . .	53
4.1.2	Airfoil Aerodynamic Characteristics Analysis . . . . .	54
4.1.3	Wave Drag Analysis . . . . .	61
4.1.4	Selection of the Diamond Airfoil . . . . .	62
	Selection of the Diamond Airfoil . . . . .	62
4.2	OpenVSP Results for the SST Aircraft . . . . .	64
4.2.1	Baseline Wing Location (20 meters from the nose) . . . . .	64
4.2.2	Wing Location at 35 meters Aft . . . . .	66
4.2.3	Wing Location at 50 meters Aft . . . . .	67
4.2.4	Comparative Analysis of Wing Locations . . . . .	69
4.3	Results from ANSYS Fluent . . . . .	73
4.3.1	Wing Location at 20 meters . . . . .	73
	Aerodynamic Coefficients . . . . .	73
	Mach Number and Pressure Contours . . . . .	74

Interpretation of Results . . . . .	74
Wing Location at 20 Meters . . . . .	78
4.3.2 Wing Location at 35 meters aft . . . . .	79
Aerodynamic Coefficients . . . . .	79
Pressure and Mach Number Contours . . . . .	79
Interpretation of Results . . . . .	79
Wing Location at 35 Meters . . . . .	83
4.3.3 Comparative Analysis Across Wing Locations . . . . .	84
<b>5 Summary, Conclusion, Recommendation</b>	<b>86</b>
5.1 Summary, Conclusion, Recommendation . . . . .	86
5.1.1 Summary . . . . .	86
5.1.2 Conclusion . . . . .	87
5.1.3 Recommendation . . . . .	87
<b>Bibliography</b>	<b>89</b>
<b>Appendices</b>	<b>92</b>
.1 OpenVSP Results . . . . .	93
.1.1 Airfoil Candidates . . . . .	93
.1.2 SST Wing Locations . . . . .	97
.1.3 SST OpenVSP Model Four View . . . . .	98
.2 ANSYS Fluent Results . . . . .	99
.2.1 Aerodynamic Coefficients of wing location at 20 m . . . . .	99
.2.2 Aerodynamic Coefficients of wing location at 35 m . . . . .	99
<b>Turnitin Report</b>	<b>100</b>
<b>Curriculum Vitae</b>	<b>107</b>

# List of Figures

1.1 Boeing 2707-300 [3]. . . . .	2
1.2 Concorde [4]. . . . .	2
1.3 Shockwave formation on a X-15 model [5]. . . . .	3
2.1 Illustration of pressure and shear stress on an aerodynamic surface.	10
2.2 Resultant aerodynamic force and moment on the body . . . . .	11
2.3 Resultant aerodynamic force and the components into which it splits	11
2.4 Airfoil geometry . . . . .	13
2.5 Airfoil nomenclature . . . . .	14
2.6 F-104 Starfighter [10]. . . . .	17
2.7 Typical shapes of supersonic airfoil. . . . .	17
2.8 Oblique shock and expansion waves. . . . .	21
3.1 Research Methodology . . . . .	29
3.2 NACA2412 . . . . .	32
3.3 NACA0005 . . . . .	32
3.4 Hexagonal . . . . .	32
3.5 Diamond . . . . .	32
3.6 Configuration parameters on Concorde and a next generation SST [2]. . . . .	34
3.7 Overall dimension of a next generation SST. . . . .	34
3.8 OpenVSP workflow flowchart. . . . .	35
3.9 Wing Model for Airfoil Selection. . . . .	37
3.10 Wing Position Variation. . . . .	39
3.11 ANSYS spaceclaim computational domain dimension. . . . .	42
3.12 ANSYS meshes results and topology. . . . .	43

3.13 ANSYS meshes results and topology zoomed. . . . .	43
3.14 ANSYS project schematic . . . . .	47
3.15 Schematic Diagram of ANSYS Fluent Workflow . . . . .	48
3.16 Drag characteristics of a next generation SST from JAXA paper [2].	50
3.17 L/D characteristics of a next generation SST from JAXA paper [2]. .	50
4.1 Airfoil Aerodynamic Characteristics at Mach 0.6 . . . . .	56
4.2 Airfoil Aerodynamic Characteristics at Mach 1.2 . . . . .	56
4.3 Airfoil Aerodynamic Characteristics at Mach 2.0 . . . . .	57
4.4 20 meters Wing Location OpenVSP Model . . . . .	65
4.5 Aerodynamic Characteristics of Wing Location at 20 m at Mach 2.0	65
4.6 35 meters Wing Location OpenVSP Model . . . . .	66
4.7 Aerodynamic Characteristics of Wing Location at 35 m at Mach 2.0	67
4.8 50 meters Wing Location OpenVSP Model . . . . .	68
4.9 Aerodynamic Characteristics of Wing Location at 50 m at Mach 2.0	68
4.10 Aerodynamic Coefficient of Wing Location at 20 meters . . . . .	75
4.11 Mach Contour of Wing Location at 20 meters . . . . .	76
4.12 Pressure Contour of Wing Location at 20 meters . . . . .	77
4.13 Moment Coefficient of 20m wing location following Center of Grav- ity . . . . .	78
4.14 Aerodynamic Coefficient of Wing Location at 35 meters . . . . .	80
4.15 Mach Contour of Wing Location at 35 meters . . . . .	81
4.16 Pressure Contour of Wing Location at 35 meters . . . . .	82
4.17 Moment Coefficient of 35m wing location following Center of Grav- ity . . . . .	83

## List of Tables

4.1	Airfoils Aerodynamic Parameters at Mach 0.6 . . . . .	58
4.2	Airfoils Aerodynamic Parameters at Mach 1.2 . . . . .	59
4.3	Airfoils Aerodynamic Parameters at Mach 2.0 . . . . .	60
4.4	Airfoils $C_{D_{0w}}$ Values at Different Mach Numbers . . . . .	62
4.5	Aerodynamic Parameters for Different Wing Locations and AoA . . .	72
4.6	$C_{D_{0w}}$ Values for Different Wing Locations . . . . .	73
4.7	ANSYS Fluent Results at AoA = $5^\circ$ . . . . .	84

## List of Abbreviations

<b>SST</b>	<b>Supersonic Transport</b>
<b>CFD</b>	<b>Computational Fluid Dynamics</b>
<b>NACA</b>	<b>National Advisory Committee for Aeronautics</b>
<b>VSP</b>	<b>Vehicle Sketch Pad</b>
<b>NASA</b>	<b>National Aeronautics and Space Administration</b>
<b>VLM</b>	<b>Vortex Lattice Method</b>
<b>Cl</b>	<b>Coefficient of Lift (airfoil)</b>
<b>Cd</b>	<b>Coefficient of Drag (airfoil)</b>
<b>Cm</b>	<b>Coefficient of Moment (airfoil)</b>
<b>CL</b>	<b>Coefficient of Lift (aircraft)</b>
<b>CD</b>	<b>Coefficient of Drag (aircraft)</b>
<b>CM</b>	<b>Coefficient of Moment (aircraft)</b>
<b>CAD</b>	<b>Computer Aided Design</b>
<b>AoA</b>	<b>Angle of Attack</b>
<b>BOI</b>	<b>Body of Influence</b>

*Dedicated to my parents*

# CHAPTER 1

## INTRODUCTION

### 1.1 Background

Supersonic transport (SST) aircraft have been a topic of extensive research and development since the mid-20th century, driven by the goal of achieving high-speed commercial travel. Early efforts, such as the Boeing 2707 (shown in Figure 1.1) and the Concorde (shown in Figure 1.2), demonstrated the feasibility of supersonic flight but faced significant limitations related to aerodynamic performance, fuel efficiency, and environmental concerns, particularly noise pollution and high operational costs. Unlike conventional aircraft, SST designs face unique challenges due to the complexities of supersonic flight, such as shockwave formation (shown in Figure 1.3), wave drag, and stability issues. These factors necessitate precise optimization of key design elements, including airfoil shapes, fuselage geometry, and, crucially, wing placement [1], [2].

In recent years, advancements in computational tools and materials have reignited interest in SST design, with modern approaches focusing on improving aerodynamic efficiency while mitigating previous challenges. A critical aspect of this improvement lies in optimizing wing placement and airfoil selection, as these factors directly influence the lift-to-drag ratio, wave drag, and overall flight stability in supersonic regimes.

EFFECT OF WING LOCATION ON THE AERODYNAMIC PROFILE OF A SUPERSONIC AIRCRAFT  
 USING ANSYS FLUENT

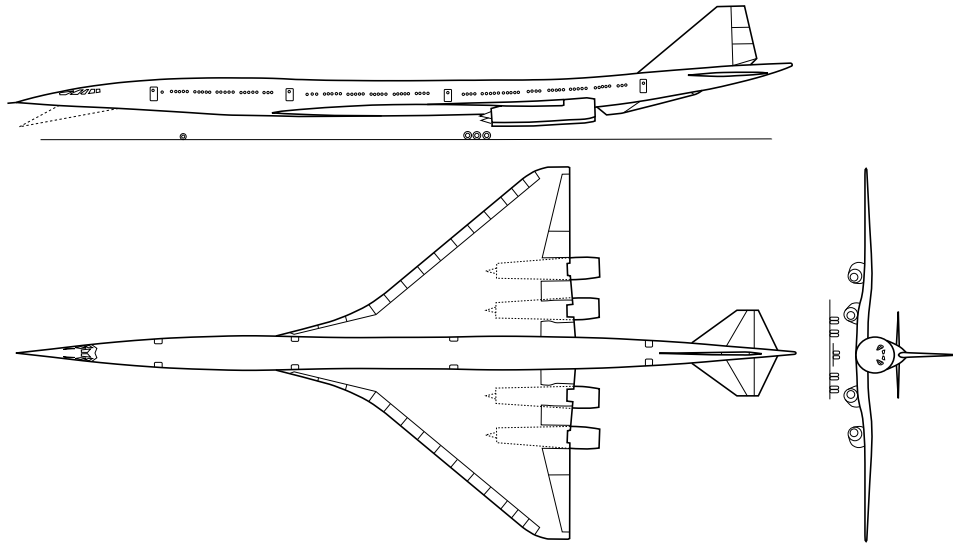


FIGURE 1.1: Boeing 2707-300 [3].

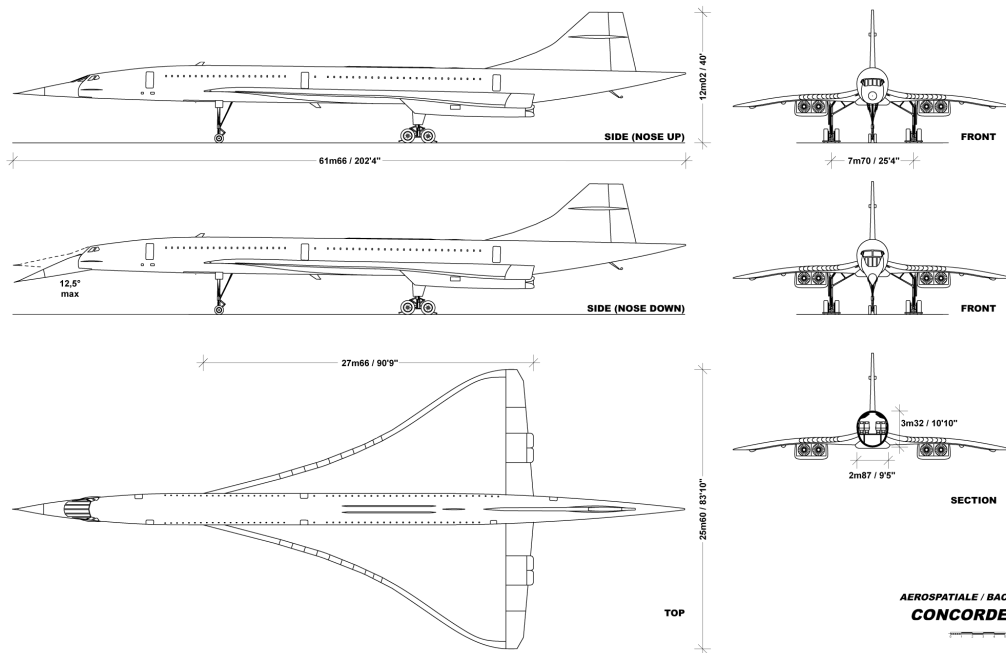


FIGURE 1.2: Concorde [4].

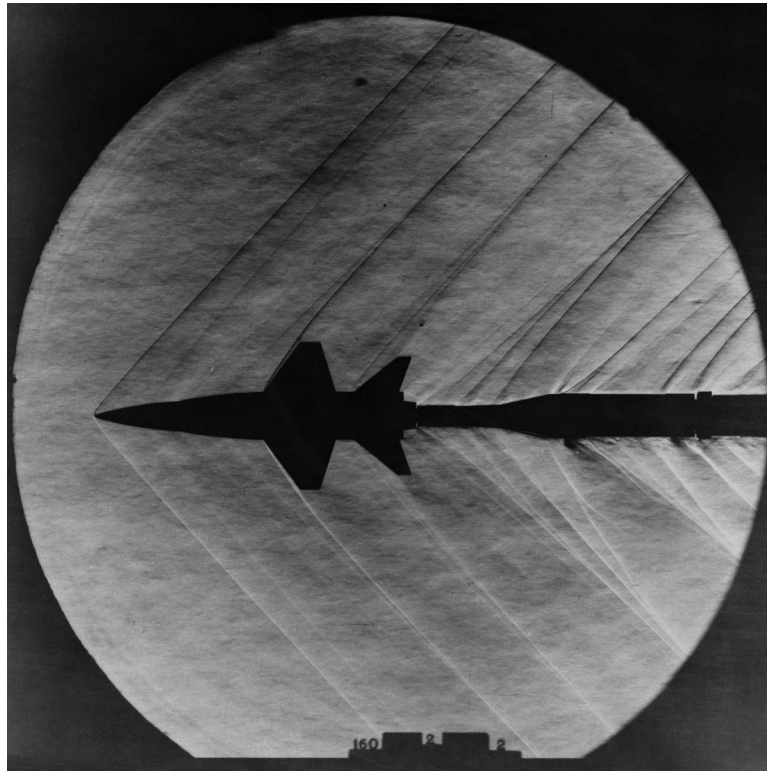


FIGURE 1.3: Shockwave formation on a X-15 model [5].

The current state of knowledge indicates that wing placement affects the distribution of aerodynamic forces, including lift and drag, and plays a crucial role in determining the aircraft's stability. Previous studies, such as those conducted by Yoshida (2009) [2], have explored the importance of reducing wave drag through optimal wing and fuselage designs. Computational fluid dynamics (CFD) simulations and panel methods have been widely employed in evaluating the impact of design parameters, including airfoil thickness, cross-sectional area distribution, and wing position.

Despite these advances, a gap remains in identifying the specific wing configuration that balances lift, drag, and stability under varying supersonic flight conditions. Existing studies often focus on individual aerodynamic components, leaving room for further exploration using high-fidelity simulations. By integrating OpenVSP and ANSYS Fluent, this thesis aims to address this knowledge gap by evaluating multiple wing configurations and identifying the optimal placement for maximizing aerodynamic performance.

To address this knowledge gap, this study focuses on the aerodynamic implications of varying wing placements for an SST aircraft. Using advanced computational tools such as OpenVSP for preliminary modeling and ANSYS Fluent for detailed CFD simulations, the research aims to provide insights into the relationship between wing placement and aerodynamic performance. By evaluating different wing configurations, this work contributes to the development of optimized SST designs that balance efficiency and stability.

## 1.2 Problem Statement

The design of supersonic transport (SST) aircraft presents significant challenges in achieving optimal aerodynamic performance and stability due to the complex interaction between lift, drag, and moment forces. Wing placement, a critical design variable, directly influences these aerodynamic parameters and plays a key role in minimizing wave drag, maximizing lift efficiency, and ensuring longitudinal stability [2]. However, determining the optimal wing configuration remains a complex task due to the varying effects of wing position under different supersonic flight conditions.

Previous research has primarily focused on general aerodynamic improvements, with limited studies comprehensively addressing how specific wing placements influence the overall aerodynamic profile. While lower-order methods such as panel-based models and empirical formulations have been used to approximate aerodynamic forces, they often neglect detailed shockwave interactions and pressure distributions that significantly affect the pitching moment and drag characteristics in supersonic flight. As a result, there is a knowledge gap in accurately predicting and validating wing placement impacts using high-fidelity computational tools.

This problem warrants investigation because improper wing placement can lead to increased drag, inefficient lift generation, and stability issues, compromising fuel efficiency, structural design, and overall aircraft performance. Addressing this gap is essential for the development of next-generation SST aircraft, which aim to balance high-speed performance with environmental and operational efficiency. Accordingly, it is interesting and important to see the interaction of those

waves for various shape configurations to investigate its effect to the aerodynamic characteristics.

In the broader context, solving this problem contributes to advancements in aerospace design by improving the understanding of key aerodynamic principles. The findings can guide design optimizations not only for commercial SSTs but also for supersonic military aircraft, drones, and high-speed transport systems.

### 1.3 Research Objectives

The primary objective of this thesis is to evaluate the impact of wing placement on the aerodynamic performance of a supersonic transport (SST) aircraft and identify the best configuration for maximizing aerodynamic efficiency and stability.

The specific research objectives are as follows:

1. To analyze the effects of wing placement on key aerodynamic parameters, including lift coefficient ( $C_L$ ), drag coefficient ( $C_D$ ), and moment coefficient ( $C_M$ ).
2. To evaluate additional aerodynamic characteristics, including wave drag, for each wing configuration.
3. To compare and validate aerodynamic trends using OpenVSP and ANSYS Fluent.
4. To provide a comprehensive understanding of how wing placement influences the aerodynamic profile of an SST aircraft.

### 1.4 Research Scope and Limitation

**Scope:** This research focuses on evaluating the aerodynamic performance of a supersonic transport (SST) next generation aircraft model by analyzing different wing placement configurations using computational tools OpenVSP and ANSYS Fluent. The study covers three wing locations (20 meters, 35 meters, and 50 meters from the nose) and assesses key aerodynamic parameters, including lift

coefficient ( $C_L$ ), drag coefficient ( $C_D$ ), and moment coefficient ( $C_M$ ). The analysis is conducted under supersonic conditions at Mach 1.2 and Mach 2.0 with a fixed angle of attack of  $5^\circ$  at Reynolds number  $Re = 1 \times 10^7$ .

**Limitations:** While the study offers valuable insights, certain limitations are acknowledged:

- The simulations are conducted only for Mach 1.2 and Mach 2.0 with a fixed angle of attack of 5 degrees. Variations in angles of attack, Mach numbers, and altitudes are not covered.
- Only geometry of wing and fuselage were analyzed.
- For the CFD simulations, only steady analysis is conducted.
- Mesh refinement and boundary conditions were set within resource limits for the student version of ANSYS Fluent.

**Justification for Limitations:** These limitations are justified by the focus of this study on preliminary aerodynamic design optimization. While real-world conditions may introduce additional complexities, the scope and approach are sufficient for identifying key aerodynamic trends and optimal wing placement.

## 1.5 Significance of the Study

**Theoretical Contributions:** This study contributes to the field of aerodynamics by providing a detailed evaluation of wing placement and its effects on the aerodynamic performance of supersonic transport (SST) aircraft. The findings enhance the understanding of how aerodynamic coefficients, such as lift coefficient ( $C_L$ ), drag coefficient ( $C_D$ ), and moment coefficient ( $C_M$ ), are influenced by wing location under supersonic flight conditions. The research bridges the gap between low-order analytical models and high-fidelity computational fluid dynamics (CFD) simulations, offering a more comprehensive framework for aerodynamic design optimization.

**Practical Implications:** The study offers practical insights for aerospace engineers and aircraft manufacturers by identifying the wing location that maximizes

the lift-to-drag ratio while maintaining stability. The recommendations derived from the simulation results can be applied to the design of future SSTs, ensuring enhanced fuel efficiency and operational stability. By evaluating multiple wing configurations, the research supports decision-making processes in the early design phases.

**Potential Impact:** The results of this study have implications beyond the design of commercial supersonic transport. The optimized wing placement strategies can be adapted to the development of high-speed military aircraft, unmanned aerial vehicles (UAVs), and advanced transport systems. The reduction of wave drag and the improvement in aerodynamic efficiency can contribute to the advancement of sustainable and cost-effective supersonic aviation.

**Stakeholder Benefits:** Aircraft manufacturers and designers can benefit from the findings by implementing the optimal wing placement strategies to reduce operational costs and environmental impact. Government and defense organizations involved in high-speed military applications may also leverage the results for improving the performance of next-generation supersonic vehicles. Additionally, the academic community benefits from the enhanced understanding of supersonic aerodynamics, which can be extended in future research efforts.

## CHAPTER 2

### LITERATURE REVIEW

## 2.1 Airfoil Fundamentals

### 2.1.1 Introduction to Airfoil

The concept of an airfoil has always been fundamental to the design of aircraft and is still a basic subject in aerospace engineering. Because of its significance, a large amount of the literature in this topic is devoted to discussions of airfoils. The airfoil section is the fundamental component of a wing or any lifting surface, as Lissaman stated in 1983. This basic structure forms the foundation of many fluid mechanics related design fields, such as marine propellers, helicopter rotors, aircraft wings, and even some aspects of animal flight [6].

Abbott and von Doenhoff work "*Theory of Wing Sections*" is one of the most thorough sources on airfoils. First published in 1949, this 700-page book underwent a widespread edition in 1959. It is still useful even after all these years. Although the book was written before the advent of contemporary numerical analysis methods for airfoil design, it is still a great resource for learning the fundamentals of airfoil theory and applications [6].

Since powered flight became successful in the early 1900s, the significance of aerodynamics has gained more attention. People became more interested in the aerodynamic behavior of different lift surfaces, like rotors and fixed wings, as their interest in flying grew. This concept was further advanced between 1912 and 1918 by Ludwig Prandtl and his team in Göttingen, Germany, who claimed that the aerodynamic properties of a wing might be divided into two parts: (1) the analysis of airfoil sections and (2) the changes required for the wing profile.

This is a complete wing, given its small span. In modern aerodynamics, this two-part method, which distinguishes the assessment of an isolated airfoil's properties from the impact of the complete wing remains the norm [7].

### 2.1.2 Airfoil Definition

The simplest definition of an airfoil is any wing cross-section that is produced by slicing through the wing parallel to the incoming airflow (also known as the free stream velocity). When exposed to airflow, this region, which runs the length of the wing's wingspan, is intended to provide lift. The wing's shape, curvature, and pressure distribution during flight are the main factors that influence its characteristics, including its capacity to produce lift and, under some situations, its drag characteristics [7].

Analysis of airfoils in theoretical aerodynamics usually begins with the assumption of inviscid flow, which eliminates the effects of viscosity. With this method, we can predict and simplify the airfoil's lift and moment properties. However, it is impossible to estimate drag accurately since viscous effects are absent. The D'Alembert paradox, which states that an object in inviscid flow experiences zero drag, is a well-known example of this absence. Viscous flow must be taken into account in order to produce realistic drag predictions [7].

## 2.2 Aerodynamics Principles

### 2.2.1 Aerodynamics Forces and Moments

The sole basic causes of the aerodynamic forces and moments acting on the body are:

1. Pressure distribution over the body surface
2. Shear stress distribution over the body

Pressure and shear stress distributions on the body surface are the only ways nature may convey a force to a body moving through a fluid. The force per unit area (pounds per square foot or newtons per square meter) is the same for both pressure ( $p$ ) and shear stress ( $\tau$ ). As shown in Figure 2.1,  $\tau$  operates tangentially

to the surface and  $p$  acts normal to it. The "tugging action" on the surface, which results from friction between the body and the air, is what causes shear stress [7].

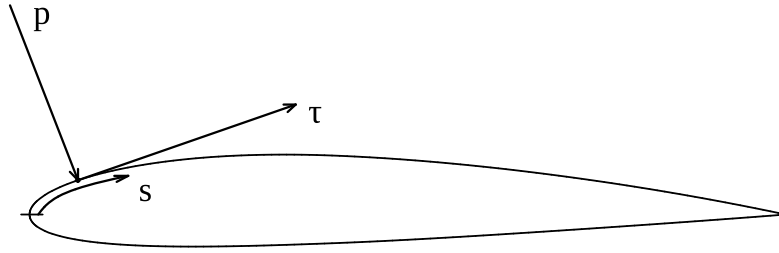


FIGURE 2.1: Illustration of pressure and shear stress on an aerodynamic surface.

As seen in Figure 2.2, the aerodynamic force  $R$  and moment  $M$  on the body are the net outcome of the integration of the  $p$  and  $\tau$  distributions over the entire body surface. The resulting  $R$  can then be divided into two sets of components and the relative wind, or  $V_\infty$ , is the flow velocity far forward of the body, as illustrated in Figure 2.3.  $V_\infty$  is also known as the freestream velocity since the flow that is far from the body is referred to as the freestream [7].

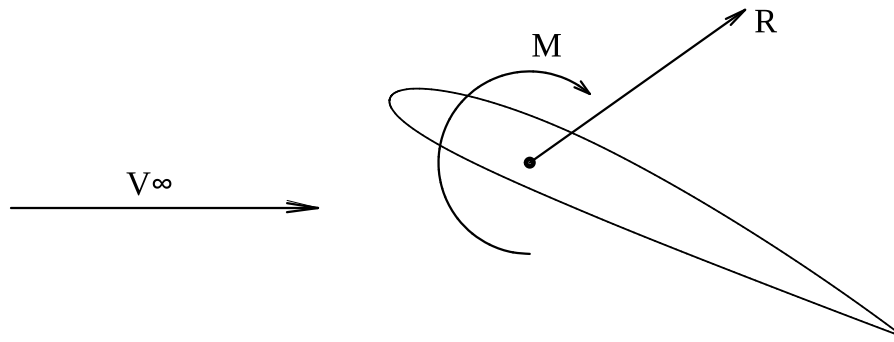


FIGURE 2.2: Resultant aerodynamic force and moment on the body

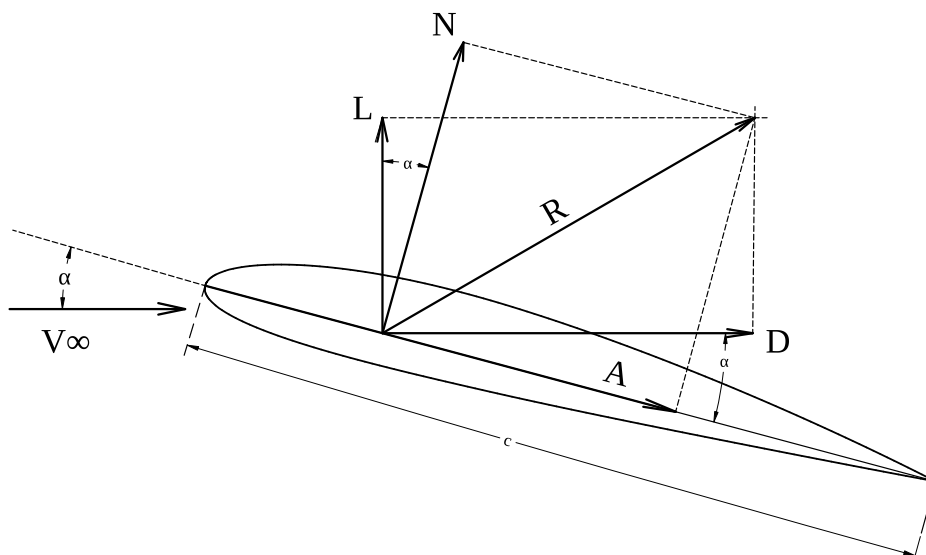


FIGURE 2.3: Resultant aerodynamic force and the components into which it splits

Based on Figure 2.3, resultant force is split into several components, by definition:

- $V_\infty$  = Free stream velocity
- $L$  = lift = component of  $R$  perpendicular to  $V_\infty$
- $D$  = drag = component of  $R$  parallel to  $V_\infty$
- $N$  = normal force = component of  $R$  perpendicular to  $c$
- $A$  = axial force = component of  $R$  parallel to  $c$

The angle between  $c$  and  $V_\infty$  is known as the angle of attack, or  $\alpha$ . Therefore, the angle between  $L$  and  $N$  and between  $D$  and  $A$  is likewise  $\alpha$ . As shown in Figure 2.3, the geometric relationship between these two groups of components is,

$$L = N \cos(\alpha) - A \sin(\alpha) \quad (2.1)$$

$$D = N \sin(\alpha) - A \cos(\alpha) \quad (2.2)$$

## 2.3 Airfoil Design

Airfoil sections must satisfy certain design requirements in order to function at their best in a variety of applications, including aircraft wings, tail, and other aerodynamic surfaces.

### 2.3.1 Airfoil Geometry

The contour form, also known as the envelope, of an airfoil describes its basic geometric shape by defining the curvature of its top and lower surfaces. An airfoil may be cambered, which means the upper and lower surfaces have distinct shapes, or symmetrical, which means the upper and lower surfaces have the same shapes and curvatures, as seen in Figure 2.4.

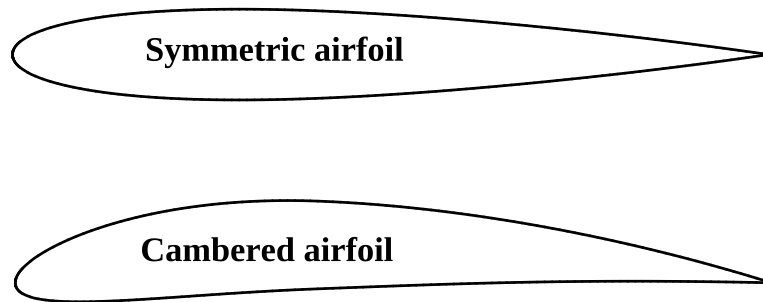


FIGURE 2.4: Airfoil geometry

### 2.3.2 Airfoil Nomenclature

Consider the airfoil depicted in Figure 2.5. The *mean camberline* is the trajectory of the midpoint between the upper and lower surfaces measured perpendicular to the mean camber line itself. The *leading and trailing edges* of the mean camber line are the foremost and rearmost points, respectively [8].

The straight line connecting the leading edge and the trailing edge is the airfoil's *chordline*, and the precise distance measured along the chord line from the leading edge to the trailing edge is referred to as the *chord  $c$*  of the airfoil [8].

The maximum distance, measured perpendicular to the chord line, between the chord line and the mean camber line is known as the *camber*. The *thickness*, which is also measured perpendicular to the chord line, is the gap between the upper and lower surfaces [8].

With a leading-edge radius of approximately  $0.02c$ , the airfoil's leading edge typically has a circular form. By first defining the geometry of the mean camber line and then encircling it with a predetermined symmetrical thickness distribution, the shapes of all typical NACA airfoils are produced [7].

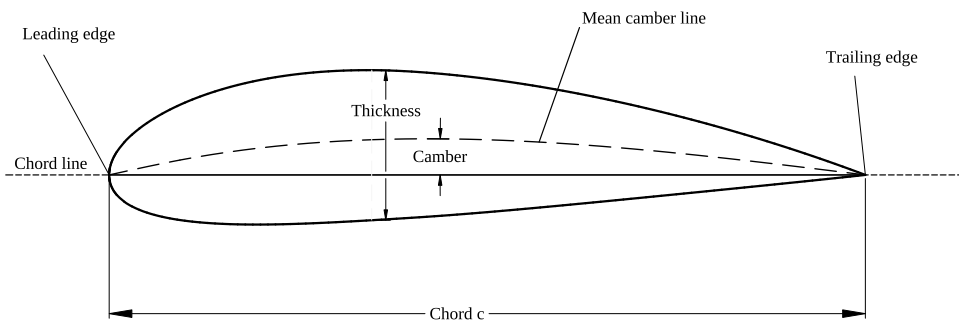


FIGURE 2.5: Airfoil nomenclature

The NACA has developed different airfoil shapes with a logical numbering system that can be used in aircraft wings depending on their application. The first family of NACA airfoils was the four digit series, like the NACA 2412 airfoil. The maximum camber in hundredths of the chord is shown by the first digit, the maximum camber position from the leading edge along the chord is indicated by the second digit in tenths of the chord, and the maximum thickness of the airfoil is indicated by the final two digits in hundredths of the chord. The NACA 2412 airfoil has a maximum thickness of  $0.12c$  and a maximum camber of  $0.02c$ , which is  $0.4c$  from the leading edge. These figures are typically expressed as a percentage of the chord, i.e., 12% thickness and 2% camber at 40% of the chord [7].

The second family of NACA airfoils was the five digit series, such as the NACA 23012 airfoil. The lift coefficient in tenths is obtained by multiplying the first digit by  $\frac{3}{2}$ . The position of the maximum camber along the chord from the leading, expressed as a percentage of the chord, is given by the next two digits divided by 2, and the last two digits give the maximum thickness in percentage of chord. The NACA23012 airfoil has a maximum thickness of 12%, a maximum camber position of  $0.15c$ , and a design lift coefficient of 0.3 [7].

The most used family of NACA airfoils is the 6-series laminar flow airfoils. An example is the NACA 65-128 airfoil. Here, the series can simply be determined by the first digit. The position of the minimum pressure at the chords leading edge is indicated by the second digit in tenths, the lift coefficient is shown by the third digit in tenths, and the chords maximum thickness is shown by the last two digits in hundredths. The NACA 65-218 airfoil has a series name of 6, a thickness of 18%, a design lift coefficient of 0.2, and a minimum pressure of  $0.5c$  for the basic symmetrical thickness distribution at zero lift [7].

## 2.4 Evolution of Airfoil Design

The design of an airfoil keeps changing as it advances from subsonic to supersonic flight. While the shape of the airfoil changes, their aerodynamic characteristics also change [9]. Subsonic, transonic, and supersonic states all necessitate distinct airfoil characteristics and provide unique challenges. It is essential to comprehend how airfoil design adjusts to different regimes in order to fully grasp the unique needs of supersonic airfoils [8].

### 2.4.1 Subsonic Airfoil Design

Subsonic airfoil may be the most common airfoil, with the applications involving free flow velocities up to roughly 0.8 mach. A common geometric characteristic of these airfoils is a large leading edge radius. This often ensures robust behavior, meaning that slight changes in the angle of attack do not cause the airfoil to behave significantly differently. This can be achieved at subsonic speeds without a large drag loss [6].

### 2.4.2 Transonic Airfoil Design

Transonic airfoil operate in subsonic, but supercritical free streams. The latter indicates that somewhere in the flow field, the local mach number is more than 1.0. In general, this initially happens at a key free stream Mach number of 0.7 to 0.8.

This is typically followed closely by the drag divergence free stream Mach number, that is the Mach number when the shock wave formation abruptly increases the wave drag [6].

Maximizing the drag divergence Mach number is the goal in transonic airfoil in order to delay the formation of these shock waves and reduce drag. This was achieved through the inverse design method, where the intended pressure distribution with a flattened pressure peak and a gentle transition to the airfoil aft was created and the geometry was tailored to reproduce this target. The more simple method of maximizing the drag rise Mach number or decreasing the drag at a specific Mach number could be used in an optimization process based on a flow simulation that is reliable enough to produce an appropriate drag estimate [6].

### 2.4.3 Supersonic Airfoil Design

Supersonic airfoil operate at cruise conditions where the free-stream Mach number exceeds 1.0, but is less than about 5.0. The challenge for this free-stream condition is reducing the wave drag, and it can be achieved by reducing the thickness to chord ratio of the airfoil, and also by sharpening the leading edge [6].

A notable example of this design is the biconvex airfoil, as seen on the Lockheed F-104 Starfighter (shown in Figure 2.6). This airfoil has an extremely thin profile, with a thickness of only 3.36 percent of the chord. As shown in Figure 2.7, other supersonic airfoil shapes have also been developed to optimize performance in high-speed regime. These diverse airfoil shapes highlight the customized aerodynamic solutions developed for supersonic speeds to balance performance, structural integrity, and drag reduction.



FIGURE 2.6: F-104 Starfighter [10].

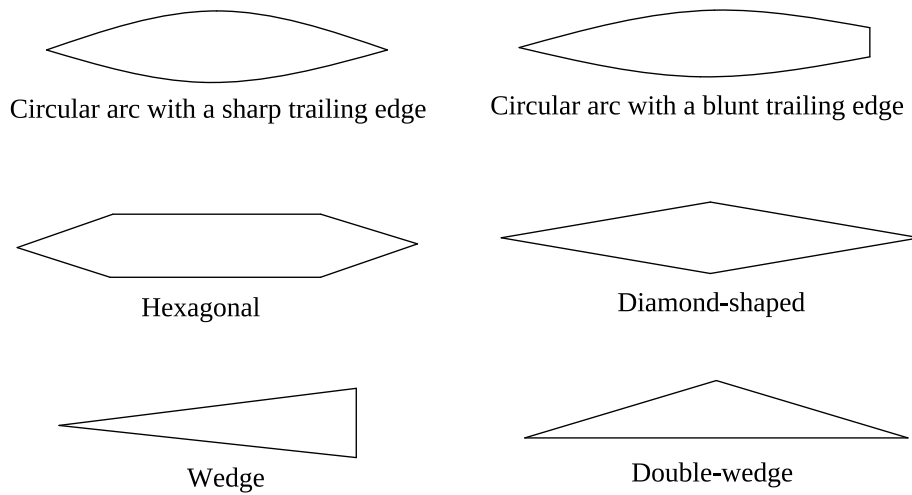


FIGURE 2.7: Typical shapes of supersonic airfoil.

## 2.5 Supersonic Aerodynamics

Supersonic aerodynamics deals with the behavior of airflow when an aircraft travels at speeds greater than the speed of sound (Mach 1). This regime introduces unique phenomena, such as shockwaves, compressibility effects, and significant changes in aerodynamic forces. Understanding these concepts is critical for optimizing the design of supersonic aircraft, particularly in minimizing drag and ensuring stability [11].

### 2.5.1 The Physics of Supersonic Flight

When an aircraft travels faster than the speed of sound, pressure waves generated by its movement coalesce into shockwaves, which have a profound impact on aerodynamic performance [12]. These shockwaves result in sudden changes in pressure, density, and velocity of the airflow, leading to the following key effects:

- **Shockwave Formation:** The formation of oblique shocks, normal shock waves, and expansion waves increases pressure drag (wave drag) and creates energy losses through irreversible heat.
- **Compressibility Effects:** The compressibility of air becomes significant, altering the pressure distribution over the airframe and leading to changes in lift and drag characteristics.
- **Drag Divergence Mach Number:** As the aircraft approaches supersonic speeds, a rapid increase in drag occurs, known as drag divergence. The drag divergence Mach number is a critical design consideration for reducing wave drag.

### 2.5.2 Key Aerodynamic Challenges in Supersonic Transport

Designing an efficient supersonic transport (SST) aircraft requires overcoming several aerodynamic challenges:

**Wave Drag Reduction:** Wave drag is the dominant source of drag in supersonic flight and occurs due to the shockwaves generated by the airframe, particularly

the wing and fuselage. Minimizing wave drag is essential for reducing fuel consumption and improving overall efficiency [2].

**Lift-to-Drag Ratio Optimization:** Supersonic aircraft typically suffer from a lower lift-to-drag ratio compared to subsonic aircraft due to higher wave drag and compressibility effects. Achieving an optimal lift-to-drag ratio requires careful design of airfoils, wing placement, and fuselage cross-sectional distribution (area ruling).

**Maintaining Stability and Control:** High-speed flight introduces challenges in maintaining longitudinal and lateral stability due to changes in the aerodynamic center and the presence of shock-induced flow separation. Wing placement and airfoil shape must be optimized to maintain stable aerodynamic moments.

### 2.5.3 Introduction to Oblique Shocks and Expansion Wave

The performance of airfoils at high speeds is significantly affected by oblique shock waves and expansion waves, shown in Figure 2.8, two crucial phenomena in supersonic aerodynamics. A shockwave is created when airflow suddenly shift from supersonic to subsonic velocity, resulting in a notable variations in density, temperature, and pressure. The formation of shock waves are located at the leading and trailing edges of the airfoil, which cause a sudden increase in temperature and pressure. The effectiveness of supersonic flight may be harmed by the higher drag caused by these sudden changes, which also known as wave drag. To preserve aerodynamic stability and reduce drag, shockwave location and intensity must be managed [8].

On the other hand, expansion waves happen when airflow accelerates over curved surfaces or in areas where pressure decrease. By reducing unwanted pressure gradients and facilitating smoother flow transitions, these wave improve overall performance. in order to manage these waves and reduce shockwave strength while utilizing expansion effects to improve lift-to-drag ratios, supersonic airfoil features thin profiles and sharp leading edge [13].

At high Mach numbers, airfoils experience an increase in pressure drag, and the formation and management of shockwave are critical to minimizing wave drag. This drag increase can be minimized by the use of thin airfoils and sharp leading edge [13]. The formation of shock waves are located at the leading and trailing edges of the airfoil, which cause a sudden increase in temperature and pressure. This, in turn, causes a fast increase in drag. Maintaining effective performance at supersonic speeds requires careful wing design to control these shock waves. Techniques for managing shock waves are crucial for reducing wave drag that is directly brought on by sudden changes in the pressure surrounding the wing [8].

The variation in pressure across the airfoil, particularly where  $p_2 > p_3$ , generates a net aerodynamic force in the stream wise direction, leading to wave drag. This drag is a fundamental factor in supersonic aerodynamics, as it directly affects aircraft performance. Equation 2.3 highlights that wave drag increases with stronger pressure variations across the airfoil. It also shows the dependence of drag on the Mach number, meaning that higher supersonic speeds result in greater wave drag effects. By understanding these aerodynamic interactions, engineers can design airfoils with optimized shapes to minimize wave drag, improving overall efficiency in supersonic flight.

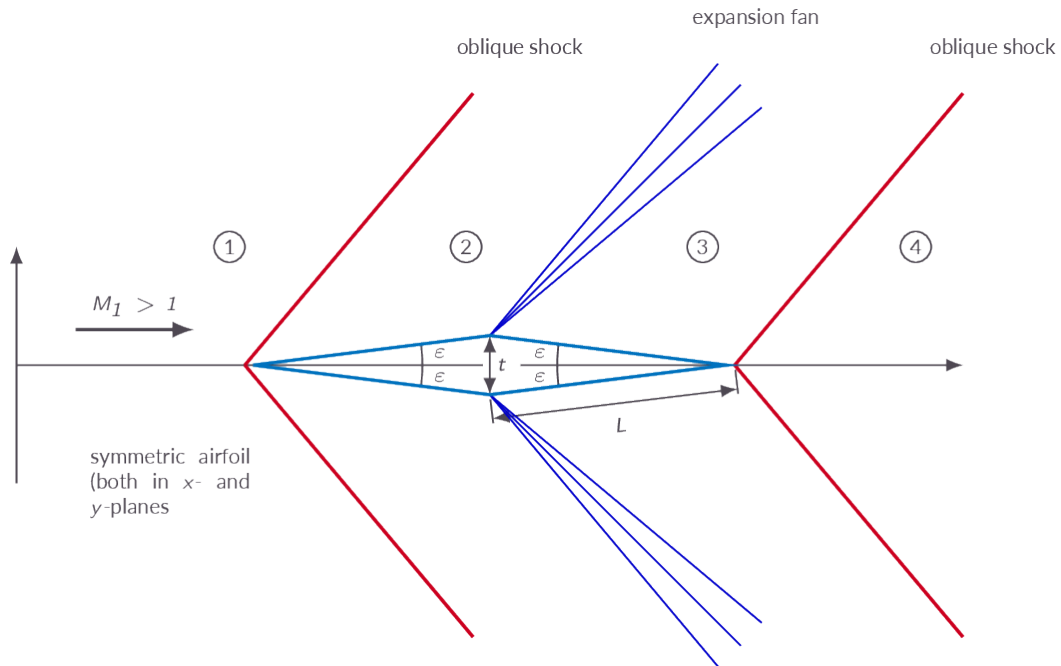


FIGURE 2.8: Oblique shock and expansion waves.

$$c_d = f\left(\frac{p_n}{p_\infty}\right) = \frac{2}{\gamma M_1^2} \left(\frac{p_3}{p_1} - \frac{p_2}{p_1}\right) \sin \alpha \quad (2.3)$$

Quantifies the contribution of these pressure changes to the total drag. Here's what each term represents:

- $c_d$ : Drag coefficient due to wave drag
- $f\left(\frac{p_n}{p_\infty}\right)$ : Function describing the pressure ratio effect on drag
- $\gamma$ : Ratio of specific heats for the gas
- $M_1$ : Freestream Mach number
- $p_1, p_2, p_3$ : Pressures at different points on the airfoil surface
- $\alpha$ : Angle of attack

## 2.5.4 Design Strategies for Managing Supersonic Aerodynamics

Engineers have developed several design strategies to address the aerodynamic challenges of supersonic flight:

**Area Rule:** The area rule minimizes wave drag by ensuring a smooth distribution of cross-sectional area along the length of the aircraft. By preventing abrupt changes in volume, this technique reduces shockwave intensity and drag [14].

**Thin Airfoils:** Thin airfoils are commonly used in supersonic aircraft because they reduce the shockwave strength and pressure drag. The thickness-to-chord ratio is typically kept low to maintain a streamlined shape.

**Swept Wings:** Sweeping the wings backward reduces the effective Mach number seen by the wing and delays the formation of shockwaves. This helps in maintaining higher lift and reducing drag at supersonic speeds [15].

**Diamond Airfoil Shape:** The diamond airfoil, characterized by sharp leading and trailing edges, is an effective design for minimizing wave drag. Its geometry allows for efficient shockwave management and pressure distribution, making it ideal for supersonic applications [16].

## 2.6 Wing Placement in Supersonic Aircraft

The placement of the wing relative to the aircraft's fuselage significantly influences the aerodynamic forces acting on the airframe, particularly in supersonic flight. Wing location affects lift, drag, and stability by altering the distribution of aerodynamic loads and the interaction of airflow with the airframe. This section explores the historical context of wing placement, the effects of wing location on key aerodynamic parameters, and the findings from previous studies that provide insights into optimizing wing placement for supersonic aircraft.

### 2.6.1 Historical and Modern Wing Designs for SST

Historically, supersonic transport (SST) aircraft such as the Concorde and Boeing 2707 utilized delta-wing configurations with wings positioned toward the rear of the aircraft [1], [3]. These designs aimed to balance aerodynamic performance with structural feasibility while minimizing wave drag. The rearward placement of wings in delta configurations was chosen to delay shockwave formation and reduce the effective Mach number seen by the wing.

Modern SST concepts, including designs proposed by Boom Supersonic and NASAs X-59 QueSST, take a different approach by integrating more advanced wing profiles and optimized placements. These designs focus on achieving higher lift-to-drag ratios, minimizing sonic boom intensity, and enhancing fuel efficiency. Unlike the fixed-wing configurations of earlier SSTs, modern designs often explore variable wing placements and hybrid wing-body configurations to improve aerodynamic performance [15].

### 2.6.2 Effects of Wing Placement on Lift, Drag, and Stability

Wing placement influences key aerodynamic characteristics, including the lift coefficient ( $C_L$ ), drag coefficient ( $C_D$ ), and moment coefficient ( $C_M$ ). These effects are primarily determined by how the wing interacts with the flow of air at supersonic speeds and how the resulting aerodynamic forces are distributed along the airframe [17].

**Lift Generation:** Forward wing positions typically enhance lift generation by placing the wing closer to the fuselage's aerodynamic center. This placement results in a more favorable pressure distribution over the wing, increasing the overall lift coefficient. However, excessive forward placement can lead to higher induced drag due to increased downwash on the tail surfaces.

**Wave Drag and Compressibility Effects:** Wing placement also affects wave drag, which is a major contributor to overall drag in supersonic flight. Aft wing positions reduce wave drag by minimizing the effective cross-sectional area exposed to shockwaves. Wings placed toward the rear reduce the pressure buildup

ahead of the wing, thereby delaying shockwave formation. However, this configuration can also result in adverse flow separation near the trailing edge, reducing lift efficiency [2].

**Stability and Moment Coefficient:** Wing placement affects the pitching moment of the aircraft, which is critical for maintaining longitudinal stability. Forward wing positions tend to generate a positive moment (nose-up tendency), which can enhance stability during takeoff and landing but may cause instability at supersonic speeds. Conversely, aft wing positions generate negative pitching moments (nose-down tendency), which can destabilize the aircraft if not properly managed. Therefore, the selection of an appropriate wing location requires a balance between lift efficiency and stability.

## 2.7 Supersonic Airfoil Characteristics

At high Mach numbers, airfoils experience an increase in pressure drag, and the formation and management of shockwave are critical to minimizing wave drag. This drag increase can be minimized by the use of thin airfoils and sharp leading edge [13]. The formation of shock waves are located at the leading and trailing edges of the airfoil, which cause a sudden increase in temperature and pressure. This, in turn, causes a fast increase in drag. Maintaining effective performance at supersonic speeds requires careful wing design to control these shock waves. Techniques for managing shock waves are crucial for reducing wave drag that is directly brought on by sudden changes in the pressure surrounding the wing [8].

### 2.7.1 Thin Airfoils and Drag Reduction

It is impossible to overestimate how effective thin airfoils are at reducing drag at supersonic speeds. Because thicker airfoils produce larger shock waves, which significantly increase drag, supersonic airfoils are typically much thinner than subsonic airfoils.

By reducing the thickness of the airfoil shock wave intensity is decreased, helping maintain a streamlined airflow over the wing, reducing pressure drag

and improving overall aerodynamic efficiency, as well as managing the boundary layer which reduces the risk of flow separation and ensures that drag remains under control. Reducing the chamber also contributes to drag reduction, as the airfoil generates less pressure differential that could intensify shockwave.

### Supersonic Drag Components

The aerodynamic drag acting on a supersonic aircraft can be categorized into various components. For a complete aircraft configuration, consisting of a wing, fuselage, tail surfaces, propulsion systems, and other appendages, the total drag can be approximated as:

$$D_{\text{total}} = D_{\text{airframe}} + D_{\text{propulsion}} + D_{\text{interference}} \quad (2.4)$$

Here:

- $D_{\text{airframe}}$ : Drag due to the airframe without propulsion systems.
- $D_{\text{propulsion}}$ : Drag associated with the propulsion system, including intake spillage, nacelle friction, and bleed drag.
- $D_{\text{interference}}$ : Drag arising from interactions between different aircraft components.

Among these, the dominant component for supersonic cruise is airframe drag, further divided into zero-lift drag and lift-dependent drag.

### Drag Breakdown

Aerodynamic drag is a combination of friction drag and pressure drag:

$$C_{D_{\text{airframe}}} = C_{D_f} + C_{D_p} \quad (2.5)$$

Pressure drag ( $C_{D_p}$ ) itself is composed of wave drag ( $C_{D_w}$ ) and vortex drag ( $C_{D_v}$ ), as expressed below:

$$C_{D_p} = C_{D_w} + C_{D_v} \quad (2.6)$$

The wave drag component ( $C_{D_w}$ ) can be further divided into drag due to volume ( $C_{D_{wv}}$ ) and drag due to lift ( $C_{D_{wl}}$ ):

$$C_{D_w} = C_{D_{wv}} + C_{D_{wl}} \quad (2.7)$$

Finally, the total drag can be expressed in terms of zero-lift drag ( $C_{D_0}$ ) and lift-dependent drag ( $C_{D_l}$ ):

$$C_{D_{\text{airframe}}} = C_{D_0} + C_{D_l} \quad (2.8)$$

### Drag Formulation

To estimate the drag components, empirical relationships are often utilized. Friction drag is calculated using the following formulation:

$$C_{D_f} = C_f(Re_L, M) \frac{S_{\text{wet}}}{S_w} \quad (2.9)$$

where:

- $C_f(Re_L, M)$ : Skin friction coefficient, which is a function of Reynolds number ( $Re_L$ ) and Mach number ( $M$ ).
- $S_{\text{wet}}$ : Wetted surface area of the component.
- $S_w$ : Reference wing area.

The skin friction coefficient is determined using Prandtl's and Hoerner's formulas for incompressible and compressible flows, respectively:

$$C_f(Re_L) = \frac{0.455}{(\log_{10} Re_L)^{2.58}} \quad (2.10)$$

$$f(M) = (1 + 0.15M^2)^{-0.58} \quad (2.11)$$

### Wave Drag Due to Volume

Wave drag due to volume arises from the shock waves generated by the body shape of the aircraft. It is primarily influenced by the cross-sectional area distribution of the fuselage and the thickness-to-chord ratio of the wings. This drag can

be minimized through techniques such as area ruling, which ensures a smooth cross-sectional variation along the length of the aircraft. Effective area ruling is critical for maintaining low wave drag at supersonic speeds [2].

### Summary

The supersonic drag components are integral to aircraft design, especially for high-speed regimes. The breakdown and formulation provided in this section serve as a foundation for analyzing and minimizing drag components, particularly airframe drag, which is the dominant contributor during supersonic cruise [2].

## 2.8 Custom Airfoils vs. NACA Airfoils

The transition from standard NACA airfoils to custom airfoils has been driven by the need for more specialized performance in high-speed regimes. With the invention of the aircraft, it has become faster and larger than the first ever aircraft [18]. NACA airfoils served as the foundation for the engineering for early aircraft, but their intrinsic limitations in supersonic applications (such as increased drag and less control over the formation of shock waves) led to the development of custom airfoil design for supersonic flight.

### 2.8.1 Benefits of Custom Airfoil Design

An airfoil has various parameters, controlling which, it is possible to design an application specific shape to serve a certain purpose. These parameters include, but are not limited to, Chord, Camber, Maximum Camber Position, Thickness, Maximum Thickness Position, Leading Edge Radius and Trailing Edge Radius [19].

Custom airfoils have several key advantages, especially in high-speed and specific applications. Their ability to give customized performance for specific Mach ranges is one of their main advantages. Engineers can guarantee that wave drag is minimized and aerodynamic efficiency is maximized, depending on the

mission profile, by designing custom airfoils that function efficiently at the desired supersonic speed.

Custom airfoils can also improve the control of shock waves as mentioned before. By fine tuning geometric properties including camber, leading edge sharpness, and thickness-to-chord ratio, shock wave production and location can be controlled, resulting in reducing the drag associated with these high speeds. Advanced design tools such as XFLR, OpenVSP, and ANSYS Fluent allows engineers to stimulate and improve custom airfoil configurations, providing airflow configurations, shock wave prediction, and geometric optimization.

### **2.8.2 Tools for Custom Airfoil and Wing Design and Analysis**

OpenVSP (Vehicle Sketch Pad) is a parametric modeling tool that supports airfoil and complete aircraft design. This tool can precisely control the geometry of the wings and provides a visual platform to integrate the wings into a complete aircraft model. OpenVSP is very suitable for creating airfoil shapes and exporting geometries for further detailed analysis in computational fluid dynamics (CFD) tools [20].

ANSYS Fluent is a CFD software, highly suitable for simulating supersonic airflow around wings. It models shock wave interactions, boundary layer behavior, and drag characteristics, and supports complex turbulence models. Fluent's detailed simulations are very valuable in supersonic design because they allow engineers to optimize airfoil designs based on pressure distribution and drag [21].

## CHAPTER 3

### RESEARCH METHODOLOGY

In this chapter the systematic method to designing and analyzing supersonic airfoils will be discussed. The main objective of this research is to estimate the aerodynamic performance of an airfoil appropriate for supersonic flight using advanced computational methods. Wave resistance reduction, lift-to-drag ratio optimization, and shockwave behavior management are among the research objective for the results that this methodology aims to achieve

#### 3.1 Research Flowchart

The study process followed a clear flow chart, beginning with a baseline study followed by design, simulation and analysis phases. The sequence of steps provides a logical approach from defining the existing design to final analysis and reporting. Figure 3.1 shows a schematic of this flowchart outlining the methodological steps.

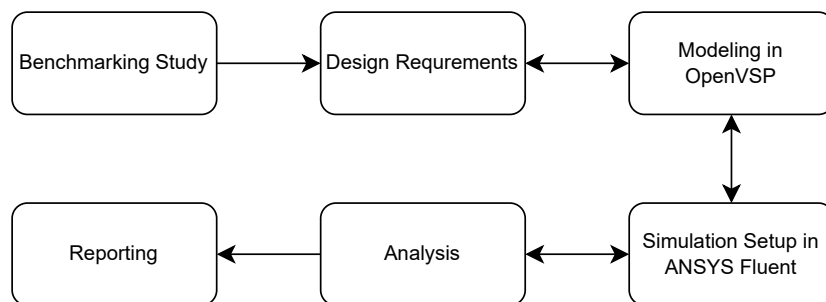


FIGURE 3.1: Research Methodology

## 3.2 Benchmarking Study

As an initial phase of the study, a benchmarking study was conducted to establish a foundation for the design and analysis of supersonic airfoils. The objective was to identify key performance indicators and aerodynamic characteristics of various airfoil profiles optimized for supersonic flight. The results from this phase informed the selection of the most efficient airfoil for subsequent analyses.

The benchmarking involved analyzing existing supersonic airfoil shapes, such as the NACA 0005, hexagonal, and the diamond airfoil, which are widely known for their efficiency at supersonic flights. These airfoils were chosen because they have effective shockwave management and minimal wave resistance, making them suitable for high-speed applications. The performance data of these airfoils were collected from the literature and evaluated for key parameters such as lift to drag ratio, wave drag coefficient, and pressure distribution.

The study showed that thin airfoils with sharp leading edges perform well in minimizing wave drag while maintaining structural integrity. This airfoil consistently outperformed the other candidates in terms of aerodynamic efficiency, making it the optimal choice for further testing. The benchmarking study also confirmed the reliability of ANSYS Fluent as a CFD tool for the next phase of analysis, as the OpenVSP results closely aligned with the findings from published literature.

## 3.3 Airfoil and Wing Geometry Modeling

### 3.3.1 Introduction to OpenVSP

OpenVSP (Open Vehicle Sketch Pad) is a versatile parametric geometry tool that is widely used in the conceptual design phase of aerospace engineering. J.R. Gloudemans et al. developed OpenVSP for NASA in the early 1990s, and it has now evolved into a complete platform that facilitates geometry generation and rally engineering analysis. The aerospace community has unlimited access to it as an open-source tool for ongoing enhancements [20].

With the ability to define and modify factors like wingspan, chord length, fuselage size, and airfoil shape, OpenVSP allows users to produce precise 3D representations of aircraft. It facilitates quick design configuration exploration and easily combines with structural and aerodynamic analysis tools later on. Early in the design process, OpenVSP real-time, accurate geometry allows for quick iterations and optimization [20].

OpenVSP began as a simple visualization tool and has since developed into a fundamental geometry and analysis engine used in many different aeronautical design workflows. Supporting projects involving drones, electric vertical take-off and landing, supersonic and hypersonic aircraft, space launch systems, and small satellites, its adoption spans major aerospace sectors, including business, government, academia, and startups. The software is a useful tool for interdisciplinary design frameworks because of its export features, which make it easier to integrate with CAD applications, finite element analysis (FEA) software, and computational fluid dynamics (CFD) tools like ANSYS Fluent.

In addition to geometric modeling, OpenVSP offers advanced aerodynamic analysis tools, such as VSPAERO, which can calculate aerodynamic properties in a variety of flight conditions, including lift, drag, and moment coefficients. The software also includes a wave drag analysis module specifically designed to evaluate compression effects and drag caused by shock waves in supersonic flight conditions. These tools allow engineers to perform preliminary aerodynamic assessments directly in OpenVSP, making them an invaluable tool for early aircraft design and optimization [20].

### 3.3.2 Initial Airfoil Configuration

The NACA 0005, biconvex, and diamond airfoils were the first three airfoils examined in order to choose the best airfoil for supersonic flight. These airfoils can be seen in Figure 3.2, 3.3, 3.4, 3.5. To be able to demonstrate the clear performance variations of airfoils designed for various flight regimes, the NACA 2412, a subsonic airfoil, was also included for comparison. Aerodynamic properties and wave drag coefficient were used to assess each airfoil.

EFFECT OF WING LOCATION ON THE AERODYNAMIC PROFILE OF A SUPERSONIC AIRCRAFT  
USING ANSYS FLUENT

---

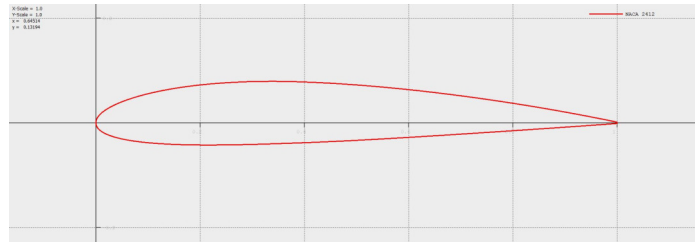


FIGURE 3.2: NACA2412



FIGURE 3.3: NACA0005



FIGURE 3.4: Hexagonal



FIGURE 3.5: Diamond

The baseline for examining supersonic properties was the NACA 0005 airfoil, which has a thin cross-section and a symmetric profile. Its wave drag was larger than that of more specialized designs, despite its moderate aerodynamic performance. The biconvex airfoil had a higher efficiency at high speeds and better shockwave management, but did not outperform the diamond airfoil.

The diamond airfoil was chosen as the best option because of the narrow profile and sharp leading edge, both of which are critical for reducing wave drag and controlling shock waves. It is essential to use airfoils that are optimized for particular flight regimes since the NACA 2412 airfoil, which was made for subsonic purposes, suffered from severe wave drag and instability at supersonic speeds. To ensure consistency across analyses and simplify comparative analysis, all three supersonic airfoils had a thickness-to-chord ratio of 5%.

The airfoils were ranked according to their aerodynamic performance using a scoring system as part of the evaluation process. Chapter 4 provides the detailed results and comparison metrics from this process, offering a quantitative justification of the diamond airfoil's selection as the best option for further refinement and analysis. Insights from benchmarking studies were used to determine the airfoil shape.

### **3.3.3 SST Aircraft Modeling**

Following the selection of the Diamond Airfoil as the optimal candidate, a complete Supersonic Transport (SST) aircraft was designed in OpenVSP, as shown in Figure 3.7. The design was based on a next-generation SST aircraft model referenced from existing literature [2]. The Diamond Airfoil was applied to the aircraft wings, and the full 3D model was developed for both OpenVSP analysis and further CFD simulations.

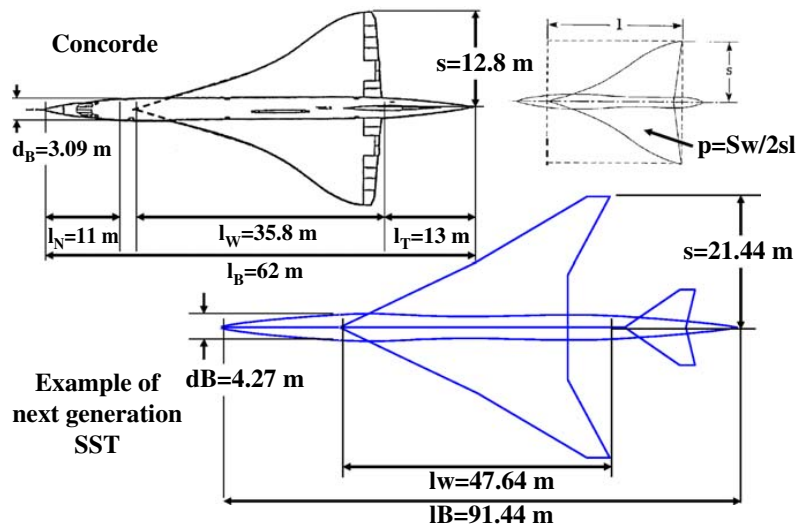


FIGURE 3.6: Configuration parameters on Concorde and a next generation SST [2].

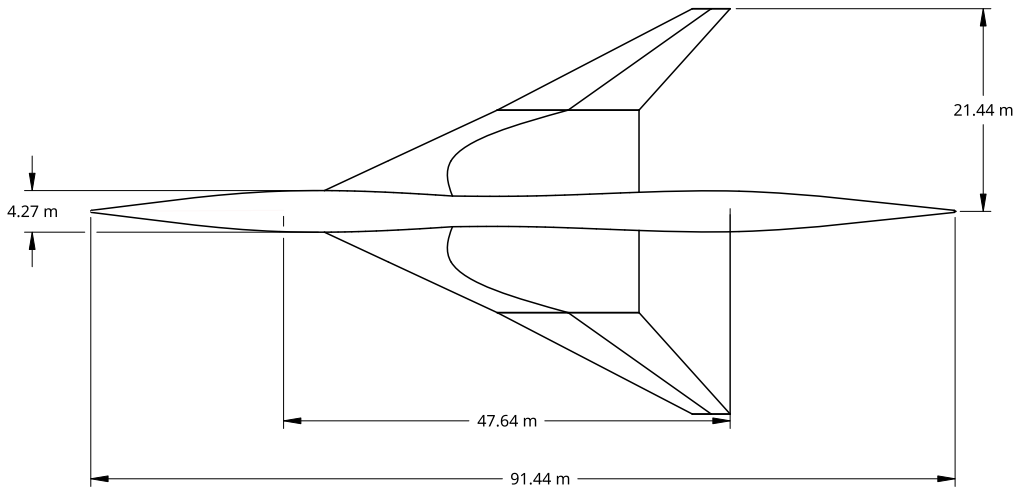


FIGURE 3.7: Overall dimension of a next generation SST.

### 3.3.4 Workflow in OpenVSP

The Workflow in OpenVSP (OpenVSP-3.40.1-win64-Python), shown in Figure 3.8, was conducted in two main phases: the airfoil selection and testing phase, followed by the creation and analysis of the next-generation Supersonic Transport (SST) aircraft model. Each phase incorporated detailed steps to ensure precise modeling, thorough aerodynamic analysis, and comprehensive data validation.

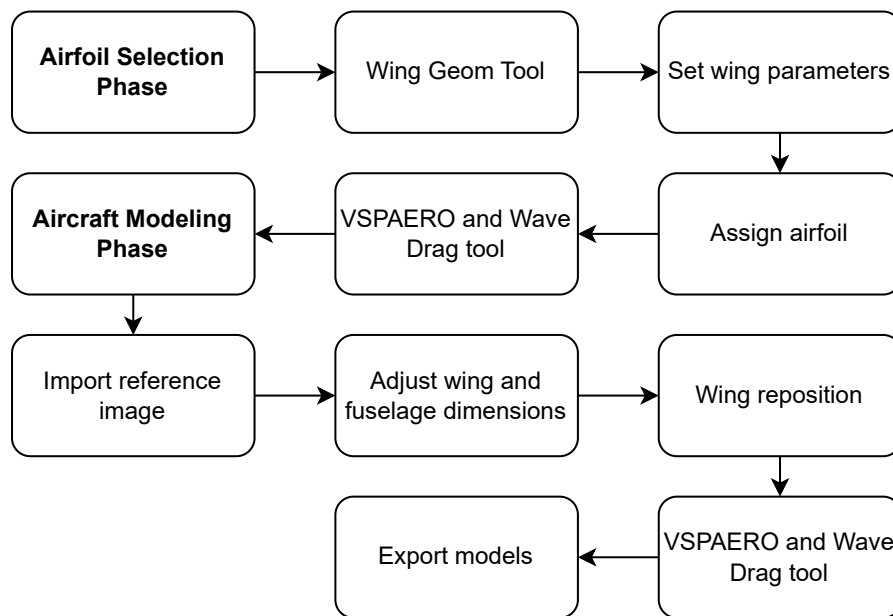


FIGURE 3.8: OpenVSP workflow flowchart.

#### Airfoil Selection and Testing Phase

##### 1. Wing Geometry Creation

The workflow began with the creation of a standardized wing geometry in OpenVSP. Using the Wing Geom tool, a wing component was added to the workspace. The parameters of the wing were modified in the Plan Editor Tab, setting the wingspan to 10 meters and the chord length to 4 meters. These dimensions were chosen to standardize the testing conditions for all airfoil configurations. The wing model is shown in Figure 3.9

## 2. Airfoil Assignment

The next step was the assignment of airfoil profiles to the wing geometry. This was performed using the Airfoil Editor Tab, which allowed for the selection and customization of airfoil shapes:

- Predefined Airfoils: NACA 2412, NACA 0005, and the Diamond Airfoil were directly selected from OpenVSP's built-in airfoil library.
- Custom Airfoil Creation: The Hexagonal Airfoil was manually designed by editing the coordinates of the Diamond Airfoil. Adjustments were made to flatten surfaces and sharpen edges, characteristic of the hexagonal profile.

Each airfoil was configured with a thickness-to-chord ratio of 5% to ensure uniformity across all test cases. Once assigned, each airfoil configuration was saved as an individual model for further aerodynamic analysis.

## 3. Aerodynamic Analysis

The airfoils were analyzed at three Mach numbers: 0.6, 1.2, and 2.0, to evaluate their performance across subsonic, transonic, and supersonic regimes. The following tools were used for aerodynamic evaluation:

### (a) VSPAERO Tool:

- The Vortex Lattice Method (VLM) was applied to compute aerodynamic coefficients, including:
  - Lift Coefficient ( $C_l$ )
  - Drag Coefficient ( $C_d$ )
  - Moment Coefficient ( $C_{m_y}$ )
- The Karman-Tsien Mach Correction was applied to incorporate compressibility effects at higher Mach numbers.

### (b) Wave Drag Analysis Tool:

- Evaluated wave drag by analyzing pressure distribution and shock-wave formation at supersonic speeds.

The results for each airfoil were saved as polar files for further data processing and visualization.

#### 4. Data Management and Visualization

The aerodynamic results were exported to Google Sheets, where line graphs and comparative plots were generated. These visualizations displayed trends in Lift, Drag, Moment Coefficients, and Wave Drag Coefficients, aiding in the identification of the most efficient airfoil.

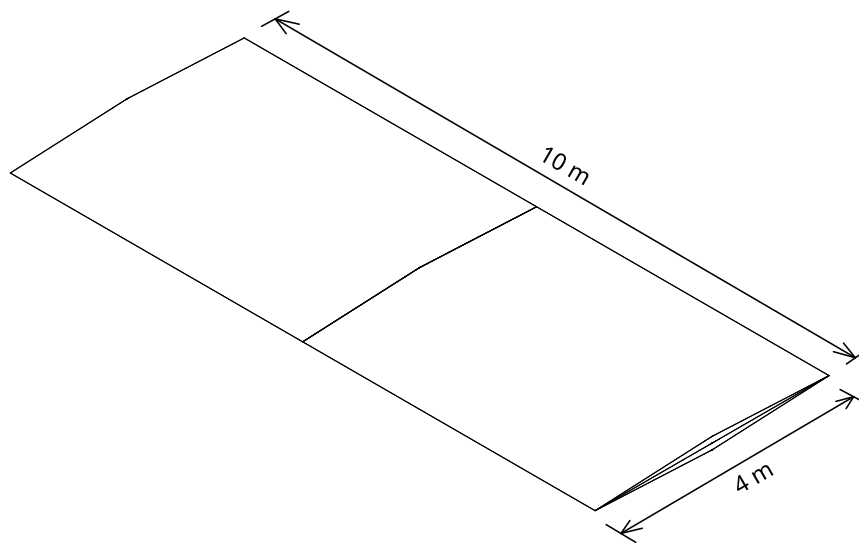


FIGURE 3.9: Wing Model for Airfoil Selection.

### SST Aircraft Modeling and Analysis Phase

#### 1. Model Creation and Reference Setup

The SST aircraft model was based on the reference paper project by JAXA [2]. A scaled reference image of the SST aircraft design was imported into OpenVSP to guide the adjustment of wing and fuselage dimensions. The configuration parameters were adjusted to match the dimensions outlined in the paper. This ensured that the model closely resembled the original design while allowing for further aerodynamic analysis.

## 2. Fuselage and Wing Construction

- The fuselage was created using the Fuselage Geom Tool. Cross-sectional dimensions were manually adjusted to closely replicate the SST's geometry.
- The Diamond Airfoil, identified as the optimal airfoil from the selection phase, was applied to the wing. A thickness-to-chord ratio of 5% was maintained.

## 3. Wing Position Variation Analysis

To study the effect of wing location on aerodynamic performance, the wing was systematically repositioned along the fuselage at:

- 0 meters (from nose to wing's leading edge)
- 10 m
- 20 m (original position)
- 35 m
- 50 m

Each wing configuration was saved as a separate model for aerodynamic analysis. The variation of wing positions are shown in [Figure 3.10](#)

## 4. Aerodynamic Analysis

The SST models were evaluated using OpenVSP tools:

### (a) VSPAERO Tool:

- Lift, drag, and pressure distribution coefficients were calculated for each wing location.

### (b) Wave Drag Analysis Tool:

- Wave drag coefficients were analyzed for varying wing positions.

## 5. Data Management and Visualization

The results for each wing position were exported as polar files and analyzed in Google Sheets. Comparative graphs and plots were generated to visualize performance trends.

## 6. Export for CFD Analysis

Once the OpenVSP analysis was complete, the SST models were exported in STL and STEP formats for further analysis in ANSYS Fluent. These exports ensured compatibility with advanced CFD tools.

## 7. Purpose of OpenVSP Analysis

The OpenVSP analysis served as a preliminary step to validate aerodynamic performance and establish baseline metrics. The results were compared with those from the JAXA SST paper and ANSYS Fluent simulations to ensure accuracy and reliability in the findings.

This revised workflow offers a clear and detailed structure of the modeling and analysis performed in OpenVSP, incorporating the evaluation of airfoil performance at multiple Mach numbers and providing robust data for subsequent validation.

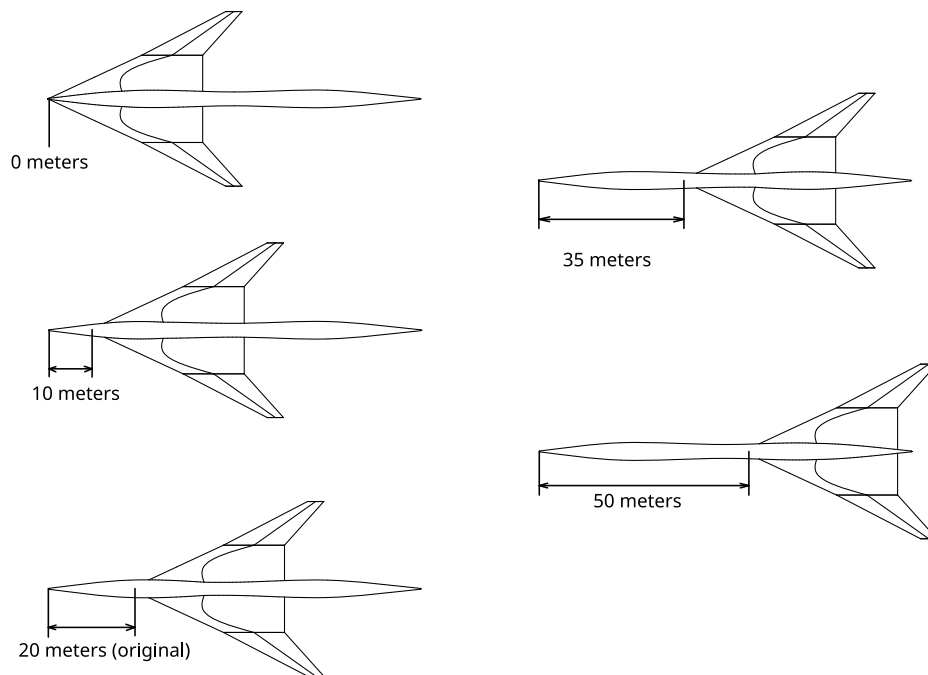


FIGURE 3.10: Wing Position Variation.

## 3.4 Computational Fluid Dynamics Simulation

### 3.4.1 Introduction to ANSYS Fluent

ANSYS Fluent is a Computational Fluid Dynamics (CFD) software widely used in aerospace applications for simulating compressible, high-speed flows. A single simulation environment that supports many analysis systems, component systems, and design exploration tools is one advantage of Fluent's integration within the ANSYS Workbench platform. For extensive simulations, the workbench project schematic is a straightforward tool that provides a clear workflow for managing operations such as geometry creation, meshing, setup, solution, and results [21], [22].

DesignModeler, a parametric modeling tool designed for creating 2D sketches and 3D CAD models, can be used to create the geometry for Fluent simulations. DesignModeler makes it easier to create intricate geometries while maintaining compliance with ANSYS and Fluent. High-quality computational grids are produced using meshing, which gives users control over mesh size and resolution for accurate simulation results [21].

For the analysis of supersonic flows, where shockwave and boundary layer interactions are important, Fluent is a very useful tool because of its strong solvers and advanced turbulence models, including  $k - \omega$  SST. It offers thorough analyses of aerodynamic characteristics, such as pressure distributions, moment coefficients, and lift and drag forces, providing a complete understanding of the airfoil's aerodynamic performance. Fluent is an essential tool for supersonic airfoil research and development because of its post-processing tools, which allow users to view flow fields, create contour plots, and extract aerodynamic performance data [21].

### 3.4.2 Workflow in ANSYS Fluent

The aerodynamic analysis of the supersonic aircraft was conducted using ANSYS Fluent 2024 R2.1 Student Version. The workflow was divided into several key stages, including Geometry Setup, Meshing, Solver Setup, and Post-Processing.

Each step was carefully executed to ensure accurate simulation results while considering the limitations of the student license.

### **Geometry Setup in SpaceClaim**

#### **1. Loading the Geometry:**

- The aircraft model was imported as a .STP file into SpaceClaim within the ANSYS Workbench environment.
- The aircraft was rotated by 5° to set the angle of attack.

#### **2. Creating the Enclosure:**

- A rectangular enclosure was created around the aircraft with the following dimensions:
  - 100 m to the left, right, top, and bottom.
  - 100 m in the front.
  - 300 m at the back (to account for wake effects).

#### **3. Hollow and Symmetry Preparation:**

- The aircraft model was subtracted from the enclosure, creating a hollow space shaped like the aircraft.
- A symmetry plane along the z-axis was used to simulate only half of the enclosure, reducing computational demand.

#### **4. Boundary Naming:**

- Boundary conditions were defined by naming key surfaces: *Inlet* (front surface), *Outlet* (rear surface), *Upper Wall*, *Bottom Wall*, *Left Wall*, *Symmetry Wall*, and *Aircraft Wall*.

#### **5. Body of Influence (BOI):**

- A rectangular BOI was added to refine the mesh around the aircraft. It extended 6 m to fully cover the aircraft geometry.

Click an object. Double-click to select an edge loop. Triple-click to select a solid.

**Ansys**  
2024 R2  
STUDENT

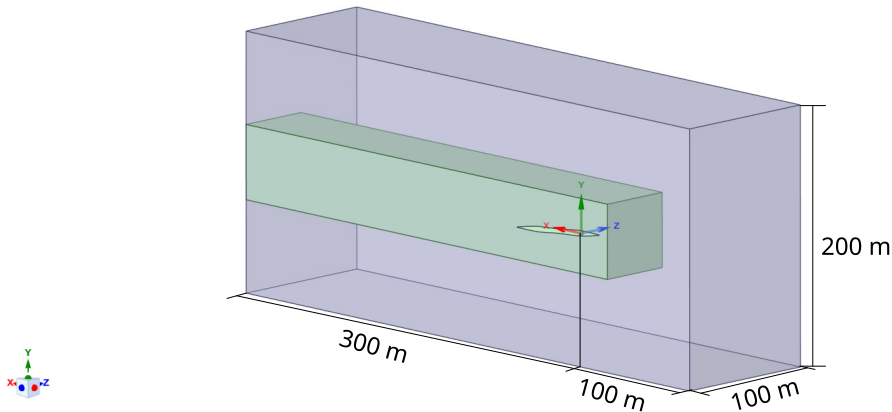


FIGURE 3.11: ANSYS spaceclaim computational domain dimension.

## Meshing

### 1. Importing Geometry:

- The prepared geometry was imported into the Meshing tool in ANSYS Workbench.

### 2. Local Sizing:

- A body of influence (BOI) method was applied for local sizing with a target mesh size of 1.5 m.
- Adjustments to the mesh sizes were made iteratively to ensure the total number of cells remained under the student license limit of 1,048,576 cells.

### 3. Boundary Layer Mesh:

- Three boundary layers were added with a transition ratio of 0.272 and a growth rate of 1.2.

### 4. Volume Mesh:

- A poly-hexcore method was used to generate the volume mesh, optimizing computational efficiency and accuracy.
- Final mesh quality checks confirmed orthogonal quality and cell count compliance.

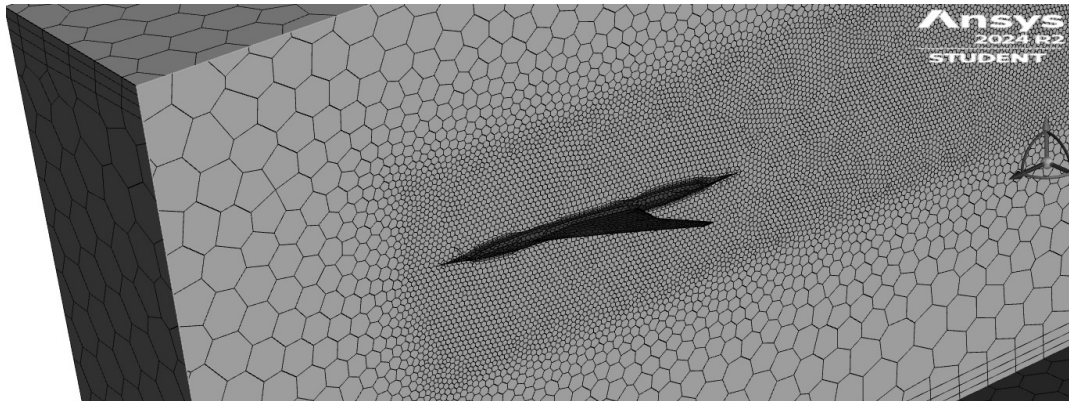


FIGURE 3.12: ANSYS meshes results and topology.

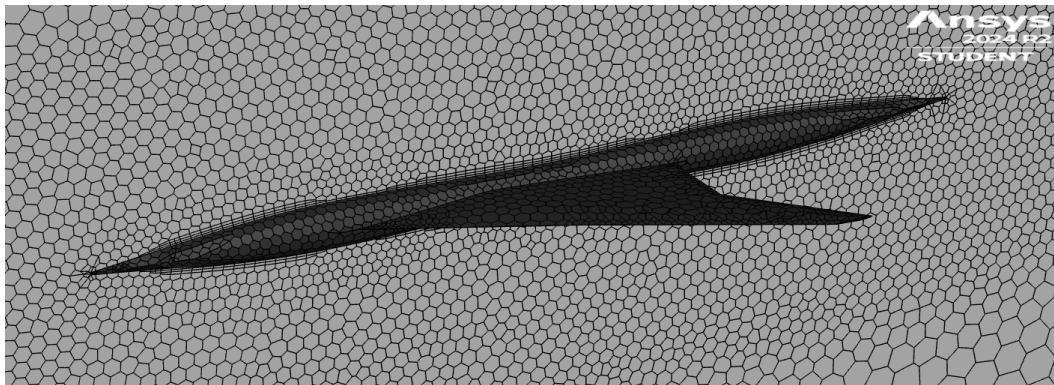


FIGURE 3.13: ANSYS meshes results and topology zoomed.

## Setup and Solution

### 1. General Setup:

- Solver: Density-Based (for compressible flows) with Double Precision.
- Time: Steady-State (for analyzing flow without transient effects).
- Velocity Formulation: Absolute (since dealing with high-speed external aerodynamics)

### 2. Models Selection: Go to Models and ensure the following settings:

- Energy Equation: Enabled to capture compressibility effects.
- Turbulence Model: SST  $k - \omega$  (Shear Stress Transport model for accurate boundary layer resolution).

- Radiation, Heat Exchanger, Species, Discrete Phase, Virtual Blade Model, Acoustics, and Structural Models: All set to Off (not required for this analysis)
3. **Materials Properties:** Define Air with the following properties:
- Density:  $1.225 \text{ kg/m}^3$  (Ideal Gas)
  - Specific Heat:  $1006.43 \text{ J/kg K}$ .
  - Thermal Conductivity:  $0.0242 \text{ W/m K}$ .
  - Viscosity: Sutherland Law
4. **Boundary Conditions:** set up boundary conditions to properly define the computational domain.
- Aircraft Wall
    - Type: Wall
    - Wall Motion: Stationary Wall
    - Shear Condition: No Slip (standard for solid surfaces)
  - Walls (Upper, Bottom, Left)
    - Type: Wall
    - Wall Motion: Stationary Wall
    - Shear Condition: Specified Shear
  - Inlet (Freestream Conditions)
    - Type: Velocity Inlet
    - Velocity Specification Method: Magnitude, Normal to Boundary
    - Reference Frame: Absolute
    - Velocity Magnitude:  $686 \text{ m/s}$  (corresponding to Mach 2)
    - Supersonic/initial Gauge Pressure:  $0 \text{ Pa}$
  - Outlet (Pressure Outlet Conditions)
    - Type: Pressure Outlet
    - Backflow Reference Frame: Absolute
    - Gauge Pressure:  $0 \text{ Pa}$
    - Pressure Profile Multiplier: 1
    - Backflow Direction Specification: Normal to Boundary
    - Backflow Pressure Specification: Total Pressure

- Symmetry Plane
  - Type: Symmetry

5. **Reference Values:** Set reference values based on the inlet conditions to properly normalize aerodynamic coefficients.

- Compute from: Inlet
- Area: 387.852 m<sup>2</sup>
- Density: 1.225 kg/m<sup>3</sup>
- Temperature: 300 K
- Velocity: 686 m/s
- Viscosity:  $1.84618 \times 10^{-5}$  kg/(m s)
- Ratio of Specific Heats: 1.4
- Reference Zone: Enclosure

6. **Solution Methods:**

- Numerical Methods
  - Formulation: Implicit
  - Flux Type: Roe-FDS (Flux-Difference Splitting for better shock resolution)
- Spatial Discretization
  - Gradient: Least Squares Cell-Based.
  - Flow: Second Order Upwind.
  - Turbulent Kinetic Energy: Second Order Upwind.
  - Specific Dissipation Rate: Second Order Upwind.
- Pseudo Time Method
  - Off (since performing a steady-state simulation)

7. **Solution Controls:**

- Courant Number: 5
- turbulent Kinetic Energy: 0.8
- Specific Dissipation: 0.8
- Turbulent Viscosity: 1
- Solid Properties: 1

8. **Report Definitions:** set up live monitoring for key aerodynamic forces:

- Lift Coefficient
  - Report Type: Lift Coefficient
  - Zone: Aircraft
  - Force Vector: (0, 1, 0) (aligned with the lift direction)
- Drag Coefficient
  - Report Type: Drag Coefficient
  - Zone: Aircraft
  - Force Vector: (1, 0, 0) (aligned with the stream wise direction)
- Moment Coefficient
  - Report Type: Moment Coefficient
  - Zone: Aircraft
  - Moment Axis: (0, 0, 1) (around the aircraft's center of gravity)

#### 9. Solution Initialization:

- Initialization Method
  - Standard Initialization
  - Compute from: Inlet
  - Reference Frame: Relative to Cell Zone
- Initial Conditions
  - Gauge Pressure: 0 Pa
  - X Velocity: 686 m/s
  - Y Velocity: 0 m/s
  - Z Velocity: 0 m/s
  - Turbulent Kinetic Energy:  $1764.735 \text{ m}^2/\text{s}^2$ .
  - Specific Dissipation Rate:  $1.201001 \times 10^7 \text{ s}^{-1}$ .
  - Temperature: 300 K

#### 10. Running the Simulation

- Number of iterations: 500 (may increase if convergence is not reached).
- Profile Update Interval: 1
- Reporting Interval: 1

11. **Post-Processing:** once the solution converges, analyze the aerodynamic performance using:

- Aerodynamic Coefficient
  - Extract values for lift, drag, and moment coefficients to evaluate aircraft performance
- Visualization
  - Pressure Contour: Display pressure variations across the aircraft surfaces.
  - Mach Contour: Analyze changes in flow velocity, mach, and shock interactions.

Post-processing involved generating contour plots for pressure, velocity, and Mach number to visualize flow behavior and identify critical aerodynamic features. Additionally, the lift, drag, and moments coefficients were analyzed, and results were exported for further comparison and validation. The ANSYS project schematic is shown in Figure 3.14 and the schematic diagram of the workflow steps is shown in Figure 3.15

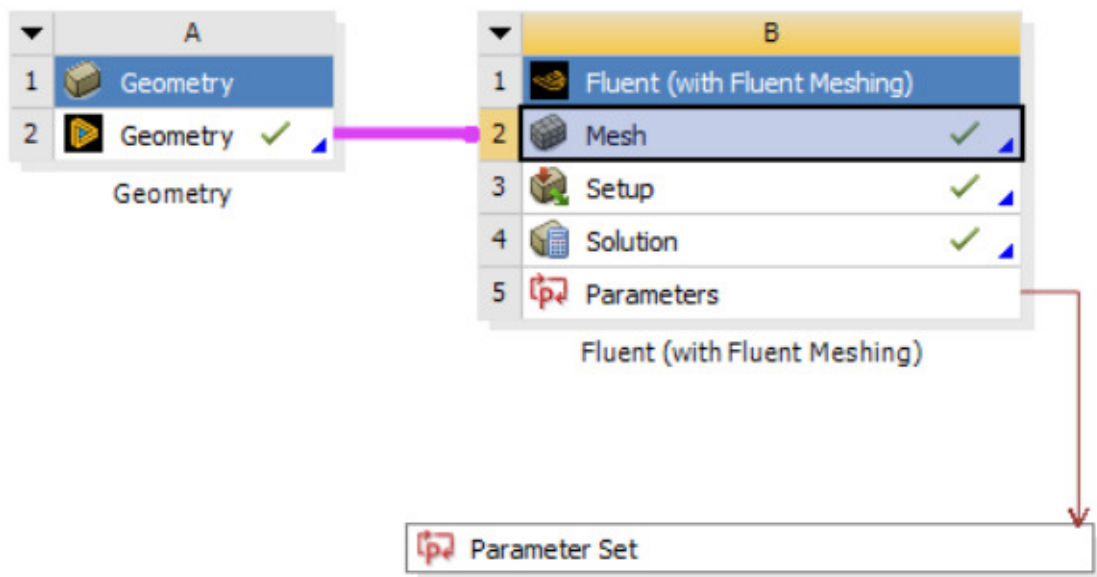


FIGURE 3.14: ANSYS project schematic

EFFECT OF WING LOCATION ON THE AERODYNAMIC PROFILE OF A SUPERSONIC AIRCRAFT  
USING ANSYS FLUENT

---

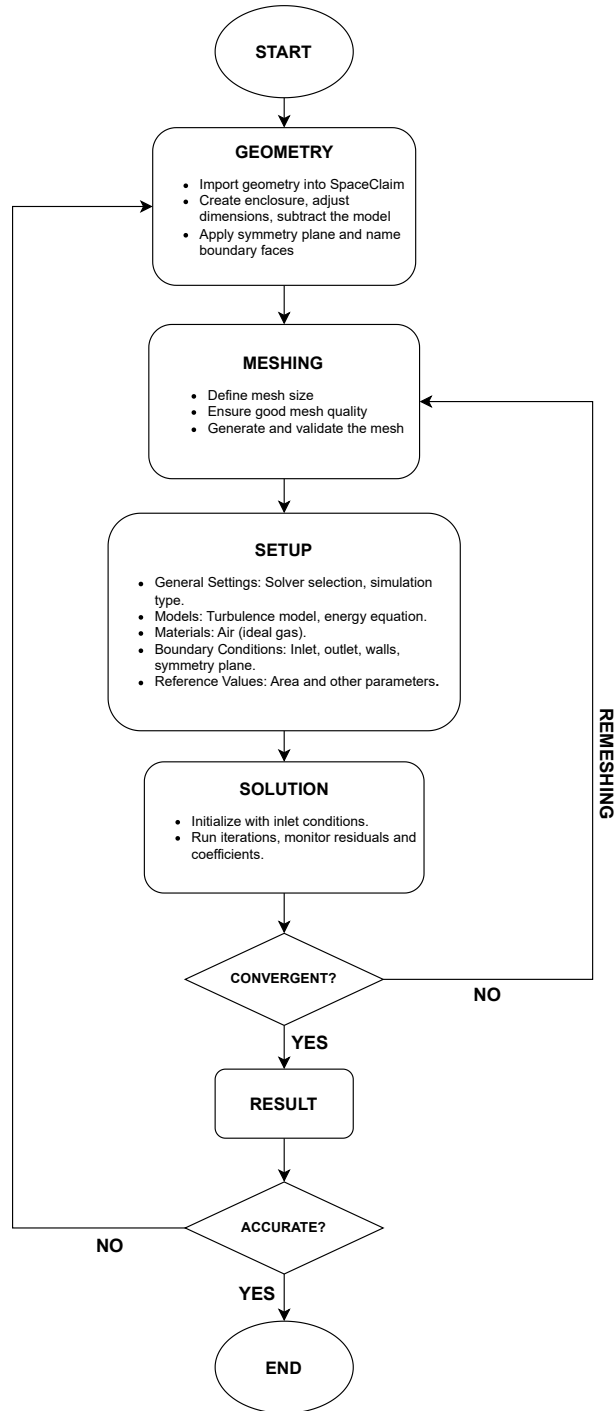


FIGURE 3.15: Schematic Diagram of ANSYS Fluent Workflow

### 3.4.3 Validation of Simulation Process Results

To ensure the accuracy of the computational fluid dynamics simulation conducted in ANSYS Fluent, validation was performed through comparison with OpenVSP results and benchmarking against reference studies [2]. Validation of the simulation process were ensured that the methodology used in ANSYS Fluent followed the best practices for supersonic aerodynamic analysis. These steps provided confidence in the numerical approach despite computational constraints.

#### Comparison with OpenVSP Results

The aerodynamic trends obtained from ANSYS Fluent were compared with the results generated using OpenVSP's solver. OpenVSP provides a first-order approximation of aerodynamic coefficient. To ensure the accuracy of the simulations, results from OpenVSP were first compared with those presented in the reference study [2]. Subsequently, a three-way comparison was conducted between OpenVSP, ANSYS Fluent, and the reference paper, assessing the consistency of key aerodynamic parameters. This approach helped confirm that both numerical simulations aligned closely with established aerodynamic data, reinforcing the reliability of the computational results.

#### Benchmarking Against Reference Studies

To further validate the numerical approach, results were compared with previously published studies on supersonic aircraft aerodynamics, specifically the JAXA SST study [2]. The comparison showed that the variation in the aerodynamic coefficient followed similar trends observed in high-fidelity CFD and experimental studies, with deviations remaining within expected ranges for this class of simulation. The results of lift coefficient and drag coefficients from OpenVSP and ANSYS Fluent were compared with the drag characteristic and lift characteristic of the next generation SST from the JAXA paper as shown in Figure 3.16 and 3.17

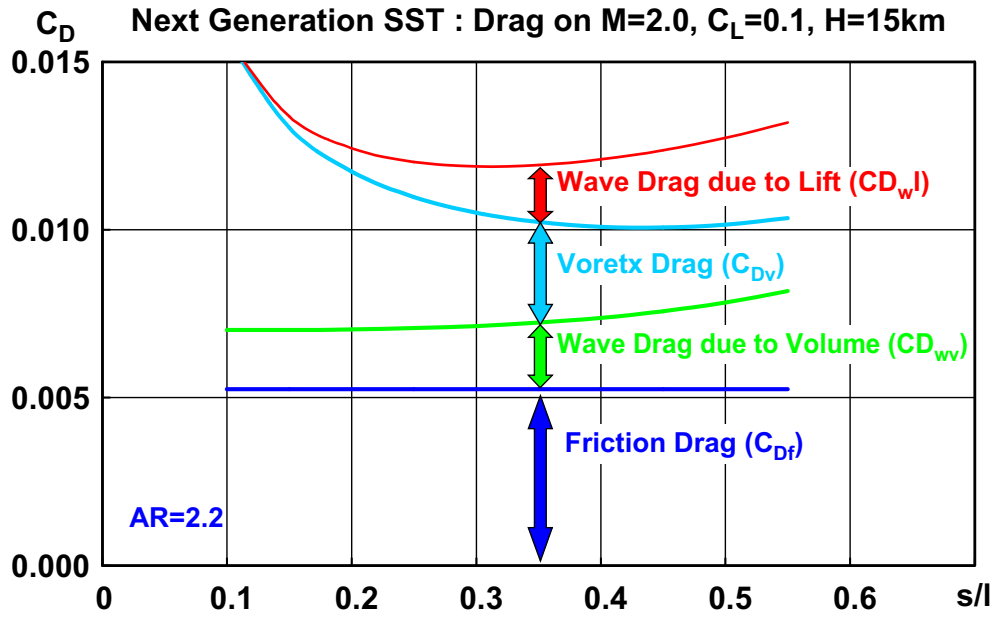


FIGURE 3.16: Drag characteristics of a next generation SST from JAXA paper [2].

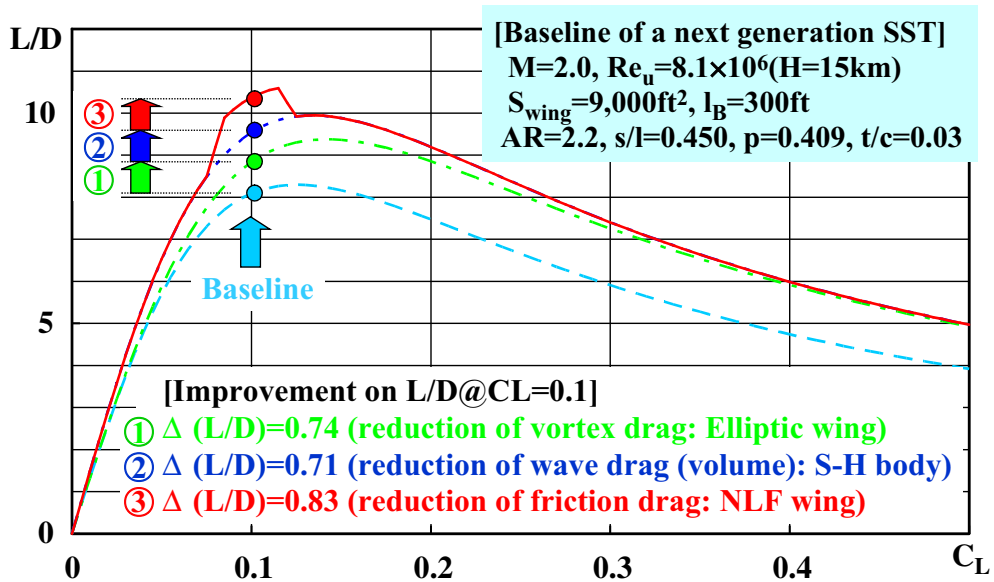


FIGURE 3.17: L/D characteristics of a next generation SST from JAXA paper [2].

### 3.4.4 Computational Hardware and Software Setup

The CFD simulations in this study were conducted using ANSYS Fluent 2024 R2.1 Student Version on a personal computer with the following specifications:

- Processor: 13th Gen Intel Core i7-13620H 2.40 GHz
- RAM: 16 GB
- GPU: NVIDIA GeForce RTX 3050 (4GB GDDR6)
- Operating System: Windows 11 (64-bit)

Due to the limitations of the ANSYS Student Version, the maximum allowable mesh size was restricted, impacting the refinement of computational grids. ANSYS Fluent primarily relies on CPU performance, which influenced the selection of numerical solvers and convergence settings.

The simulations were performed using parallel processing on available CPU cores. Given these hardware constraints, adjustments were made to maintain a reasonable simulation runtime while ensuring meaningful aerodynamic insights.

#### Minimum Hardware Requirements

The minimum hardware requirements for ANSYS Fluent commonly include:

- Processor: a multi-core processor (e.g., Intel Core i5 or equivalent)
- RAM: at least 8 GB RAM
- Graphics Card: a dedicated graphics card with OpenGL support
- Storage: a minimum of 10 GB of free disk space

## CHAPTER 4

### RESULTS AND DISCUSSIONS

In this chapter, the results of simulations using OpenVSP and ANSYS Fluent are presented and analyzed. The aerodynamic performance of the SST aircraft was assessed through various parameters, including lift coefficient ( $C_L$ ), drag coefficient ( $C_D$ ), and moment coefficient ( $C_M$ ). Additionally, detailed contour plots for pressure and Mach number are discussed. The insights gained from these results are interpreted to provide recommendations for supersonic aircraft design.

#### 4.1 Airfoil Selection and Preliminary Analysis

The selection of a suitable airfoil for the SST aircraft was a critical step in the design process. To ensure optimal aerodynamic performance, four candidate airfoils were evaluated: NACA 2412, NACA 0005, Hexagonal Airfoil, and Diamond Airfoil. The evaluation considered key aerodynamic metrics, including lift coefficient ( $C_l$ ), drag coefficient ( $C_d$ ), and moment coefficient ( $C_m$ ), across varying angles of attack (AoA) and Mach numbers (0.6, 1.2, and 2.0). The results of these analyses are summarized and discussed below.

##### 4.1.1 Airfoil Candidates and Comparison

###### NACA 2412

The airfoil demonstrated good lift performance at subsonic speeds (Mach 0.6), particularly at lower angles of attack. However, its thick profile caused a sharp rise in wave drag at supersonic speeds, leading to a poor lift-to-drag ratio ( $\frac{L}{D}$ ).

While the moment coefficient ( $C_m$ ) remained stable at subsonic speeds, significant variability was observed at higher Mach numbers, indicating potential control challenges in supersonic regimes. This variability made it unsuitable for consistent supersonic applications.

### **NACA 0005**

The NACA 0005 airfoil performed consistently across all Mach numbers, with modest lift generation. Its thin profile helped to maintain relatively low drag coefficients, particularly at supersonic speeds. However, its lift coefficients were lower than those of the Diamond Airfoil, limiting its effectiveness for applications requiring high aerodynamic loads. The moment coefficient remained stable, suggesting good control characteristics but insufficient overall performance for supersonic flight.

### **Hexagonal Airfoil**

The Hexagonal Airfoil displayed performance characteristics similar to the NACA 0005, with moderate lift and drag values. Its angular design contributed to slightly higher wave drag at supersonic speeds, but the differences were not substantial. Stability, as reflected by the moment coefficient, was generally acceptable, though minor fluctuations at higher AoA indicated potential control issues during extreme maneuvers.

### **Diamond Airfoil**

Among the candidates, the Diamond Airfoil provided the best overall performance. At Mach 0.6, it achieved slightly higher lift coefficients compared to the Hexagonal and NACA 0005 airfoils. At Mach 1.2 and 2.0, its sharp leading edge minimized wave drag effectively, resulting in the lowest drag coefficients among all profiles. Its lift-to-drag ratio ( $\frac{L}{D}$ ) was consistently superior, making it the most efficient airfoil for both subsonic and supersonic regimes. The moment coefficient was stable across all conditions, ensuring reliable handling and control.

## 4.1.2 Airfoil Aerodynamic Characteristics Analysis

The aerodynamic characteristics analysis evaluates the performance of four airfoil configurations, NACA 2412, NACA 0005, Hexagonal, and Diamond, at different angles of attack (AoA) and Mach numbers (0.6, 1.2, and 2.0). The results were obtained using OpenVSP, focusing on lift coefficient ( $C_l$ ), drag coefficient ( $C_d$ ), and moment coefficient ( $C_m$ ), shown in Figure 4.1, 4.2, and 4.3, and Table 4.1, 4.2, and 4.3.

**Lift Coefficient ( $C_l$ )** The lift coefficient ( $C_l$ ) varies with AoA, revealing significant differences in performance across airfoil configurations:

- **NACA 2412:** At Mach 0.6, this airfoil exhibits high lift coefficients, achieving a peak of  $C_l = 0.2757$  at AoA  $10^\circ$ . However, its performance diminishes at Mach 1.2 and Mach 2.0, where shockwave formation negatively impacts its lift generation.
- **NACA 0005:** The symmetric profile produces consistent lift coefficients across all Mach numbers. At Mach 2.0,  $C_l$  peaks at 0.1428 for AoA  $10^\circ$ , demonstrating moderate lift capabilities compared to other configurations.
- **Hexagonal Airfoil:** This configuration performs similarly to NACA 0005, with slightly improved lift coefficients at higher Mach numbers. At Mach 2.0 and  $10^\circ$ ,  $C_l$  reaches 0.1437.
- **Diamond Airfoil:** The Diamond Airfoil consistently outperforms other profiles in generating lift at all Mach numbers. At Mach 2.0,  $C_l$  peaks at 0.1426 for AoA  $10^\circ$ , indicating excellent lift characteristics in supersonic regimes.

**Drag Coefficient ( $C_d$ )** The drag coefficient ( $C_d$ ) analysis reveals the efficiency of each airfoil in minimizing aerodynamic resistance:

- **NACA 2412:** At Mach 0.6,  $C_d$  is relatively low (0.0260 at  $10^\circ$ ), but it increases significantly at higher Mach numbers due to shockwave-induced drag.
- **NACA 0005:** This airfoil maintains low drag coefficients, particularly at Mach 1.2 and 2.0, where  $C_d$  values are around 0.056 and 0.028, respectively, at  $10^\circ$ .

- **Hexagonal Airfoil:** Drag characteristics are slightly higher than those of the Diamond Airfoil but remain competitive. At Mach 2.0,  $C_d$  is approximately 0.0279 at  $10^\circ$ .
- **Diamond Airfoil:** The Diamond Airfoil consistently records the lowest drag coefficients at all Mach numbers. At Mach 2.0 and  $10^\circ$ ,  $C_d = 0.0277$ , confirming its aerodynamic efficiency.

**Moment Coefficient ( $C_m$ )** The moment coefficient ( $C_m$ ) indicates stability and control characteristics:

- **NACA 2412:** Exhibits unstable  $C_m$  trends, particularly at higher Mach numbers and AoA. At Mach 2.0 and  $10^\circ$ ,  $C_m$  is  $-0.0633$ , suggesting control challenges.
- **NACA 0005:** Displays stable  $C_m$  values across all conditions. At Mach 2.0,  $C_m$  is approximately  $-0.0176$  at  $10^\circ$ , indicating consistent control characteristics.
- **Hexagonal Airfoil:** Moment coefficients show slight fluctuations, but overall stability is maintained. At Mach 2.0,  $C_m = 0.0312$  at  $10^\circ$ .
- **Diamond Airfoil:** The Diamond Airfoil provides the most stable  $C_m$  trends, with minimal variations. At Mach 2.0 and  $10^\circ$ ,  $C_m$  is 0.0311, ensuring excellent stability and control.

**Summary of Aerodynamic Performance** The results emphasize the superior aerodynamic performance of the Diamond Airfoil across all metrics, particularly in supersonic regimes. Its high  $C_l$ -to- $C_d$  ratio and stable  $C_m$  trends make it the most efficient and controllable airfoil among the configurations analyzed. Conversely, the NACA 2412 airfoil underperforms at higher Mach numbers, highlighting its unsuitability for supersonic applications.

EFFECT OF WING LOCATION ON THE AERODYNAMIC PROFILE OF A SUPERSONIC AIRCRAFT  
 USING ANSYS FLUENT

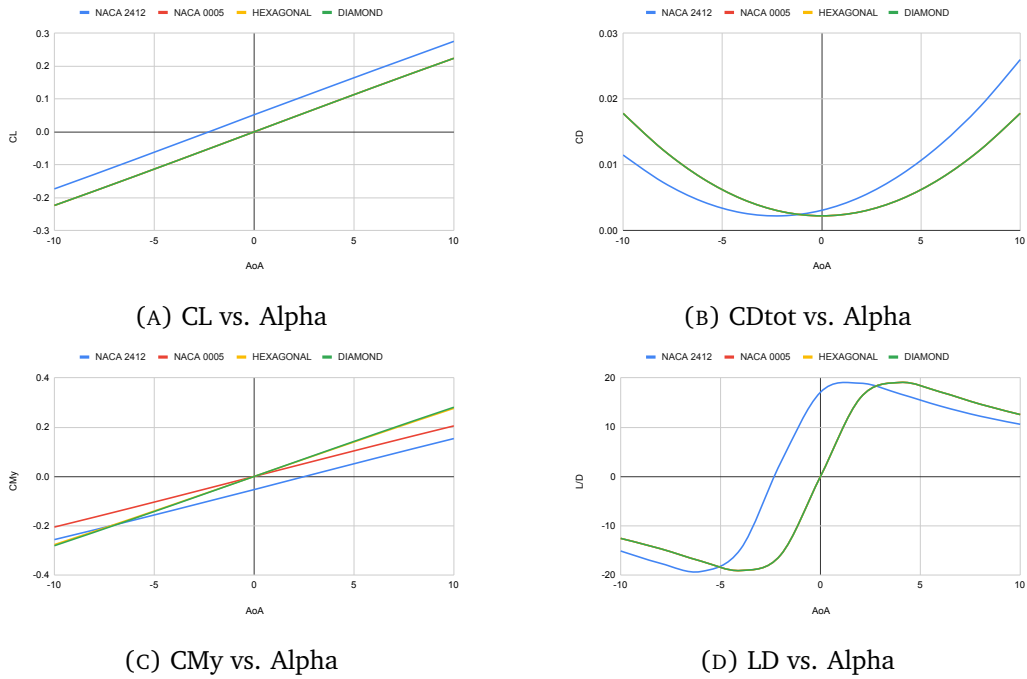


FIGURE 4.1: Airfoil Aerodynamic Characteristics at Mach 0.6

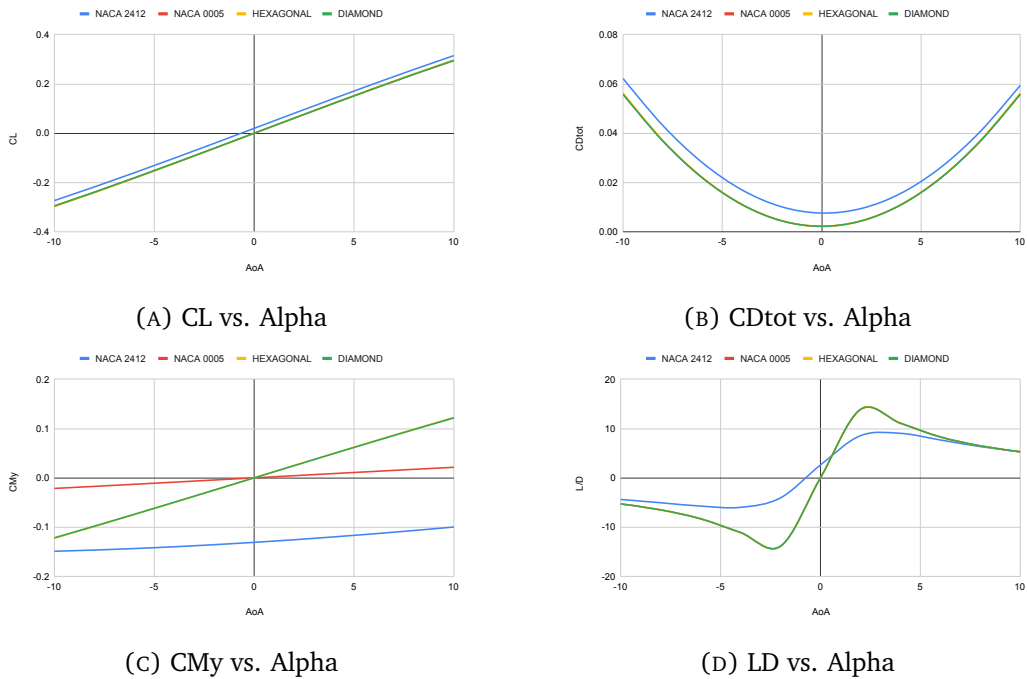
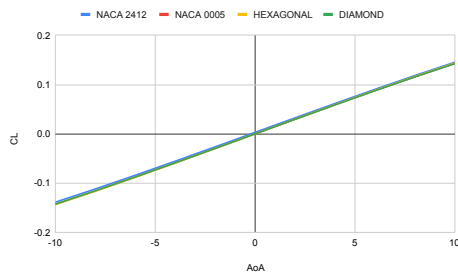


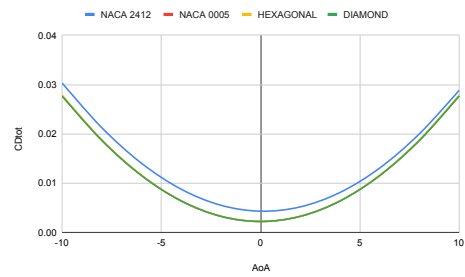
FIGURE 4.2: Airfoil Aerodynamic Characteristics at Mach 1.2

EFFECT OF WING LOCATION ON THE AERODYNAMIC PROFILE OF A SUPERSONIC AIRCRAFT  
 USING ANSYS FLUENT

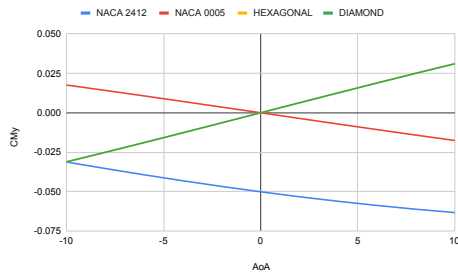
---



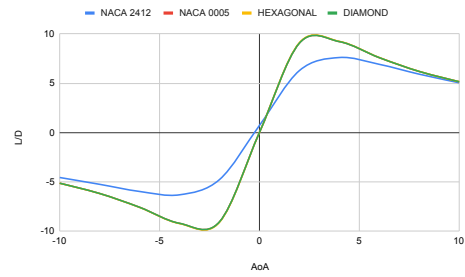
(A) CL vs. Alpha



(B) CDtot vs. Alpha



(C) CM\_y vs. Alpha



(D) LD vs. Alpha

FIGURE 4.3: Airfoil Aerodynamic Characteristics at Mach 2.0

EFFECT OF WING LOCATION ON THE AERODYNAMIC PROFILE OF A SUPERSONIC AIRCRAFT  
USING ANSYS FLUENT

---

TABLE 4.1: Airfoils Aerodynamic Parameters at Mach 0.6

AoA	NACA 2412	NACA 0005	HEXAGONAL	DIAMOND
$C_l$				
-10	-0.1736	-0.2240	-0.2241	-0.2240
-8	-0.1295	-0.1803	-0.1803	-0.1803
-6	-0.0847	-0.1359	-0.1359	-0.1359
-4	-0.0393	-0.0909	-0.0909	-0.0909
-2	0.0061	-0.0455	-0.0456	-0.0455
0	0.0522	0.0000	0.0000	0.0000
2	0.0972	0.0455	0.0456	0.0455
4	0.1423	0.0909	0.0909	0.0909
6	0.1871	0.1359	0.1359	0.1359
8	0.2313	0.1803	0.1803	0.1803
10	0.2757	0.2240	0.2241	0.2240
$C_d$				
-10	0.0115	0.0178	0.0178	0.0178
-8	0.0073	0.0123	0.0123	0.0123
-6	0.0044	0.0079	0.0079	0.0079
-4	0.0027	0.0048	0.0048	0.0048
-2	0.0022	0.0029	0.0029	0.0029
0	0.0031	0.0022	0.0022	0.0022
2	0.0051	0.0029	0.0029	0.0029
4	0.0085	0.0048	0.0048	0.0048
6	0.0131	0.0079	0.0079	0.0079
8	0.0189	0.0123	0.0123	0.0123
10	0.0260	0.0178	0.0178	0.0178
$C_{m_y}$				
-10	-0.2563	-0.2054	-0.2767	-0.2811
-8	-0.2169	-0.1653	-0.2227	-0.2263
-6	-0.1767	-0.1246	-0.1679	-0.1706
-4	-0.1359	-0.0833	-0.1123	-0.1141
-2	-0.0945	-0.0417	-0.0562	-0.0571
0	-0.0533	0.0000	0.0000	0.0000
2	-0.0112	0.0417	0.0562	0.0571
4	0.0308	0.0833	0.1123	0.1141
6	0.0724	0.1246	0.1679	0.1706
8	0.1135	0.1653	0.2227	0.2263
10	0.1540	0.2054	0.2767	0.2811

EFFECT OF WING LOCATION ON THE AERODYNAMIC PROFILE OF A SUPERSONIC AIRCRAFT  
USING ANSYS FLUENT

---

TABLE 4.2: Airfoils Aerodynamic Parameters at Mach 1.2

AoA	NACA 2412	NACA 0005	HEXAGONAL	DIAMOND
$C_l$				
-10	-0.2733	-0.2956	-0.2976	-0.2952
-8	-0.2180	-0.2396	-0.2413	-0.2393
-6	-0.1605	-0.1816	-0.1828	-0.1813
-4	-0.1013	-0.1219	-0.1228	-0.1218
-2	-0.0410	-0.0612	-0.0617	-0.0612
0	0.0199	0.0000	0.0000	0.0000
2	0.0809	0.0612	0.0617	0.0612
4	0.1414	0.1219	0.1228	0.1218
6	0.2010	0.1816	0.1828	0.1813
8	0.2591	0.2396	0.2413	0.2393
10	0.3152	0.2956	0.2976	0.2952
$C_d$				
-10	0.0622	0.0559	0.0563	0.0558
-8	0.0431	0.0369	0.0371	0.0368
-6	0.0280	0.0218	0.0220	0.0218
-4	0.0169	0.0110	0.0110	0.0110
-2	0.0101	0.0044	0.0044	0.0044
0	0.0076	0.0022	0.0022	0.0022
2	0.0094	0.0044	0.0044	0.0044
4	0.0156	0.0110	0.0110	0.0110
6	0.0261	0.0218	0.0220	0.0218
8	0.0408	0.0369	0.0371	0.0368
10	0.0594	0.0559	0.0563	0.0558
$C_{m_y}$				
-10	-0.1490	-0.0215	-0.1227	-0.1216
-8	-0.1466	-0.0173	-0.0989	-0.0980
-6	-0.1436	-0.0130	-0.0746	-0.0739
-4	-0.1399	-0.0087	-0.0499	-0.0495
-2	-0.1357	-0.0044	-0.0250	-0.0248
0	-0.1310	0.0000	0.0000	0.0000
2	-0.1257	0.0044	0.0250	0.0248
4	-0.1198	0.0087	0.0499	0.0495
6	-0.1136	0.0130	0.0746	0.0739
8	-0.1069	0.0173	0.0989	0.0980
10	-0.0998	0.0215	0.1227	0.1216

EFFECT OF WING LOCATION ON THE AERODYNAMIC PROFILE OF A SUPERSONIC AIRCRAFT  
USING ANSYS FLUENT

---

TABLE 4.3: Airfoils Aerodynamic Parameters at Mach 2.0

AoA	NACA 2412	NACA 0005	HEXAGONAL	DIAMOND
$C_l$				
-10	-0.1386	-0.1428	-0.1437	-0.1426
-8	-0.1118	-0.1158	-0.1165	-0.1156
-6	-0.0840	-0.0877	-0.0882	-0.0876
-4	-0.0554	-0.0589	-0.0593	-0.0588
-2	-0.0263	-0.0296	-0.0298	-0.0295
0	0.0031	0.0000	0.0000	0.0000
2	0.0325	0.0296	0.0298	0.0295
4	0.0617	0.0589	0.0593	0.0588
6	0.0904	0.0877	0.0882	0.0876
8	0.1185	0.1158	0.1165	0.1156
10	0.1455	0.1428	0.1437	0.1426
$C_d$				
-10	0.0303	0.0277	0.0279	0.0277
-8	0.0212	0.0187	0.0188	0.0187
-6	0.0140	0.0115	0.0116	0.0115
-4	0.0088	0.0064	0.0064	0.0064
-2	0.0055	0.0033	0.0033	0.0033
0	0.0043	0.0022	0.0022	0.0022
2	0.0052	0.0033	0.0033	0.0033
4	0.0081	0.0064	0.0064	0.0064
6	0.0131	0.0115	0.0116	0.0115
8	0.0200	0.0187	0.0188	0.0187
10	0.0288	0.0277	0.0279	0.0277
$C_{m_y}$				
-10	-0.0313	0.0176	-0.0312	-0.0311
-8	-0.0354	0.0142	-0.0251	-0.0251
-6	-0.0394	0.0107	-0.0190	-0.0189
-4	-0.0432	0.0072	-0.0127	-0.0127
-2	-0.0467	0.0036	-0.0064	-0.0063
0	-0.0501	0.0000	0.0000	0.0000
2	-0.0533	-0.0036	0.0064	0.0063
4	-0.0562	-0.0072	0.0127	0.0127
6	-0.0588	-0.0107	0.0190	0.0189
8	-0.0612	-0.0142	0.0251	0.0251
10	-0.0633	-0.0176	0.0312	0.0311

### 4.1.3 Wave Drag Analysis

Wave drag is a critical component of the total drag experienced by an airfoil, particularly at supersonic speeds. This section analyzes the wave drag coefficients  $C_{D_{0w}}$  for four airfoil configurations, NACA 2412, NACA 0005, Hexagonal, and Diamond, at Mach numbers of 1.2 and 2.0, as presented in Table 4.4.

- **NACA 2412 Airfoil:**
  - At Mach 1.2, the  $C_{D_{0w}}$  is the highest among all airfoils at 0.4874, reflecting its unsuitability for supersonic flight due to substantial shock-wave formation and inefficient aerodynamic design.
  - At Mach 2.0, the  $C_{D_{0w}}$  decreases slightly to 0.3869, but it remains significantly higher than the other airfoils, indicating persistent drag issues at higher supersonic speeds.
- **NACA 0005 Airfoil:**
  - This symmetric airfoil demonstrates much lower  $C_{D_{0w}}$  values than NACA 2412, with 0.094 at Mach 1.2 and 0.0656 at Mach 2.0.
  - The reduced drag can be attributed to its streamlined design, which minimizes shockwave intensity compared to the cambered NACA 2412.
- **Hexagonal Airfoil:**
  - The hexagonal airfoil exhibits an even lower wave drag, with values of 0.056 at Mach 1.2 and 0.0447 at Mach 2.0.
  - These results suggest that its blunt but symmetric geometry is more optimized for supersonic regimes, effectively reducing the formation of strong shockwaves.
- **Diamond Airfoil:**
  - The diamond airfoil achieves the lowest  $C_{D_{0w}}$  values among all configurations, with 0.0175 at Mach 1.2 and 0.010 at Mach 2.0.
  - This significant reduction in wave drag is consistent with its supersonic-optimized geometry, where sharp leading and trailing edges minimize the formation of shockwaves and ensure smooth airflow expansion.

**Implications of the Results** The results highlight the aerodynamic superiority of the diamond airfoil for supersonic applications. Its minimal wave drag makes it the most efficient choice, particularly in high-speed regimes, as it substantially reduces energy losses caused by shockwaves. In contrast, the high  $C_{D_{0w}}$  values of the NACA 2412 airfoil demonstrate its unsuitability for supersonic aircraft, emphasizing the importance of selecting or designing airfoils specifically tailored for such flight conditions.

**Conclusion** The wave drag analysis confirms the critical role of airfoil geometry in determining aerodynamic efficiency at supersonic speeds. Among the analyzed airfoils, the diamond airfoil is the most aerodynamically efficient, followed by the hexagonal and NACA 0005 airfoils. The NACA 2412 airfoil, on the other hand, exhibits poor performance, underlining the need for supersonic-optimized designs in high-speed applications.

TABLE 4.4: Airfoils  $C_{D_{0w}}$  Values at Different Mach Numbers

	NACA 2412	NACA 0005	HEXAGONAL	DIAMOND
$C_{D_{0w}}$ at Mach 1.2	0.4874	0.094	0.056	0.0175
$C_{D_{0w}}$ at Mach 2.0	0.3869	0.0656	0.0447	0.010

#### 4.1.4 Selection of the Diamond Airfoil

##### Selection of the Diamond Airfoil

The selection of the Diamond Airfoil as the optimal choice for supersonic flight was based on a comprehensive evaluation of its aerodynamic performance compared to other candidates, NACA 2412, NACA 0005, and Hexagonal Airfoil. The decision was supported by detailed analysis across critical metrics, including lift coefficient ( $C_l$ ), drag coefficient ( $C_d$ ), and moment coefficient ( $C_m$ ) at various angles of attack (AoA) and Mach numbers (0.6, 1.2, and 2.0).

**1. Superior Lift-to-Drag Ratio ( $\frac{L}{D}$ )** The Diamond Airfoil consistently demonstrated the highest lift-to-drag ratio across all flight regimes:

- At Mach 0.6, its sharp geometry allowed for effective airflow management, achieving a higher  $\frac{L}{D}$  compared to NACA 0005 and Hexagonal Airfoil.
- At Mach 1.2 and 2.0, the airfoil's supersonic-optimized design significantly minimized wave drag, maintaining high aerodynamic efficiency. In contrast, the NACA 2412 suffered from substantial drag penalties, resulting in poor  $\frac{L}{D}$  performance.

**2. Reduced Drag Coefficient ( $C_d$ )** The drag characteristics of the Diamond Airfoil were unmatched among the four candidates:

- At Mach 2.0, its  $C_d$  was the lowest, recorded at 0.0277 at  $10^\circ$ , owing to its sharp leading and trailing edges, which efficiently managed shockwave formation.
- The Hexagonal and NACA 0005 airfoils also exhibited low drag coefficients, but they were consistently higher than the Diamond Airfoil, particularly at higher Mach numbers.

**3. Compatibility with Supersonic Flow Conditions** The Diamond Airfoil's geometry is specifically tailored for supersonic regimes:

- Its thin profile and sharp edges effectively reduce wave drag by minimizing shockwave strength and optimizing pressure distribution.
- In comparison, the NACA 2412's thicker profile caused significant shockwave formation, resulting in higher drag and instability in supersonic conditions.

**4. Overall Aerodynamic Performance** The Diamond Airfoil emerged as the most efficient and stable option, with consistently superior performance in all analyzed parameters. Its design achieves an optimal balance of lift, drag, and stability, making it the best candidate for supersonic applications. The Hexagonal and NACA 0005 airfoils, while competitive, failed to match the Diamond Airfoil's combination of low drag and high stability. The NACA 2412, tailored for subsonic

applications, was deemed unsuitable for supersonic flight due to its high drag and poor stability.

**Conclusion** The Diamond Airfoil was selected for its unparalleled performance in supersonic regimes, offering significant advantages in aerodynamic efficiency and stability. Its ability to maintain a high  $\frac{L}{D}$ , minimal wave drag, and excellent control characteristics solidifies its position as the optimal choice for the design of supersonic aircraft wings.

## 4.2 OpenVSP Results for the SST Aircraft

This section provides a detailed analysis of the aerodynamic performance of the SST aircraft based on simulations conducted in OpenVSP. The results focus on the lift coefficient ( $C_L$ ), drag coefficient ( $C_D$ ), moment coefficient ( $C_M$ ), and wave drag coefficient ( $C_{D_{0w}}$ ) for three wing locations: the original position (20 meters from the nose), 35 meters aft, and 50 meters aft. Comparisons are drawn to highlight the effects of wing placement on overall aircraft performance.

### 4.2.1 Baseline Wing Location (20 meters from the nose)

The original wing placement at 20 meters, shown in Figure 4.4 served as the baseline configuration for comparison. The aerodynamic performance showed stable lift generation with predictable increases in  $C_L$  as the angle of attack increased.  $C_D$  values exhibited moderate growth with AoA, maintaining efficient aerodynamic flow. The  $C_M$  trends indicated stable control characteristics, essential for reliable handling. The aerodynamics characteristics are shown in Figure 4.5

Wave drag was minimal in this configuration, demonstrating effective shock-wave alignment. Parasite drag remained low, reflecting the streamlined nature of the Diamond Airfoil. The aerodynamic efficiency of this configuration ensured an optimal balance between lift generation and drag resistance, making it a reliable reference point for comparison with alternative wing locations.

EFFECT OF WING LOCATION ON THE AERODYNAMIC PROFILE OF A SUPERSONIC AIRCRAFT  
USING ANSYS FLUENT

---

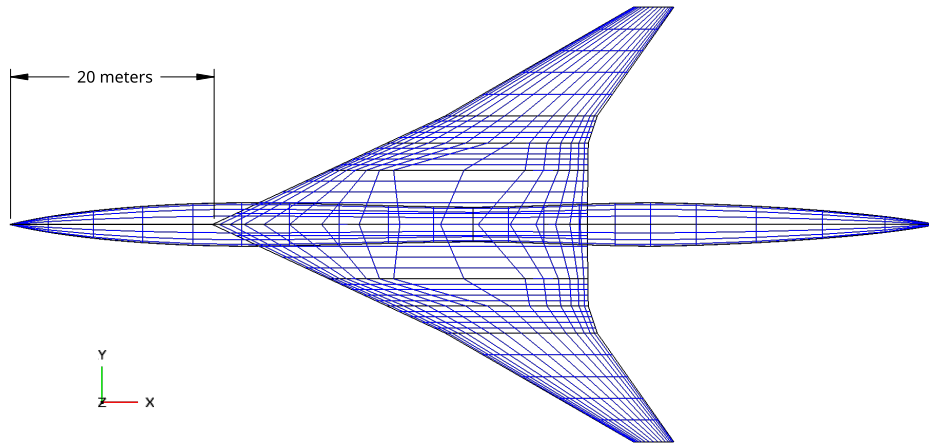


FIGURE 4.4: 20 meters Wing Location OpenVSP Model

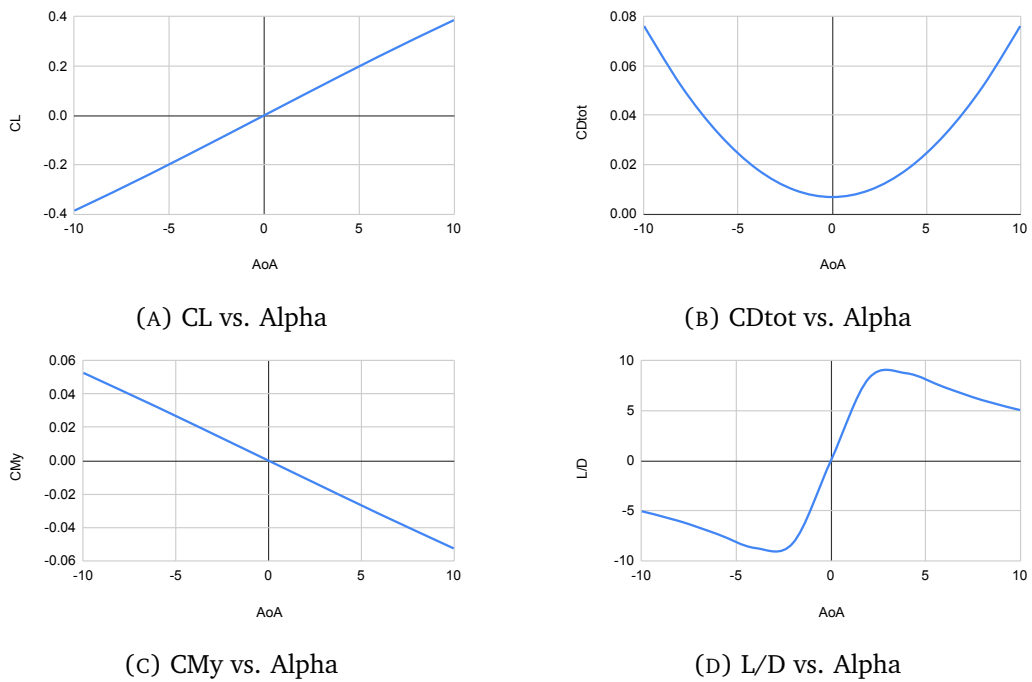


FIGURE 4.5: Aerodynamic Characteristics of Wing Location at 20 m  
at Mach 2.0

### 4.2.2 Wing Location at 35 meters Aft

When the wing was moved 35 meters aft, there were noticeable changes in aerodynamic behavior. Lift generation decreased slightly, suggesting reduced efficiency in airflow over the wing. The aerodynamic drag experienced a slight increase compared to the baseline configuration, which could be attributed to minor disruptions in flow patterns caused by the aft placement. The wing model at 35 meters aft is shown in Figure 4.6 and the aerodynamic characteristics are shown in Figure 4.7

The moment coefficient displayed higher pitching moments, reflecting reduced stability compared to the baseline. Wave drag increased marginally, indicating less efficient shockwave alignment in this configuration. Parasite drag was slightly elevated, further adding to the aerodynamic resistance. Despite these issues, the configuration retained acceptable performance metrics, though it was slightly less efficient than the baseline.

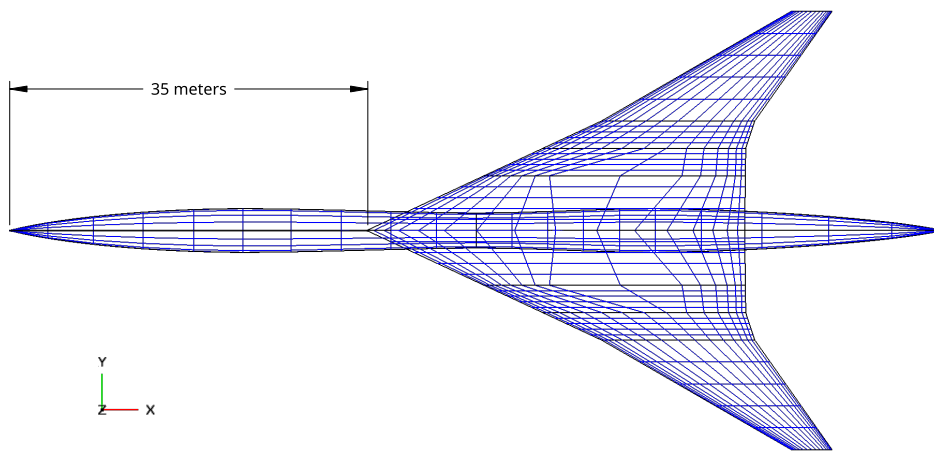


FIGURE 4.6: 35 meters Wing Location OpenVSP Model

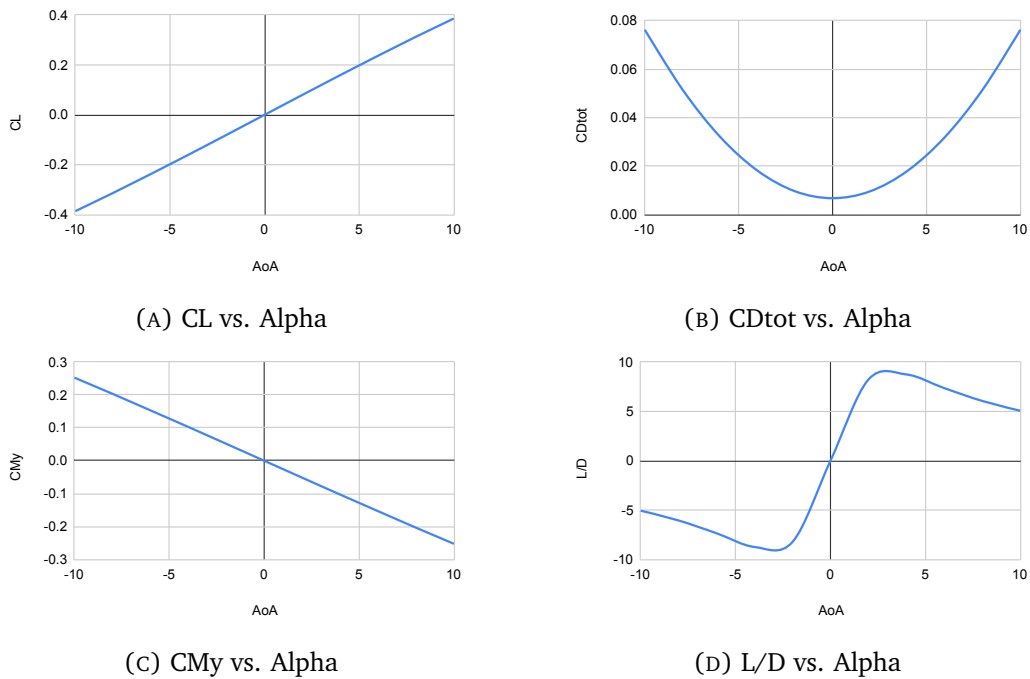


FIGURE 4.7: Aerodynamic Characteristics of Wing Location at 35 m at Mach 2.0

### 4.2.3 Wing Location at 50 meters Aft

The furthest aft wing placement, 50 meters from the nose (shown in Figure 4.8), exhibited the most significant deviations in performance. Lift generation continued to decline, indicating reduced aerodynamic efficiency. Drag remained high, consistent with the 35-meter configuration, highlighting persistent inefficiencies in flow management. Moment coefficients reflected substantial stability concerns, with increased pitching moments indicating a higher likelihood of control issues. The aerodynamic characteristics are shown in Figure 4.9

Wave drag reached its highest values, demonstrating poor shockwave alignment and increased resistance at supersonic speeds. Parasite drag also increased, compounding the aerodynamic inefficiencies. This configuration, while still operationally feasible, exhibited the greatest compromise in terms of lift, drag, and stability, rendering it the least favorable among the three placements.

EFFECT OF WING LOCATION ON THE AERODYNAMIC PROFILE OF A SUPERSONIC AIRCRAFT  
USING ANSYS FLUENT

---

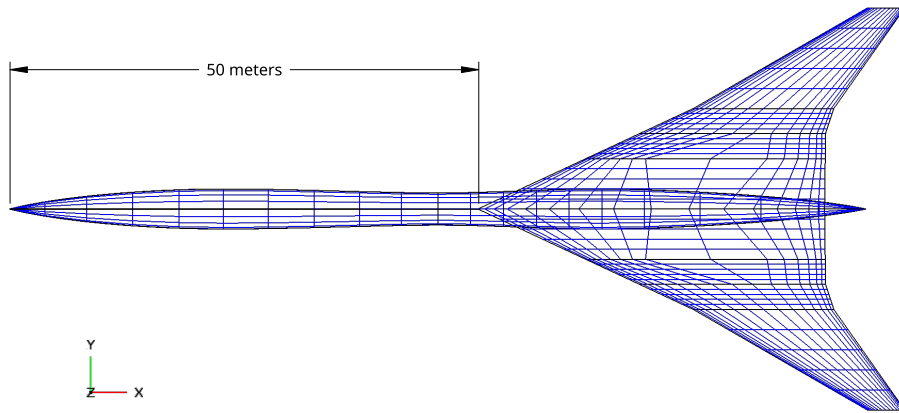


FIGURE 4.8: 50 meters Wing Location OpenVSP Model

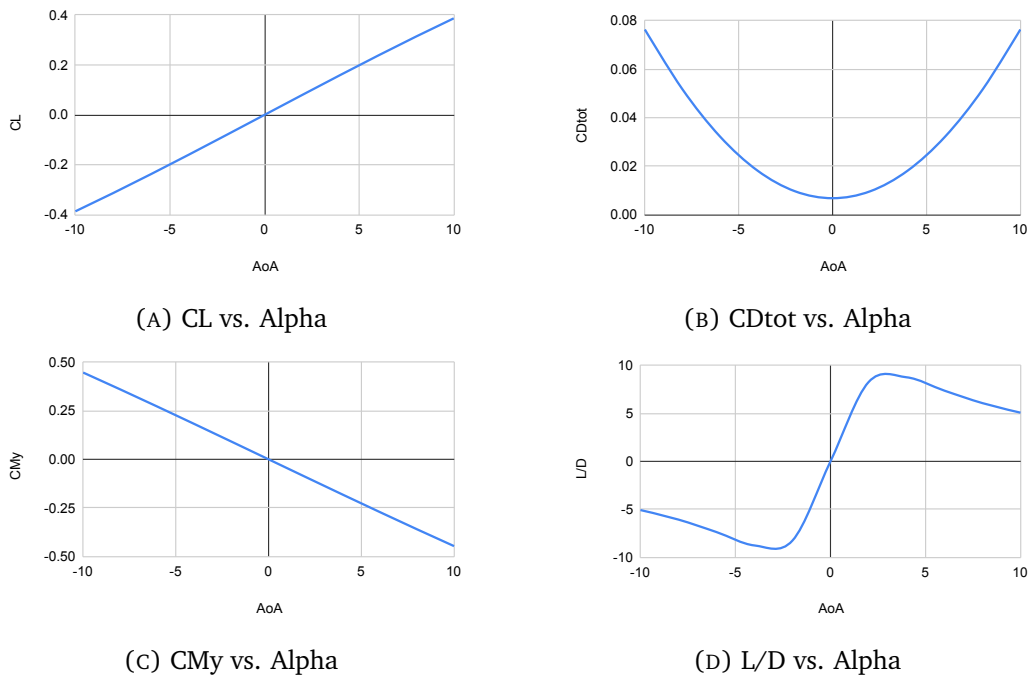


FIGURE 4.9: Aerodynamic Characteristics of Wing Location at 50 m  
at Mach 2.0

#### 4.2.4 Comparative Analysis of Wing Locations

The aerodynamic performance of the supersonic aircraft was analyzed for three wing locations, 20 meters, 35 meters, and 50 meters from the nose. The evaluation focused on the lift coefficient ( $C_L$ ), drag coefficient ( $C_D$ ), moment coefficient ( $C_M$ ), and wave drag coefficient ( $C_{D_{0w}}$ ). The results provide insights into how wing placement impacts overall aerodynamic efficiency and stability. The aerodynamic parameters for different wing locations are shown in Table 4.5

**Lift Coefficient ( $C_L$ )** The lift coefficient values for the three wing locations were nearly identical across all angles of attack, with only minor variations:

- At AoA  $10^\circ$ ,  $C_L$  values were:
  - 20 meters:  $C_L = 0.3865$
  - 35 meters:  $C_L = 0.3861$
  - 50 meters:  $C_L = 0.3868$
- Although the differences were small, the slightly higher  $C_L$  at 50 meters suggests marginally improved lift generation at aft locations. However, the stability implications of these placements must also be considered.

**Drag Coefficient ( $C_D$ )** The drag coefficient remained consistent across the three wing locations, with minor differences:

- At AoA  $10^\circ$ ,  $C_D$  values were:
  - 20 meters:  $C_D = 0.0762$
  - 35 meters:  $C_D = 0.0762$
  - 50 meters:  $C_D = 0.0763$
- The results indicate minimal drag variation between wing locations, with the forward position (20 meters) slightly outperforming the aft locations.

**Moment Coefficient ( $C_M$ )** The moment coefficient ( $C_M$ ) demonstrated significant differences across wing locations, particularly at higher AoA:

- At AoA  $10^\circ$ ,  $C_M$  values were:
  - 20 meters:  $C_M = -0.0528$

- 35 meters:  $C_M = -0.2528$
- 50 meters:  $C_M = -0.4464$
- The aft wing locations (35 and 50 meters) exhibited larger negative  $C_M$ , indicating reduced stability compared to the baseline position (20 meters). The increase in pitching moments for aft placements may lead to control challenges during flight.

**Wave Drag Coefficient ( $C_{D_{0w}}$ )** Wave drag values ( $C_{D_{0w}}$ ), shown in Table 4.6, were calculated to evaluate the efficiency of each configuration in minimizing shockwave-induced drag:

- $C_{D_{0w}}$  values for the three locations were:
  - 20 meters:  $C_{D_{0w}} = 0.00457$
  - 35 meters:  $C_{D_{0w}} = 0.00631$
  - 50 meters:  $C_{D_{0w}} = 0.00624$
- The forward wing position (20 meters) significantly outperformed the aft placements by maintaining the lowest wave drag. This result highlights its superior shockwave management.

**Summary of Aerodynamic Trends** The comparative analysis of wing locations reveals important trade-offs:

- The 20-meter position offers the best balance of lift, drag, stability, and wave drag, making it the most efficient configuration overall.
- The 50-meter location, while generating slightly higher lift, suffers from increased pitching moments and wave drag, compromising stability and efficiency.
- The 35-meter position shows intermediate characteristics, with moderate lift and drag values but reduced stability compared to the baseline configuration.

**Conclusion** The analysis demonstrates that wing placement significantly influences aerodynamic performance. The 20-meter wing location emerged as the optimal configuration due to its superior stability, low wave drag, and balanced

lift-to-drag ratio. Aft wing placements, although viable, introduce stability challenges and increased drag, making them less favorable for supersonic applications.

EFFECT OF WING LOCATION ON THE AERODYNAMIC PROFILE OF A SUPERSONIC AIRCRAFT  
USING ANSYS FLUENT

---

TABLE 4.5: Aerodynamic Parameters for Different Wing Locations and AoA

Wing Location			
AoA	20 m	35 m	50 m
$C_L$			
-10	-0.386532517	-0.386088008	-0.386032094
-8	-0.313164057	-0.313664671	-0.313539559
-6	-0.237946295	-0.236267111	-0.237354504
-4	-0.159341428	-0.159228239	-0.159532196
-2	-0.080094780	-0.079956811	-0.080103428
0	0.000000000	0.000000000	0.000000000
2	0.080094781	0.079956811	0.08010342708
4	0.159351482	0.159228239	0.1595321962
6	0.237946295	0.236867211	0.2375454003
8	0.313164057	0.312966477	0.3135259504
10	0.3865352171	0.386088800	0.386809204
$C_D$			
-10	0.07622073297	0.07615473049	0.07629375712
-8	0.05162312353	0.05162714352	0.05171138161
-6	0.03227074108	0.03218133174	0.03227429188
-4	0.01820311132	0.01819737689	0.0182214421
-2	0.00971590994	0.00971071749	0.009716366256
0	0.006870588608	0.006870587592	0.006870589346
2	0.009715909941	0.00971071749	0.009716366173
4	0.01820311132	0.01819737689	0.0182214421
6	0.03227074111	0.03218133174	0.03227429188
8	0.05162312355	0.05162714352	0.05171138198
10	0.07622073297	0.07615473049	0.07629375712
$C_{M_y}$			
-10	0.05278402668	0.2527703685	0.4463957122
-8	0.04250171347	0.2037521035	0.3597518178
-6	0.03212709774	0.1534298759	0.271358875
-4	0.02148566205	0.1028846283	0.1816634554
-2	0.01074939686	0.05156527268	0.09104433184
0	0.0000000000	0.0000000000	0.0000000000
2	-0.01074939675	-0.05156527268	-0.09104432019
4	-0.02148566195	-0.1028846283	-0.1816634554
6	-0.03212709795	-0.1534298758	-0.271358875
8	-0.04250171697	-0.2037521035	-0.3597518494
10	-0.0527840256	-0.2527703684	-0.4463957122

TABLE 4.6:  $C_{D_{0w}}$  Values for Different Wing Locations

	Wing Location		
	20 meters	35 meters	50 meters
$C_{D_{0w}}$	0.00457418	0.00680787	0.0062374

## 4.3 Results from ANSYS Fluent

This chapter presents the results obtained from the computational fluid dynamics (CFD) simulations conducted using ANSYS Fluent for the SST aircraft. The analysis focuses on two wing locations: the baseline position at 20 meters from the nose and 35 meters aft. Key aerodynamic coefficients ( $C_L$ ,  $C_D$ ,  $C_M$ ), their iterative convergence during the simulation, and visualizations (pressure contours and Mach number contours) are discussed in detail. All simulations were conducted at Mach 2.0 and a 5-degree angle of attack (AoA) to ensure consistency in comparing aerodynamic performance.

### 4.3.1 Wing Location at 20 meters

#### Aerodynamic Coefficients

For the baseline configuration, the iterative convergence of  $C_l$ ,  $C_d$ , and  $C_m$  during the simulation revealed a stable aerodynamic behavior. The lift coefficient ( $C_L$ ) demonstrated effective lift generation, while the drag coefficient ( $C_D$ ) indicated minimal resistance, aligning with the streamlined geometry of the aircraft. The moment coefficient ( $C_M$ ) displayed consistent stability, reflecting reliable control characteristics for the aircraft. The aerodynamic iteration results for wing location at 20 meters are shown in Figure [4.10](#)

### **Mach Number and Pressure Contours**

Pressure contours showed well-distributed pressure fields across the surface, with high-pressure zones concentrated at the leading edges of the wing and fuselage. This contributed to the lift generation observed in the aerodynamic coefficients. Low-pressure regions over the upper wing surface further enhanced the aerodynamic performance by increasing the pressure differential.

Mach number contours depicted smooth supersonic airflow over the wing with minimal shockwave interference. The absence of significant flow separation emphasized the efficiency of the Diamond Airfoil and the baseline wing placement. The Mach and Pressure Contour of wing location at 20 meters are shown in Figure [4.11](#) and [4.12](#)

### **Interpretation of Results**

The results for the baseline configuration highlight its aerodynamic efficiency, combining stable lift generation with minimal drag and effective shockwave management. These findings establish the baseline wing placement as a robust reference point for comparison.

EFFECT OF WING LOCATION ON THE AERODYNAMIC PROFILE OF A SUPERSONIC AIRCRAFT  
USING ANSYS FLUENT

---

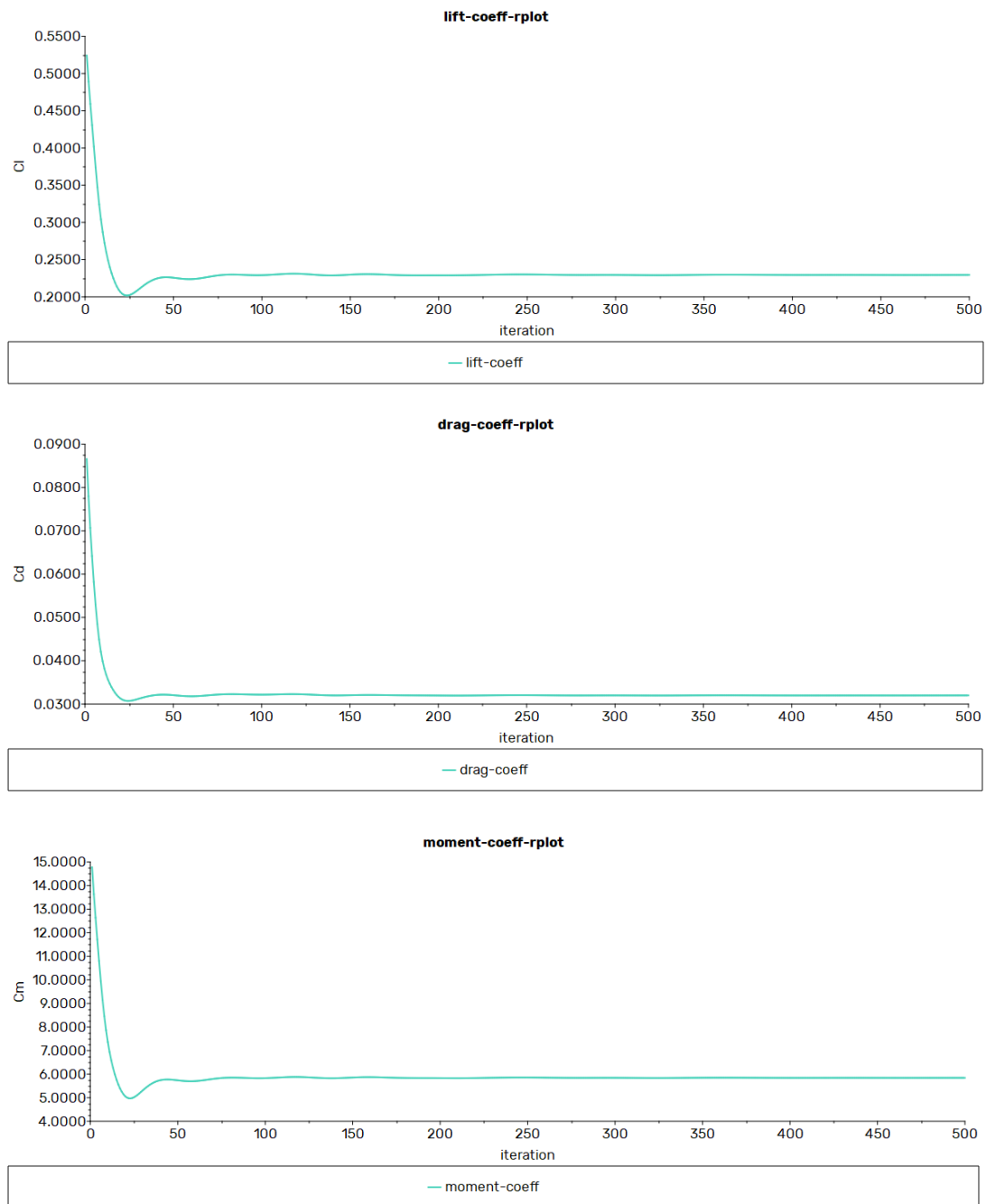


FIGURE 4.10: Aerodynamic Coefficient of Wing Location at 20 meters

EFFECT OF WING LOCATION ON THE AERODYNAMIC PROFILE OF A SUPERSONIC AIRCRAFT  
USING ANSYS FLUENT

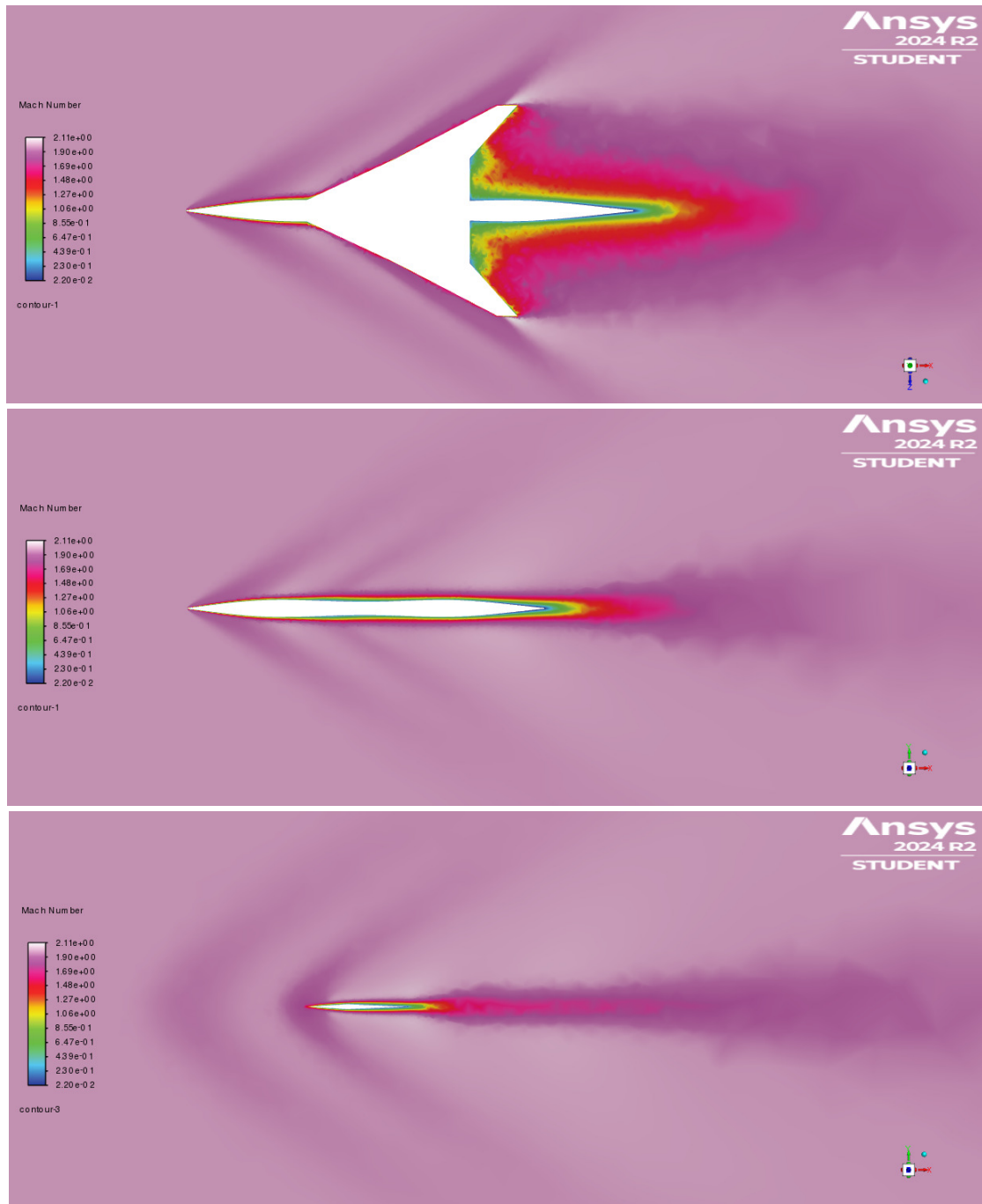


FIGURE 4.11: Mach Contour of Wing Location at 20 meters

EFFECT OF WING LOCATION ON THE AERODYNAMIC PROFILE OF A SUPERSONIC AIRCRAFT  
USING ANSYS FLUENT

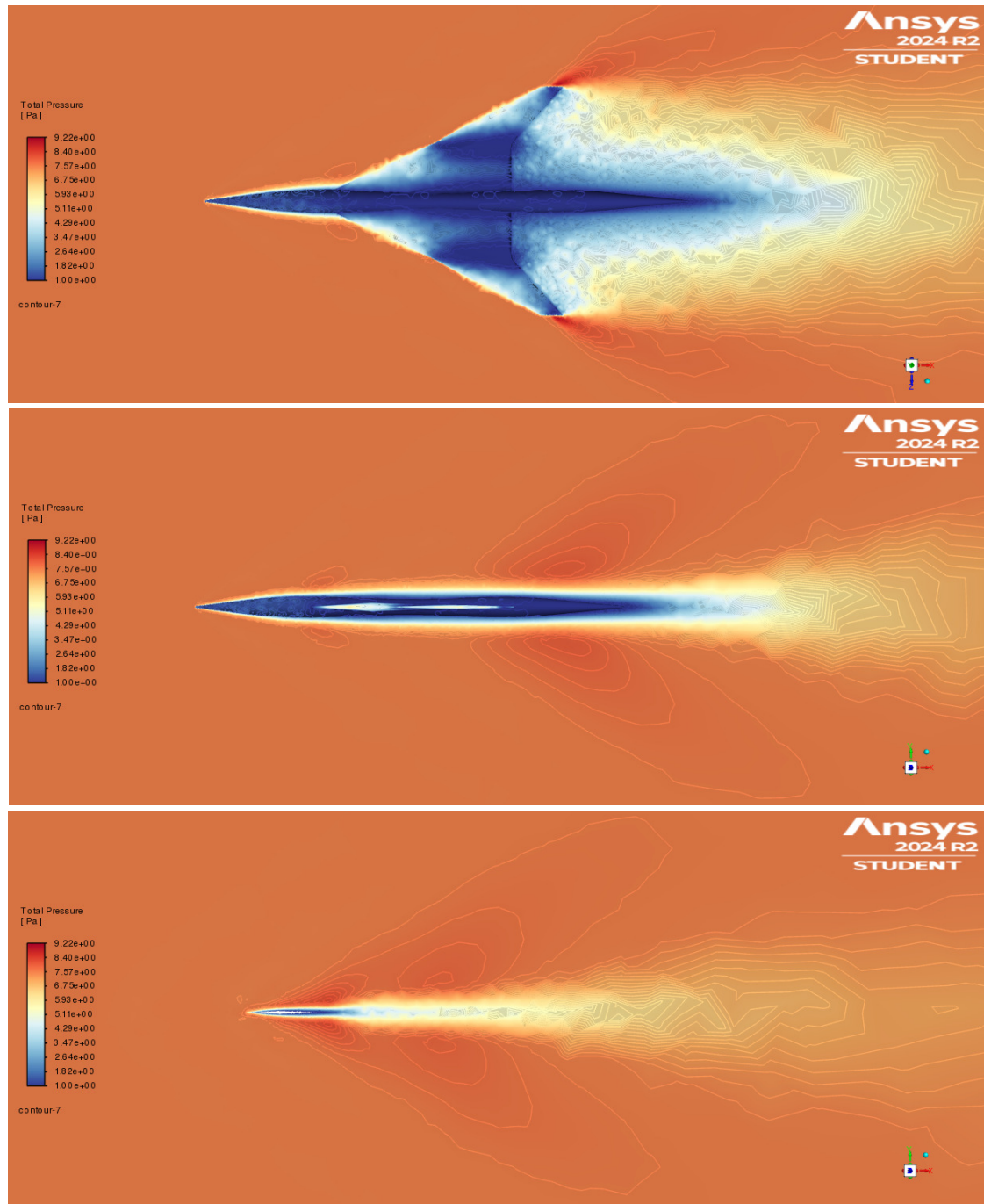


FIGURE 4.12: Pressure Contour of Wing Location at 20 meters

### Wing Location at 20 Meters

The aerodynamic performance of the wing located 20 meters from the nose was evaluated using ANSYS Fluent simulations under supersonic conditions. Initially, the moment coefficient ( $C_M$ ) was overestimated due to an incorrect center of moment. After correcting the reference point to 24.6 meters along the  $x$ -axis, corresponding to the CG location derived from OpenVSP, the new moment coefficient was calculated as:

$$C_M = 0.63319 \quad (4.1)$$

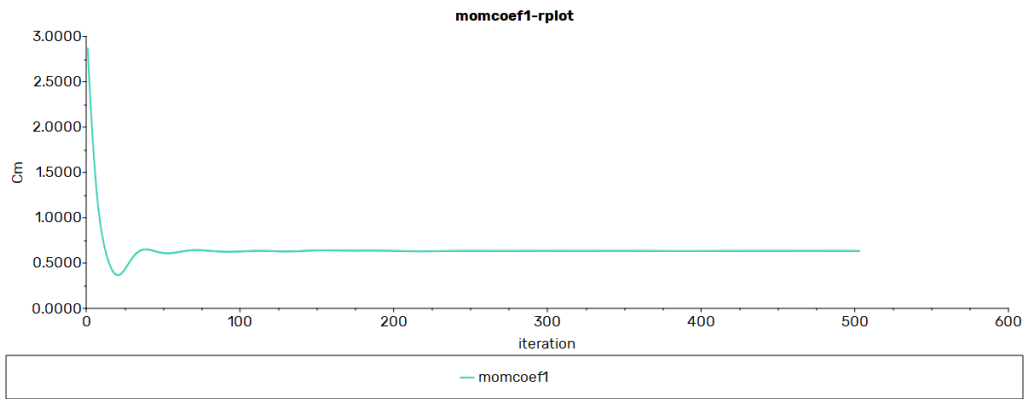


FIGURE 4.13: Moment Coefficient of 20m wing location following Center of Gravity

In comparison, the moment coefficient obtained from OpenVSP for the same configuration was around  $-0.02148$  to  $-0.03212$ . Although the values differ significantly, the trend between the two tools remains consistent.

**Following the Trend of OpenVSP** Although the absolute values differ, both tools follow the same general trend: the 20-meter wing location exhibits a relatively stable moment compared to the aft positions. This consistency in trends is important, as it validates the aerodynamic relationship between wing location and moment behavior predicted by both tools. The corrected  $C_M$  value in ANSYS Fluent reflects a more realistic estimate of the pitching moment while confirming the stability trend observed in OpenVSP.

**Conclusion** The updated moment coefficient demonstrates the importance of accurately defining the center of moment in CFD simulations. Misalignment of the CG can lead to significant errors in stability predictions, as seen in the initial overestimated value.

### 4.3.2 Wing Location at 35 meters aft

#### Aerodynamic Coefficients

In the 35-meter aft wing placement, the iterative convergence of  $C_L$ ,  $C_D$ , and  $C_M$  revealed changes in aerodynamic performance compared to the baseline. The lift coefficient ( $C_L$ ) was slightly reduced, reflecting diminished lift efficiency. Drag coefficient ( $C_D$ ) values increased marginally, indicating higher aerodynamic resistance. The moment coefficient ( $C_M$ ) exhibited greater variations, suggesting reduced stability compared to the baseline. The aerodynamic coefficients iteration plot for wing location at 35 meters are shown in Figure 4.14

#### Pressure and Mach Number Contours

Pressure contours indicated a shift in high-pressure regions toward the rear of the fuselage, altering the lift generation dynamics. The low-pressure zones on the wing's upper surface were less pronounced than in the baseline configuration, reducing the pressure differential essential for efficient lift.

Mach number contours showed regions of flow separation and turbulence near the trailing edge, contributing to increased drag. These observations highlight the aerodynamic compromises introduced by the aft wing placement. The mach and pressure contour of wing location at 35 meters are shown in Figure 4.15 and 4.16.

#### Interpretation of Results

The 35-meter aft placement resulted in reduced aerodynamic efficiency and stability compared to the baseline. While the configuration remains operationally feasible, the increased drag and reduced lift efficiency make it less optimal for supersonic flight.

EFFECT OF WING LOCATION ON THE AERODYNAMIC PROFILE OF A SUPERSONIC AIRCRAFT  
USING ANSYS FLUENT

---

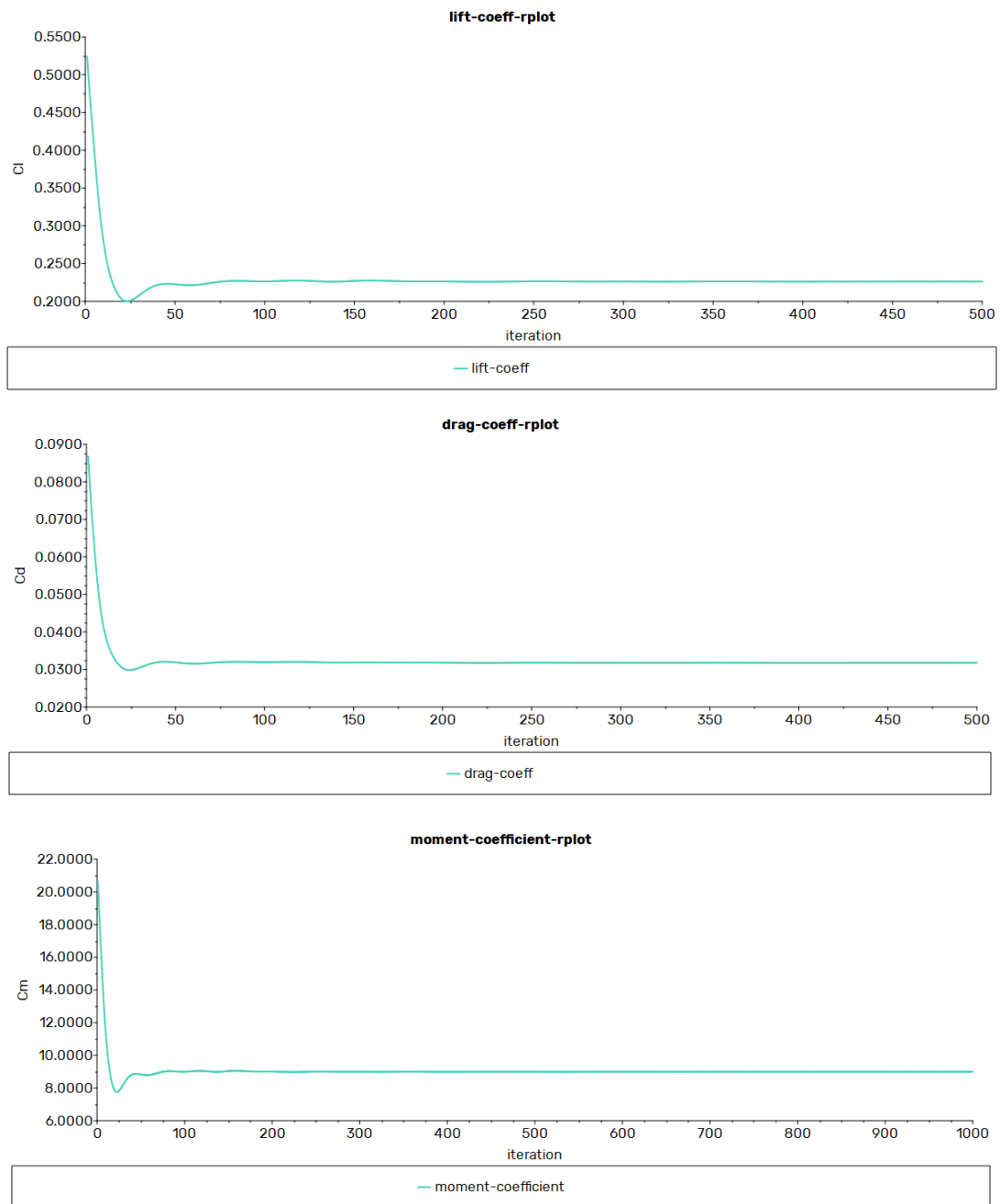


FIGURE 4.14: Aerodynamic Coefficient of Wing Location at 35 meters

EFFECT OF WING LOCATION ON THE AERODYNAMIC PROFILE OF A SUPERSONIC AIRCRAFT  
USING ANSYS FLUENT

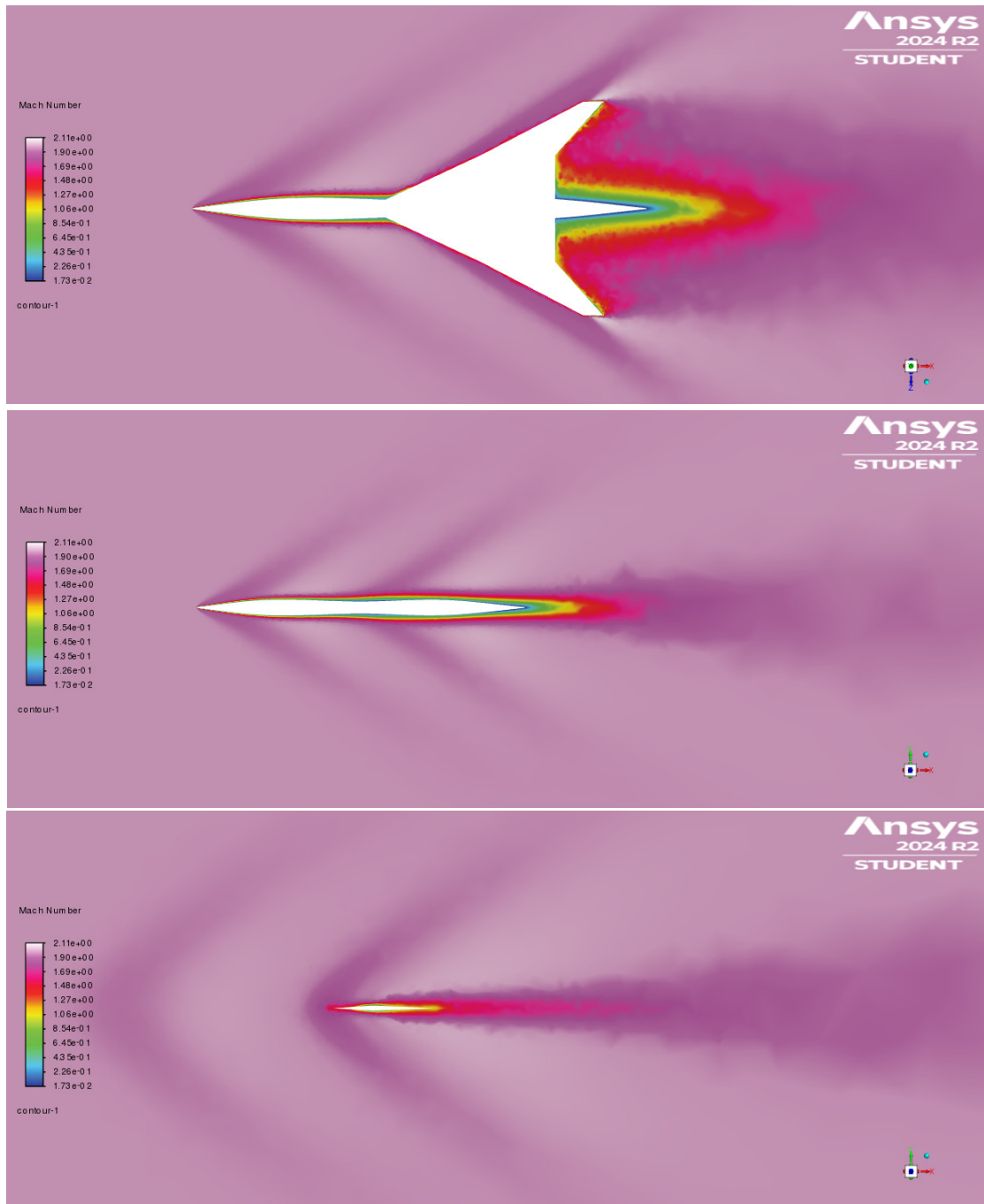


FIGURE 4.15: Mach Contour of Wing Location at 35 meters

EFFECT OF WING LOCATION ON THE AERODYNAMIC PROFILE OF A SUPERSONIC AIRCRAFT  
USING ANSYS FLUENT

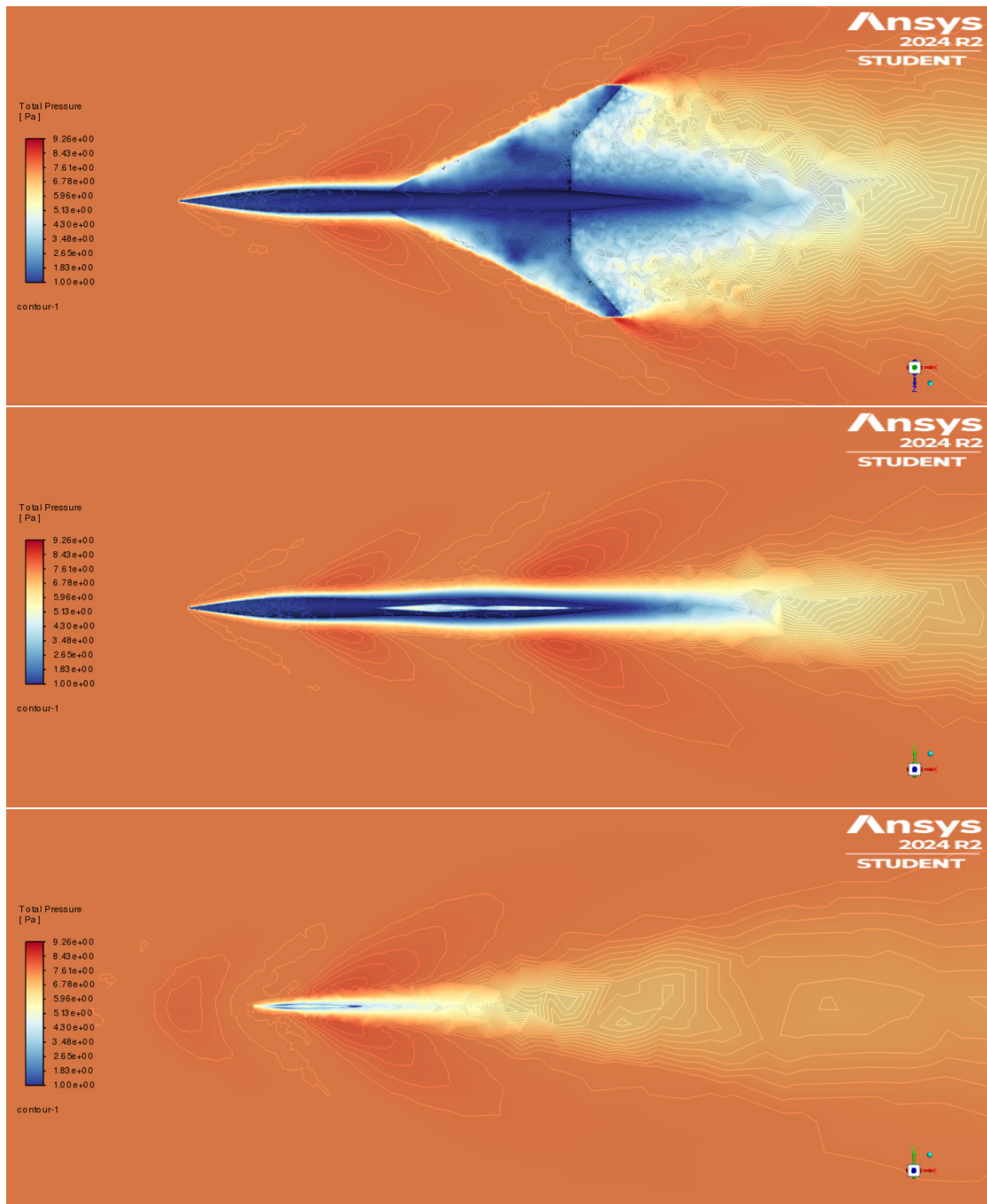


FIGURE 4.16: Pressure Contour of Wing Location at 35 meters

### Wing Location at 35 Meters

For the wing placed 35 meters from the nose, the initial simulation overestimated the moment coefficient due to an incorrect reference for the center of moment. By adjusting the center of moment to 29.267 meters along the  $x$ -axis, based on the CG location derived from OpenVSP, the updated moment coefficient was:

$$C_M = 2.3765 \quad (4.2)$$

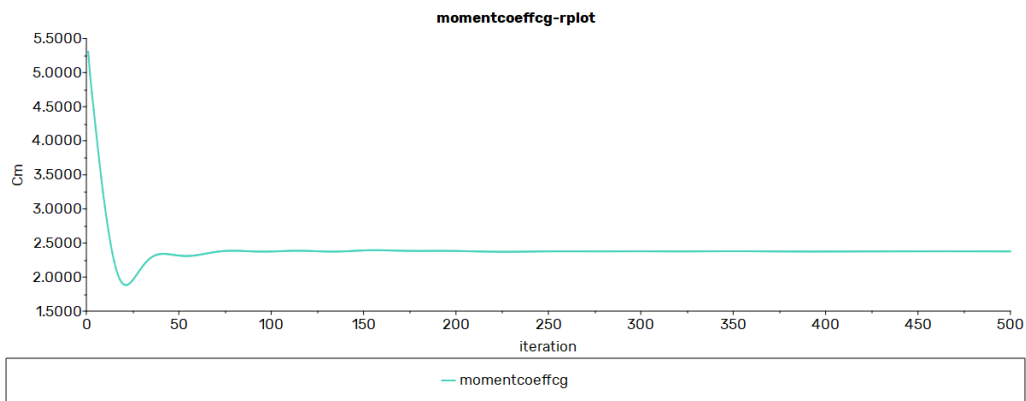


FIGURE 4.17: Moment Coefficient of 35m wing location following Center of Gravity

The moment coefficient from OpenVSP for the same configuration was around  $-0.10288$  to  $-0.1534$ . While the numerical values differ, both simulations indicate a higher moment coefficient for the 35-meter wing location compared to the 20-meter position.

**Following the Trend of OpenVSP** Despite the differences in magnitude, both OpenVSP and ANSYS Fluent follow the same trend: moving the wing further aft results in a larger moment coefficient. The 35-meter wing location shows increased pitching moments due to the extended distance between the aerodynamic center and CG, making it more prone to stability challenges.

**Conclusion** The updated moment coefficient highlights the importance of using accurate CG data in CFD simulations. While OpenVSP provides a useful preliminary estimate of stability trends, it lacks the accuracy required for precise moment predictions. The higher fidelity of ANSYS Fluent offers a more realistic assessment of the pitching moment, confirming the design trade-offs associated with aft wing placements.

### 4.3.3 Comparative Analysis Across Wing Locations

The aerodynamic performance of the supersonic aircraft was evaluated using ANSYS Fluent simulations at an angle of attack (AoA) of  $5^\circ$  for wing placements at 20 meters and 35 meters from the nose. These results were compared with OpenVSP simulations conducted at AoA values of  $0^\circ$ ,  $2^\circ$ ,  $4^\circ$ , and  $6^\circ$ . While the exact AoA does not align, the ANSYS results, shown in Table 4.7, are consistent with OpenVSP trends, providing validation for the aerodynamic performance metrics.

TABLE 4.7: ANSYS Fluent Results at AoA =  $5^\circ$

Wing Location	$C_L$	$C_D$	$C_M$
20 m	0.22936	0.03201	0.6332
35 m	0.22617	0.03179	2.3765

**Lift Coefficient ( $C_L$ )** The lift coefficient results from ANSYS Fluent at  $5^\circ$  AoA are consistent with the trends observed in OpenVSP:

- Wing at 20 meters:  $C_L = 0.22936$
- Wing at 35 meters:  $C_L = 0.22617$
- The slight reduction in  $C_L$  for the 35-meter position aligns with OpenVSP results, where aft wing placement showed marginally lower lift generation.

**Drag Coefficient ( $C_D$ )** The drag coefficient from ANSYS Fluent closely matches OpenVSP trends, with minimal differences between wing locations:

- Wing at 20 meters:  $C_D = 0.03201$

- Wing at 35 meters:  $C_D = 0.03179$
- These results reflect improved aerodynamic efficiency for the aft position, which is consistent with OpenVSP predictions.

**Moment Coefficient ( $C_M$ )** The moment coefficient ( $C_M$ ) results from ANSYS Fluent are significantly higher than those from OpenVSP, highlighting potential discrepancies:

- Wing at 20 meters:  $C_M = 0.6332$
- Wing at 35 meters:  $C_M = 2.3765$
- The elevated  $C_M$  values can be attributed to:
  - **Mesh Limitations:** Constrained cell count due to the student license may have affected the accurate computation of pressure distributions.
  - **Boundary Conditions:** Simplified boundary conditions might have introduced errors in flow modeling near the aircraft surface.
  - **Numerical Model:** The SST  $k-\omega$  model may have overestimated flow effects around the leading and trailing edges.

**Comparison with OpenVSP Results** Although OpenVSP simulations were conducted at AoA values of  $0^\circ$ ,  $2^\circ$ ,  $4^\circ$ , and  $6^\circ$ , the ANSYS results at  $5^\circ$  are closely aligned in terms of lift and drag coefficients, validating the overall trends observed across both tools. The discrepancy in moment coefficients emphasizes the importance of refining simulation setups and mesh resolution to achieve more accurate predictions.

**Conclusion** The analysis confirms that the 20-meter wing location provides a better balance of lift and drag compared to the 35-meter position, consistent with trends from OpenVSP. While the elevated moment coefficients in ANSYS Fluent highlight potential modeling limitations, the results validate the superior aerodynamic efficiency of the baseline (20-meter) configuration.

## CHAPTER 5

### SUMMARY, CONCLUSION, RECOMMENDATION

#### 5.1 Summary, Conclusion, Recommendation

##### 5.1.1 Summary

This study aimed to analyze the effect of wing placement on the aerodynamic profile of a supersonic transport (SST) aircraft using OpenVSP and ANSYS Fluent simulations. The analysis focused on three wing locations, 20 meters, 35 meters, and 50 meters from the nose, and evaluated key aerodynamic parameters, including lift coefficient ( $C_L$ ), drag coefficient ( $C_D$ ), and moment coefficient ( $C_M$ ).

The key findings are summarized as follows:

- **Airfoil Selection:** The Diamond Airfoil was selected as the optimal airfoil for supersonic regimes due to its high lift-to-drag ratio ( $\frac{L}{D}$ ) and stable moment coefficients across all Mach numbers. It consistently outperformed NACA 2412, NACA 0005, and the Hexagonal Airfoil in minimizing wave drag and maximizing aerodynamic efficiency.
- **OpenVSP Results:** The 20-meter wing position demonstrated superior aerodynamic performance with the highest lift-to-drag ratio and stable moment coefficients. The 35-meter and 50-meter placements showed reduced aerodynamic efficiency and increased pitching moments, highlighting the trade-offs in aft wing locations.
- **ANSYS Fluent Results:** Simulations at an angle of attack (AoA) of  $5^\circ$  validated the trends observed in OpenVSP for lift and drag coefficients. However, moment coefficients from ANSYS were significantly higher, likely due to limitations in mesh resolution, boundary conditions, and turbulence modeling.

- **Comparative Analysis:** The 20-meter wing location provided the best balance of lift, drag, and stability, confirming its suitability as the optimal configuration. Aft positions (35 and 50 meters) introduced higher drag and moment coefficients, compromising aerodynamic performance.

### 5.1.2 Conclusion

Based on the analysis, the following conclusions can be drawn:

- **Effect of Wing Location:** Wing placement significantly influences the aerodynamic performance of a supersonic aircraft. The 20-meter wing location achieved the most favorable lift-to-drag ratio and demonstrated stable moment coefficients, making it the optimal configuration for supersonic flight.
- **Diamond Airfoil Superiority:** The Diamond Airfoil proved to be the best candidate for supersonic regimes, minimizing wave drag and maintaining aerodynamic efficiency across varying flight conditions. Its thin profile and sharp edges contributed to effective shockwave management and reduced drag.
- **Validation Across Tools:** The consistency of results between OpenVSP and ANSYS Fluent for lift and drag coefficients validates the overall aerodynamic trends. However, the significant discrepancy in moment coefficients from ANSYS highlights the importance of refining numerical models and mesh quality to improve prediction accuracy.
- **Trade-offs in Aft Wing Locations:** Aft wing placements (35 and 50 meters) showed reduced lift efficiency and increased drag and pitching moments. While these configurations remain operationally feasible, their aerodynamic penalties make them less desirable for optimal supersonic performance.

### 5.1.3 Recommendation

This research provides a foundational understanding of the impact of wing placement on supersonic aerodynamic performance. However, further studies are recommended to address limitations and expand the scope of analysis:

- **Expanded Wing Configurations:** Future work should explore additional wing placements and hybrid configurations to identify optimal trade-offs for varying mission profiles.
- **Broader Flight Conditions:** Analyze aerodynamic performance across a wider range of Mach numbers, angles of attack, and altitudes to ensure robustness under different flight scenarios.
- **Higher Fidelity Simulations:** Utilize advanced turbulence models (e.g., Reynolds Stress Model) and higher mesh resolutions to improve the accuracy of moment coefficient predictions.
- **Validation Through Experiments:** Conduct wind tunnel testing and flight trials to validate computational findings and ensure real-world applicability.
- **Structural and Control Analysis:** Integrate structural dynamics and control surface effectiveness into the analysis to provide a holistic perspective on the design of supersonic aircraft.
- **Energy Efficiency Studies:** Investigate the relationship between wing placement and fuel efficiency to optimize SST designs for environmental and economic considerations.

This study highlights the critical role of wing placement and airfoil selection in supersonic aircraft design. The findings contribute to the broader understanding of supersonic aerodynamics and provide a strong foundation for future research and development in this field.

## Bibliography

- [1] “Supersonic transport,” *Wikipedia*, Jan. 2025. (visited on 01/30/2025).
- [2] K. Yoshida, “Supersonic drag reduction technology in the scaled supersonic experimental airplane project by JAXA,” *Progress in Aerospace Sciences*, vol. 45, no. 4-5, pp. 124–146, May 2009, ISSN: 03760421. DOI: [10.1016/j.paerosci.2009.05.002](https://doi.org/10.1016/j.paerosci.2009.05.002). (visited on 12/22/2024).
- [3] “Boeing 2707,” *Wikipedia*, Jan. 2025. (visited on 01/28/2025).
- [4] “Concorde,” *Wikipedia*, Jan. 2025. (visited on 02/03/2025).
- [5] G. E. O. o. M. and Communications, *New model simulates phenomena in a shock wave*, <https://aerospace.illinois.edu/news/43324>. (visited on 01/28/2025).
- [6] A. Sóbester, “Aircraft Aerodynamic Design,”
- [7] J. D. Anderson, *Fundamentals of Aerodynamics* (McGraw-Hill Series in Aeronautical and Aerospace Engineering), Sixth edition. New York, NY: McGraw Hill Education, 2017, ISBN: 978-1-259-12991-9.
- [8] J. D. Anderson, *Introduction to Flight*, Eighth edition. New York, NY: McGraw-Hill Education, 2016, ISBN: 978-0-07-802767-3.
- [9] A. Harikumar, “Aerodynamic Principles for Aircraft: A Study,” *International Journal for Research in Applied Science and Engineering Technology*, vol. 8, no. 7, pp. 1548–1554, Jul. 2020, ISSN: 23219653. DOI: [10.22214/ijraset.2020.30573](https://doi.org/10.22214/ijraset.2020.30573). (visited on 11/07/2024).
- [10] *F-104 | Cold War, Supersonic, Interceptor | Britannica*, <https://www.britannica.com/technology/F-104>. (visited on 01/28/2025).
- [11] *Understanding the Aerodynamic Characteristics of Supersonic Airfoils*, <https://resources.system-analysis.cadence.com/blog/msa2022-understanding-the-aerodynamic-characteristics-of-supersonic-airfoils>. (visited on 01/30/2025).

- [12] *Supersonic Physics - The Physics of Supersonic Flight*, <http://ffden-2.phys.uaf.edu/webproj/2rdewick/96210913254730c4671702/supersonic-physics.html>. (visited on 01/30/2025).
- [13] S. M. Ruffin, A. Gupta, and D. D. Marshall, "Supersonic Channel Airfoils for Reduced Drag,"
- [14] *Area Rule | SKYbrary Aviation Safety*, <https://skybrary.aero/articles/area-rule>. (visited on 01/30/2025).
- [15] B. Supersonic, *Boom - FlyBy - Aerodynamics 101: The Shape of Supersonic*, <https://boomsupersonic.com/flyby/aerodynamics-101-the-shape-of-supersonic>, Oct. 2022. (visited on 01/30/2025).
- [16] J. Siegler, J. Ren, L. Leifsson, S. Koziel, and A. Bekasiewicz, "Supersonic Airfoil Shape Optimization by Variable-fidelity Models and Manifold Mapping," *Procedia Computer Science*, vol. 80, pp. 1103–1113, 2016, ISSN: 18770509. DOI: [10.1016/j.procs.2016.05.416](https://doi.org/10.1016/j.procs.2016.05.416). (visited on 11/07/2024).
- [17] A. Goodman, "EFFECTS OF WING POSITION AND. HORIZONTAL-TAIL POSITION ON THE STATIC STABILITY CHARACTERISTICS OF MODELS WITH UNSWEPT AND 45° SWEPTBACK SURFACES WITH SOME REFERENCE TO MUTUAL INTERFERENCE,"
- [18] W. Yong, "Study on Aerodynamic Characteristics of Supersonic Airfoil," *Modern Mechanical Engineering*, vol. 09, no. 01, pp. 13–19, 2019, ISSN: 2164-0165, 2164-0181. DOI: [10.4236/mme.2019.91002](https://doi.org/10.4236/mme.2019.91002). (visited on 11/07/2024).
- [19] Anirudh Ganesh Sriraam, VIT Vellore, Tamilnadu, India Manav Badamwala, Student, VIT Vellore, Tamilnadu , India, S. K. Singh\*, S. Aggarwal, *et al.*, "An Access for Designing and Manufacturing of Aerodynamics Wings for a FSAE Vehicle," *International Journal of Recent Technology and Engineering (IJRTE)*, vol. 8, no. 4, pp. 7340–7350, Nov. 2019, ISSN: 22773878. DOI: [10.35940/ijrte.D5296.118419](https://doi.org/10.35940/ijrte.D5296.118419). (visited on 11/07/2024).
- [20] R. A. McDonald and J. R. Gloudemans, "Open Vehicle Sketch Pad: An Open Source Parametric Geometry and Analysis Tool for Conceptual Aircraft Design," in *AIAA SCITECH 2022 Forum*, San Diego, CA & Virtual: American

- Institute of Aeronautics and Astronautics, Jan. 2022, ISBN: 978-1-62410-631-6. DOI: [10.2514/6.2022-0004](https://doi.org/10.2514/6.2022-0004). (visited on 12/22/2024).
- [21] J. E. Matsson, *An Introduction to Ansys Fluent 2023*. SDC Publications, 2023, ISBN: 978-1-63057-648-6.
- [22] P. Welahettige and K. Vaagsaether, “Comparison of OpenFOAM and ANSYS Fluent,” in *Proceedings of The 9th EUROSIM Congress on Modelling and Simulation, EUROSIM 2016, The 57th SIMS Conference on Simulation and Modelling SIMS 2016*, Dec. 2018, pp. 1005–1012. DOI: [10.3384/ecp171421005](https://doi.org/10.3384/ecp171421005). (visited on 12/22/2024).

# Appendices

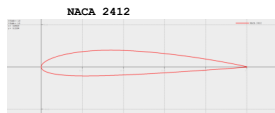
EFFECT OF WING LOCATION ON THE AERODYNAMIC PROFILE OF A SUPERSONIC AIRCRAFT  
 USING ANSYS FLUENT

# Appendix A

## .1 OpenVSP Results

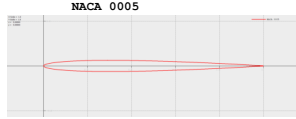
### .1.1 Airfoil Candidates

#### AIRFOIL CANDIDATES



Mach	AoA	Re/1e6	CL	CD0	CDi	CDtot	CDt	CDtot_CS	L/D	E	CFx	CFy	CFz	CMx	CMy	CMz	CMl	CMm	CMn	
0.6	-10	10	-0.1730	0.0026	0.0089	0.0115	0.0095	0.0121	0.0000	-15.1283	605	-0.0180	0.0000	-0.1730	0.0000	-0.2560	0.0000	0.0000	-0.2560	0.0000
0.6	-8	10	-0.1290	0.0024	0.0049	0.0073	0.0052	0.0076	0.0000	-17.6472	724	-0.0100	0.0000	-0.1290	0.0000	-0.2160	0.0000	0.0000	-0.2160	0.0000
0.6	-6	10	-0.0840	0.0023	0.0021	0.0044	0.0022	0.0045	0.0000	-19.3052	823	-0.0040	0.0000	-0.0840	0.0000	-0.1760	0.0000	0.0000	-0.1760	0.0000
0.6	-4	10	-0.0390	0.0022	0.0004	0.0027	0.0005	0.0027	0.0000	-14.7418	436	-0.0000	0.0000	-0.0390	0.0000	-0.1350	0.0000	0.0000	-0.1350	0.0000
0.6	-2	10	0.0061	0.0022	0.0000	0.0022	0.0000	0.0022	0.0000	2.7345	527	0.0024	0.0000	0.0060	0.0000	-0.0940	0.0000	0.0000	-0.0940	0.0000
0.6	0	10	0.0522	0.0023	0.0008	0.0031	0.0008	0.0031	0.0000	17.0982	397	0.0031	0.0000	0.0522	0.0000	-0.0530	0.0000	0.0000	-0.0530	0.0000
0.6	2	10	0.0972	0.0024	0.0028	0.0051	0.0028	0.0052	0.0000	18.9295	58	0.0017	0.0000	0.0974	0.0000	-0.0110	0.0000	0.0000	-0.0110	0.0000
0.6	4	10	0.1423	0.0025	0.0060	0.0085	0.0062	0.0088	0.0000	16.7447	850	-0.0010	0.0000	0.1426	0.0001	0.0308	0.0000	-0.0000	0.0308	0.0000
0.6	6	10	0.1871	0.0028	0.0103	0.0131	0.0103	0.0131	0.0000	14.2978	1175	-0.0060	0.0000	0.1875	0.0000	0.0724	0.0000	0.0000	0.0724	0.0000
0.6	8	10	0.2313	0.0030	0.0159	0.0189	0.0164	0.0194	0.0000	12.2359	1088	-0.0130	0.0000	0.2317	0.0000	0.1135	0.0000	0.0000	0.1135	0.0000
0.6	10	10	0.2757	0.0034	0.0226	0.0260	0.0230	0.0264	0.0000	10.6033	930	-0.0220	0.0000	0.2760	0.0000	0.1540	0.0000	0.0000	0.1540	0.0000
1.2	-10	10	-0.2730	0.0035	0.0587	0.0622	0.0587	0.0622	0.0000	-4.3953	2410	0.0138	0.0000	-0.2800	0.0000	-0.1490	0.0000	0.0000	-0.1490	0.0000
1.2	-8	10	-0.2180	0.0030	0.0402	0.0431	0.0402	0.0431	0.0000	-5.0523	2505	0.0124	0.0000	-0.2210	0.0000	-0.1460	0.0000	0.0000	-0.1460	0.0000
1.2	-6	10	-0.1600	0.0026	0.0254	0.0280	0.0254	0.0280	0.0000	-5.7322	2928	0.0113	0.0000	-0.1620	0.0000	-0.1430	0.0000	0.0000	-0.1430	0.0000
1.2	-4	10	-0.1010	0.0024	0.0146	0.0169	0.0146	0.0169	0.0000	-5.9841	3010	0.0098	0.0000	-0.1020	0.0000	-0.1390	0.0000	0.0000	-0.1390	0.0000
1.2	-2	10	-0.0410	0.0022	0.0079	0.0101	0.0079	0.0101	0.0000	-4.0625	3069	0.0087	0.0000	-0.0410	0.0000	-0.1350	0.0000	0.0000	-0.1350	0.0000
1.2	0	10	0.0199	0.0022	0.0054	0.0076	0.0054	0.0076	0.0000	2.6162	1.6544	0.0076	0.0000	0.0199	0.0000	-0.1310	0.0000	0.0000	-0.1310	0.0000
1.2	2	10	0.0809	0.0023	0.0071	0.0094	0.0071	0.0094	0.0000	8.5594	22.0330	0.0066	0.0000	0.0812	0.0000	-0.1250	0.0000	0.0000	-0.1250	0.0000
1.2	4	10	0.1414	0.0025	0.0131	0.0156	0.0131	0.0156	0.0000	9.0377	40.6730	0.0057	0.0000	0.1421	0.0000	-0.1190	0.0000	0.0000	-0.1190	0.0000
1.2	6	10	0.2010	0.0028	0.0233	0.0261	0.0233	0.0261	0.0000	7.6919	49.2040	0.0050	0.0000	0.2026	0.0000	-0.1130	0.0000	0.0000	-0.1130	0.0000
1.2	8	10	0.2591	0.0033	0.0375	0.0408	0.0375	0.0408	0.0000	6.3536	52.3940	0.0043	0.0000	0.2622	0.0000	-0.1060	0.0000	0.0000	-0.1060	0.0000
1.2	10	10	0.3152	0.0038	0.0556	0.0594	0.0556	0.0594	0.0000	5.3045	53.2170	0.0038	0.0000	0.3207	0.0000	-0.0990	0.0000	0.0000	-0.0990	0.0000
2.0	-10	10	-0.1380	0.0024	0.0279	0.0303	0.0279	0.0303	0.0000	-4.5711	20.1700	0.0058	0.0000	-0.1410	0.0000	-0.0310	0.0000	0.0000	-0.0310	0.0000
2.0	-8	10	-0.1110	0.0024	0.0189	0.0212	0.0189	0.0212	0.0000	-5.2631	18.7330	0.0055	0.0000	-0.1130	0.0000	-0.0350	0.0000	0.0000	-0.0350	0.0000
2.0	-6	10	-0.0840	0.0023	0.0117	0.0140	0.0117	0.0140	0.0000	-5.9881	16.0130	0.0052	0.0000	-0.0850	0.0000	-0.0390	0.0000	0.0000	-0.0390	0.0000
2.0	-4	10	-0.0550	0.0022	0.0065	0.0088	0.0065	0.0088	0.0000	-6.3261	11.6300	0.0049	0.0000	-0.0550	0.0000	-0.0430	0.0000	0.0000	-0.0430	0.0000
2.0	-2	10	-0.0260	0.0022	0.0033	0.0055	0.0033	0.0055	0.0000	-4.7804	0.0041	0.0046	0.0000	-0.0260	0.0000	-0.0460	0.0000	0.0000	-0.0460	0.0000
2.0	0	10	0.0031	0.0022	0.0021	0.0043	0.0021	0.0043	0.0000	0.7164	0.0703	0.0043	0.0000	0.0031	0.0000	-0.0500	0.0000	0.0000	-0.0500	0.0000
2.0	2	10	0.0325	0.0022	0.0030	0.0052	0.0030	0.0052	0.0000	6.2811	6.5003	0.0040	0.0000	0.0327	0.0000	-0.0530	0.0000	0.0000	-0.0530	0.0000
2.0	4	10	0.0617	0.0023	0.0059	0.0081	0.0059	0.0081	0.0000	7.6085	14.9450	0.0038	0.0000	0.0621	0.0000	-0.0560	0.0000	0.0000	-0.0560	0.0000
2.0	6	10	0.0904	0.0023	0.0108	0.0131	0.0108	0.0131	0.0000	6.9174	19.9120	0.0035	0.0000	0.0913	0.0000	-0.0580	0.0000	0.0000	-0.0580	0.0000
2.0	8	10	0.1185	0.0024	0.0176	0.0200	0.0176	0.0200	0.0000	5.9178	22.3170	0.0033	0.0000	0.1201	0.0000	-0.0610	0.0000	0.0000	-0.0610	0.0000
2.0	10	10	0.1455	0.0025	0.0264	0.0288	0.0264	0.0288	0.0000	5.0459	23.3670	0.0031	0.0000	0.1483	0.0000	-0.0630	0.0000	0.0000	-0.0630	0.0000

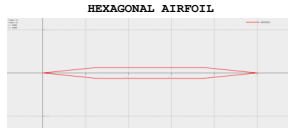
# EFFECT OF WING LOCATION ON THE AERODYNAMIC PROFILE OF A SUPERSONIC AIRCRAFT USING ANSYS FLUENT



mach 1.2 CD0\_w 0.0940  
mach 2.0 CD0\_w 0.0656

Mach	AoA	Re/1e6	CL	CD0	CDi	CDtot	CDt	CDtot_CS	L/D	E	CFx	CFy	CFz	CMx	CMy	CMz	CML	CMm	CMn	
0.6	-10	10	-0.2240	0.0030	0.0149	0.0178	0.0153	0.0182	0.0000	-12.57	89.655	-0.021	0.0000	-0.223	0.0001	-0.205	0.0000	-0.000	-0.205	0.0000
0.6	-8	10	-0.180	0.0027	0.0096	0.0123	0.0098	0.0125	0.0000	-14.67	84.219	-0.012	0.0000	-0.180	0.0001	-0.165	0.0000	-0.000	-0.165	0.0000
0.6	-6	10	-0.135	0.0025	0.0054	0.0079	0.0056	0.0080	0.0000	-17.16	74.209	-0.006	0.0000	-0.135	0.0000	-0.124	0.0000	0.000	-0.124	0.0000
0.6	-4	10	-0.090	0.0023	0.0024	0.0048	0.0025	0.0048	0.0000	-19.09	55.223	-0.001	0.0000	-0.091	0.0000	-0.083	0.0000	0.000	-0.083	0.0000
0.6	-2	10	-0.045	0.0022	0.0006	0.0029	0.0006	0.0029	0.0000	-15.96	23.154	0.001	0.0000	-0.045	0.0000	-0.041	0.0000	0.000	-0.041	0.0000
0.6	0	10	0.0000	0.0022	0.0000	0.0022	0.0000	0.0022	0.0000	0.0000	0.0000	0.0022	0.0000	0.0000	0.0000	0.0000	0.0000	0.0000	0.0000	0.0000
0.6	2	10	0.045	0.0022	0.0006	0.0029	0.0006	0.0029	0.0000	15.96	23.154	0.001	0.0000	0.045	0.0000	0.041	0.0000	0.000	0.041	0.0000
0.6	4	10	0.090	0.0023	0.0024	0.0048	0.0025	0.0048	0.0000	19.09	55.223	-0.001	0.0000	0.091	0.0000	0.083	0.0000	0.000	0.083	0.0000
0.6	6	10	0.135	0.0025	0.0054	0.0079	0.0056	0.0080	0.0000	17.16	74.209	-0.006	0.0000	0.135	0.0000	0.124	0.0000	0.000	0.124	0.0000
0.6	8	10	0.180	0.0027	0.0096	0.0123	0.0098	0.0125	0.0000	14.67	84.219	-0.012	0.0000	0.180	-0.000	0.165	0.0000	0.001	0.165	0.0000
0.6	10	10	0.2240	0.0030	0.0149	0.0178	0.0153	0.0182	0.0000	12.57	89.655	-0.021	0.0000	0.223	-0.000	0.205	0.0000	0.001	0.205	0.0000
1.2	-10	10	-0.295	0.0036	0.0522	0.0559	0.0522	0.0559	0.0000	-5.29	49.773	0.003	0.0000	-0.300	0.0000	-0.021	0.0000	0.000	-0.021	0.0000
1.2	-8	10	-0.239	0.0031	0.0337	0.0369	0.0337	0.0369	0.0000	-6.49	49.563	0.003	0.0000	-0.242	0.0000	-0.017	0.0000	0.000	-0.017	0.0000
1.2	-6	10	-0.181	0.0027	0.0191	0.0218	0.0191	0.0218	0.0000	-8.31	48.024	0.002	0.0000	-0.182	0.0000	-0.013	0.0000	0.000	-0.013	0.0000
1.2	-4	10	-0.121	0.0024	0.0085	0.0110	0.0085	0.0110	0.0000	-11.10	43.078	0.002	0.0000	-0.122	0.0000	-0.008	0.0000	0.000	-0.008	0.0000
1.2	-2	10	-0.061	0.0023	0.0021	0.0044	0.0021	0.0044	0.0000	-13.87	27.043	0.002	0.0000	-0.061	0.0000	-0.004	0.0000	0.000	-0.004	0.0000
1.2	0	10	0.0000	0.0022	0.0000	0.0022	0.0000	0.0022	0.0000	0.0000	0.0000	0.0022	0.0000	0.0000	0.0000	0.0000	0.0000	0.0000	0.0000	0.0000
1.2	2	10	0.061	0.0023	0.0021	0.0044	0.0021	0.0044	0.0000	13.87	27.043	0.002	0.0000	0.061	0.0000	0.004	0.0000	0.000	0.004	0.0000
1.2	4	10	0.121	0.0024	0.0085	0.0110	0.0085	0.0110	0.0000	11.10	43.078	0.002	0.0000	0.122	0.0000	0.008	0.0000	0.000	0.008	0.0000
1.2	6	10	0.181	0.0027	0.0191	0.0218	0.0191	0.0218	0.0000	8.31	48.024	0.002	0.0000	0.182	0.0000	0.013	0.0000	0.000	0.013	0.0000
1.2	8	10	0.239	0.0031	0.0337	0.0369	0.0337	0.0369	0.0000	6.49	49.563	0.003	0.0000	0.242	0.0000	0.017	0.0000	0.000	0.017	0.0000
1.2	10	10	0.295	0.0036	0.0522	0.0559	0.0522	0.0559	0.0000	5.29	49.773	0.003	0.0000	0.300	0.0000	0.021	0.0000	0.000	0.021	0.0000
2.0	-10	10	-0.142	0.0025	0.0253	0.0277	0.0253	0.0277	0.0000	-5.15	23.424	0.002	0.0000	-0.145	0.0000	0.017	0.0000	0.000	0.017	0.0000
2.0	-8	10	-0.115	0.0024	0.0163	0.0187	0.0163	0.0187	0.0000	-6.19	42.824	0.002	0.0000	-0.117	0.0000	0.014	0.0000	0.000	0.014	0.0000
2.0	-6	10	-0.087	0.0023	0.0092	0.0115	0.0092	0.0115	0.0000	-7.59	21.204	0.002	0.0000	-0.088	0.0000	0.010	0.0000	0.000	0.010	0.0000
2.0	-4	10	-0.058	0.0023	0.0041	0.0064	0.0041	0.0064	0.0000	-9.22	17.297	0.002	0.0000	-0.059	0.0000	0.007	0.0000	0.000	0.007	0.0000
2.0	-2	10	-0.029	0.0022	0.0010	0.0033	0.0010	0.0033	0.0000	-9.07	58.543	0.002	0.0000	-0.029	0.0000	0.003	0.0000	0.000	0.003	0.0000
2.0	0	10	0.0000	0.0022	0.0000	0.0022	0.0000	0.0022	0.0000	0.0000	0.0000	0.0022	0.0000	0.0000	0.0000	0.0000	0.0000	0.0000	0.0000	0.0000
2.0	2	10	0.029	0.0022	0.0010	0.0033	0.0010	0.0033	0.0000	9.07	58.543	0.002	0.0000	0.029	0.0000	0.003	0.0000	0.000	0.003	0.0000
2.0	4	10	0.058	0.0023	0.0041	0.0064	0.0041	0.0064	0.0000	9.22	17.297	0.002	0.0000	0.059	0.0000	0.007	0.0000	0.000	0.007	0.0000
2.0	6	10	0.087	0.0023	0.0092	0.0115	0.0092	0.0115	0.0000	7.59	21.204	0.002	0.0000	0.088	0.0000	0.010	0.0000	0.000	0.010	0.0000
2.0	8	10	0.115	0.0024	0.0163	0.0187	0.0163	0.0187	0.0000	6.19	42.824	0.002	0.0000	0.117	0.0000	0.014	0.0000	0.000	0.014	0.0000
2.0	10	10	0.142	0.0025	0.0253	0.0277	0.0253	0.0277	0.0000	5.15	23.424	0.002	0.0000	0.145	0.0000	0.017	0.0000	0.000	0.017	0.0000

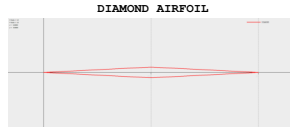
# EFFECT OF WING LOCATION ON THE AERODYNAMIC PROFILE OF A SUPERSONIC AIRCRAFT USING ANSYS FLUENT



mach 1.2 CD0\_w 0.0560  
mach 2.0 CD0\_w 0.0447

Mach	AoA	Re/1e6	CL	CD0	CDi	CDtot	CDt	CDtot_CS	L/D	E	CFx	CFy	CFz	CMx	CMy	CMz	CMl	CMm	CMn	
0.6	-10	10	-0.224	0.0030	0.0149	0.0178	0.0153	0.0182	0.0000	-12.5789	685	-0.021	0.0000	-0.2230	0.0001	-0.276	0.0000	-0.000	-0.276	0.0000
0.6	-8	10	-0.180	0.0027	0.0096	0.0123	0.0098	0.0125	0.0000	-14.6784	247	-0.012	0.0000	-0.180	0.0001	-0.222	0.0000	-0.000	-0.222	0.0000
0.6	-6	10	-0.135	0.0025	0.0054	0.0079	0.0056	0.0080	0.0000	-17.1674	236	-0.006	0.0000	-0.1360	0.0000	-0.167	0.0000	0.0000	-0.167	0.0000
0.6	-4	10	-0.090	0.0023	0.0024	0.0048	0.0025	0.0048	0.0000	-19.0955	245	-0.001	0.0000	-0.0910	0.0000	-0.112	0.0000	0.0000	-0.112	0.0000
0.6	-2	10	-0.045	0.0022	0.0006	0.0029	0.0006	0.0029	0.0000	-15.9723	164	0.0013	0.0000	-0.045	0.0000	-0.056	0.0000	0.0000	-0.056	0.0000
0.6	0	10	0.0000	0.0022	0.0000	0.0022	0.0000	0.0022	0.0000	0.0000	0.0000	0.0022	0.0000	0.0000	0.0000	0.0000	0.0000	0.0000	0.0000	0.0000
0.6	2	10	0.0456	0.0022	0.0006	0.0029	0.0006	0.0029	0.0000	15.9723	164	0.0013	0.0000	0.0456	0.0000	0.0562	0.0000	0.0000	0.0562	0.0000
0.6	4	10	0.0909	0.0023	0.0024	0.0048	0.0025	0.0048	0.0000	19.0935	245	-0.001	0.0000	0.0910	0.0000	0.1123	0.0000	0.0000	0.1123	0.0000
0.6	6	10	0.1359	0.0025	0.0054	0.0079	0.0056	0.0080	0.0000	17.1627	236	-0.006	0.0000	0.1360	0.0000	0.1679	0.0000	0.0000	0.1679	0.0000
0.6	8	10	0.1803	0.0027	0.0096	0.0123	0.0098	0.0125	0.0000	14.6768	247	-0.012	0.0000	0.1803	-0.0000	0.2227	0.0000	0.0001	0.2227	0.0000
0.6	10	10	0.2241	0.0030	0.0149	0.0178	0.0153	0.0182	0.0000	12.5738	685	-0.021	0.0000	0.2238	-0.0000	0.2767	0.0000	0.0001	0.2767	0.0000
1.2	-10	10	-0.297	0.0037	0.0526	0.0563	0.0526	0.0563	0.0000	-5.2905	121	0.0037	0.0000	-0.302	0.0000	-0.122	0.0000	0.0000	-0.122	0.0000
1.2	-8	10	-0.241	0.0031	0.0340	0.0371	0.0340	0.0371	0.0000	-6.4994	917	0.0032	0.0000	-0.244	0.0000	-0.098	0.0000	0.0000	-0.098	0.0000
1.2	-6	10	-0.182	0.0027	0.0192	0.0220	0.0192	0.0220	0.0000	-8.3134	381	0.0028	0.0000	-0.184	0.0000	-0.074	0.0000	0.0000	-0.074	0.0000
1.2	-4	10	-0.122	0.0024	0.0086	0.0110	0.0086	0.0110	0.0000	-11.1143	430	0.0025	0.0000	-0.123	0.0000	-0.049	0.0000	0.0000	-0.049	0.0000
1.2	-2	10	-0.061	0.0023	0.0022	0.0044	0.0022	0.0044	0.0000	-13.9227	323	0.0023	0.0000	-0.061	0.0000	-0.025	0.0000	0.0000	-0.025	0.0000
1.2	0	10	0.0000	0.0022	0.0000	0.0022	0.0000	0.0022	0.0000	0.0000	0.0000	0.0022	0.0000	0.0000	0.0000	0.0000	0.0000	0.0000	0.0000	0.0000
1.2	2	10	0.0617	0.0023	0.0022	0.0044	0.0022	0.0044	0.0000	13.9227	323	0.0023	0.0000	0.0618	0.0000	0.025	0.0000	0.0000	0.025	0.0000
1.2	4	10	0.1228	0.0024	0.0086	0.0110	0.0086	0.0110	0.0000	11.1133	430	0.0025	0.0000	0.1232	0.0000	0.0499	0.0000	0.0000	0.0499	0.0000
1.2	6	10	0.1828	0.0027	0.0192	0.0220	0.0192	0.0220	0.0000	8.3139	48.381	0.0028	0.0000	0.1841	0.0000	0.0746	0.0000	0.0000	0.0746	0.0000
1.2	8	10	0.2413	0.0031	0.0340	0.0371	0.0340	0.0371	0.0000	6.4996	917	0.0032	0.0000	0.2441	0.0000	0.0989	0.0000	0.0000	0.0989	0.0000
1.2	10	10	0.2976	0.0037	0.0526	0.0563	0.0526	0.0563	0.0000	5.2905	121	0.0037	0.0000	0.3029	0.0000	0.1227	0.0000	0.0000	0.1227	0.0000
2.0	-10	10	-0.143	0.0025	0.0254	0.0279	0.0254	0.0279	0.0000	-5.1542	23.576	0.0025	0.0000	-0.146	0.0000	-0.031	0.0000	0.0000	-0.031	0.0000
2.0	-8	10	-0.116	0.0024	0.0164	0.0188	0.0164	0.0188	0.0000	-6.1982	22.978	0.0024	0.0000	-0.118	0.0000	-0.025	0.0000	0.0000	-0.025	0.0000
2.0	-6	10	-0.088	0.0023	0.0093	0.0116	0.0093	0.0116	0.0000	-7.6032	21.356	0.0023	0.0000	-0.089	0.0000	-0.019	0.0000	0.0000	-0.019	0.0000
2.0	-4	10	-0.059	0.0023	0.0042	0.0064	0.0042	0.0064	0.0000	-9.2451	17.437	0.0023	0.0000	-0.059	0.0000	-0.012	0.0000	0.0000	-0.012	0.0000
2.0	-2	10	-0.029	0.0022	0.0010	0.0033	0.0010	0.0033	0.0000	-9.1128	8.6302	0.0022	0.0000	-0.029	0.0000	-0.006	0.0000	0.0000	-0.006	0.0000
2.0	0	10	0.0000	0.0022	0.0000	0.0022	0.0000	0.0022	0.0000	0.0000	0.0000	0.0022	0.0000	0.0000	0.0000	0.0000	0.0000	0.0000	0.0000	0.0000
2.0	2	10	0.0298	0.0022	0.0010	0.0033	0.0010	0.0033	0.0000	9.1121	8.6302	0.0022	0.0000	0.0299	0.0000	0.0064	0.0000	0.0000	0.0064	0.0000
2.0	4	10	0.0593	0.0023	0.0042	0.0064	0.0042	0.0064	0.0000	9.2454	17.437	0.0023	0.0000	0.0596	0.0000	0.0127	0.0000	0.0000	0.0127	0.0000
2.0	6	10	0.0882	0.0023	0.0093	0.0116	0.0093	0.0116	0.0000	7.6034	21.356	0.0023	0.0000	0.0890	0.0000	0.0190	0.0000	0.0000	0.0190	0.0000
2.0	8	10	0.1165	0.0024	0.0164	0.0188	0.0164	0.0188	0.0000	6.1980	22.978	0.0024	0.0000	0.1180	0.0000	0.0251	0.0000	0.0000	0.0251	0.0000
2.0	10	10	0.1437	0.0025	0.0254	0.0279	0.0254	0.0279	0.0000	5.1543	23.576	0.0025	0.0000	0.1464	0.0000	0.0312	0.0000	0.0000	0.0312	0.0000

# EFFECT OF WING LOCATION ON THE AERODYNAMIC PROFILE OF A SUPERSONIC AIRCRAFT USING ANSYS FLUENT



mach 1.2 CD0\_w 0.0175  
 mach 2.0 CD0\_w 0.0100

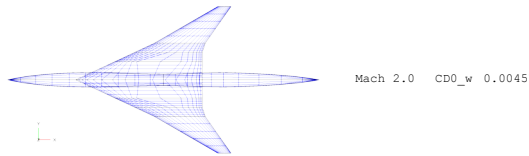
Mach	AoA	Re/1e6	CL	CD0	CDi	CDtot	CDt	CDtot_CS	L/D	E	CFx	CFy	CFz	CMx	CMy	CMz	CMl	CMm	CMn	
0.6	-10	10	-0.224	0.0030	0.0149	0.0178	0.0153	0.0182	0.0000	-12.5789	654.4	-0.021	0.0000	-0.223	0.0001	-0.281	0.0000	-0.000	-0.281	0.0000
0.6	-8	10	-0.180	0.0027	0.0096	0.0123	0.0098	0.0125	0.0000	-14.6784	217.7	-0.012	0.0000	-0.180	0.0001	-0.226	0.0000	-0.000	-0.226	0.0000
0.6	-6	10	-0.135	0.0025	0.0054	0.0079	0.0056	0.0080	0.0000	-17.1674	208.8	-0.006	0.0000	-0.135	0.0000	-0.170	0.0000	0.0000	-0.170	0.0000
0.6	-4	10	-0.090	0.0023	0.0024	0.0048	0.0025	0.0048	0.0000	-19.0955	222.2	-0.001	0.0000	-0.091	0.0000	-0.114	0.0000	0.0000	-0.114	0.0000
0.6	-2	10	-0.045	0.0022	0.0006	0.0029	0.0006	0.0029	0.0000	-15.9623	154.0	0.0013	0.0000	-0.045	0.0000	-0.057	0.0000	0.0000	-0.057	0.0000
0.6	0	10	0.0000	0.0022	0.0000	0.0022	0.0000	0.0022	0.0000	0.0000	0.0000	0.0022	0.0000	0.0000	0.0000	0.0000	0.0000	0.0000	0.0000	0.0000
0.6	2	10	0.0455	0.0022	0.0006	0.0029	0.0006	0.0029	0.0000	15.9692	23.154	0.0013	0.0000	0.0456	0.0000	0.0571	0.0000	0.0000	0.0571	0.0000
0.6	4	10	0.0909	0.0023	0.0024	0.0048	0.0025	0.0048	0.0000	19.0905	55.222	-0.001	0.0000	0.0910	0.0000	0.1141	0.0000	0.0000	0.1141	0.0000
0.6	6	10	0.1359	0.0025	0.0054	0.0079	0.0056	0.0080	0.0000	17.1607	4.208	-0.006	0.0000	0.1359	0.0000	0.1706	0.0000	0.0000	0.1706	0.0000
0.6	8	10	0.1803	0.0027	0.0096	0.0123	0.0098	0.0125	0.0000	14.6758	4.217	-0.012	0.0000	0.1802	-0.0000	0.2263	0.0000	0.0001	0.2263	0.0000
0.6	10	10	0.2240	0.0030	0.0149	0.0178	0.0153	0.0182	0.0000	12.5728	89.654	-0.021	0.0000	0.2237	-0.0000	0.2811	0.0000	0.0001	0.2811	0.0000
1.2	-10	10	-0.295	0.0036	0.0522	0.0558	0.0522	0.0558	0.0000	-5.2904	9.714	0.0037	0.0000	-0.300	0.0000	-0.121	0.0000	0.0000	-0.121	0.0000
1.2	-8	10	-0.239	0.0031	0.0337	0.0368	0.0337	0.0368	0.0000	-6.4984	9.503	0.0032	0.0000	-0.242	0.0000	-0.098	0.0000	0.0000	-0.098	0.0000
1.2	-6	10	-0.181	0.0027	0.0191	0.0218	0.0191	0.0218	0.0000	-8.3094	7.963	0.0027	0.0000	-0.182	0.0000	-0.073	0.0000	0.0000	-0.073	0.0000
1.2	-4	10	-0.121	0.0024	0.0085	0.0110	0.0085	0.0110	0.0000	-11.0943	0.018	0.0025	0.0000	-0.122	0.0000	-0.049	0.0000	0.0000	-0.049	0.0000
1.2	-2	10	-0.061	0.0023	0.0021	0.0044	0.0021	0.0044	0.0000	-13.8626	9.966	0.0023	0.0000	-0.061	0.0000	-0.024	0.0000	0.0000	-0.024	0.0000
1.2	0	10	0.0000	0.0022	0.0000	0.0022	0.0000	0.0022	0.0000	0.0000	0.0000	0.0022	0.0000	0.0000	0.0000	0.0000	0.0000	0.0000	0.0000	0.0000
1.2	2	10	0.0612	0.0023	0.0021	0.0044	0.0021	0.0044	0.0000	13.8672	6.996	0.0023	0.0000	0.0613	0.0000	0.0248	0.0000	0.0000	0.0248	0.0000
1.2	4	10	0.1218	0.0024	0.0085	0.0110	0.0085	0.0110	0.0000	11.0974	3.018	0.0025	0.0000	0.1223	0.0000	0.0495	0.0000	0.0000	0.0495	0.0000
1.2	6	10	0.1813	0.0027	0.0191	0.0218	0.0191	0.0218	0.0000	8.3093	4.963	0.0027	0.0000	0.1826	0.0000	0.0739	0.0000	0.0000	0.0739	0.0000
1.2	8	10	0.2393	0.0031	0.0337	0.0368	0.0337	0.0368	0.0000	6.4983	4.9.503	0.0032	0.0000	0.2421	0.0000	0.0980	0.0000	0.0000	0.0980	0.0000
1.2	10	10	0.2952	0.0036	0.0522	0.0558	0.0522	0.0558	0.0000	5.2903	4.9.714	0.0037	0.0000	0.3004	0.0000	0.1216	0.0000	0.0000	0.1216	0.0000
2.0	-10	10	-0.142	0.0025	0.0252	0.0277	0.0252	0.0277	0.0000	-5.1512	3.386	0.0025	0.0000	-0.145	0.0000	-0.031	0.0000	0.0000	-0.031	0.0000
2.0	-8	10	-0.115	0.0024	0.0163	0.0187	0.0163	0.0187	0.0000	-6.1932	2.786	0.0024	0.0000	-0.117	0.0000	-0.025	0.0000	0.0000	-0.025	0.0000
2.0	-6	10	-0.087	0.0023	0.0092	0.0115	0.0092	0.0115	0.0000	-7.5932	2.1.165	0.0023	0.0000	-0.088	0.0000	-0.018	0.0000	0.0000	-0.018	0.0000
2.0	-4	10	-0.058	0.0023	0.0041	0.0064	0.0041	0.0064	0.0000	-9.2217	1.261	0.0023	0.0000	-0.059	0.0000	-0.012	0.0000	0.0000	-0.012	0.0000
2.0	-2	10	-0.029	0.0022	0.0010	0.0033	0.0010	0.0033	0.0000	-9.0658	8.5212	0.0022	0.0000	-0.029	0.0000	-0.006	0.0000	0.0000	-0.006	0.0000
2.0	0	10	0.0000	0.0022	0.0000	0.0022	0.0000	0.0022	0.0000	0.0000	0.0000	0.0022	0.0000	0.0000	0.0000	0.0000	0.0000	0.0000	0.0000	0.0000
2.0	2	10	0.0295	0.0022	0.0010	0.0033	0.0010	0.0033	0.0000	9.0656	8.5212	0.0022	0.0000	0.0296	0.0000	0.0063	0.0000	0.0000	0.0063	0.0000
2.0	4	10	0.0588	0.0023	0.0041	0.0064	0.0041	0.0064	0.0000	9.2219	1.261	0.0023	0.0000	0.0591	0.0000	0.0127	0.0000	0.0000	0.0127	0.0000
2.0	6	10	0.0876	0.0023	0.0092	0.0115	0.0092	0.0115	0.0000	7.5931	2.1.165	0.0023	0.0000	0.0883	0.0000	0.0189	0.0000	0.0000	0.0189	0.0000
2.0	8	10	0.1156	0.0024	0.0163	0.0187	0.0163	0.0187	0.0000	6.1931	2.786	0.0024	0.0000	0.1171	0.0000	0.0251	0.0000	0.0000	0.0251	0.0000
2.0	10	10	0.1426	0.0025	0.0252	0.0277	0.0252	0.0277	0.0000	5.1518	2.3.386	0.0025	0.0000	0.1453	0.0000	0.0311	0.0000	0.0000	0.0311	0.0000

EFFECT OF WING LOCATION ON THE AERODYNAMIC PROFILE OF A SUPERSONIC AIRCRAFT  
 USING ANSYS FLUENT

**.1.2 SST Wing Locations**

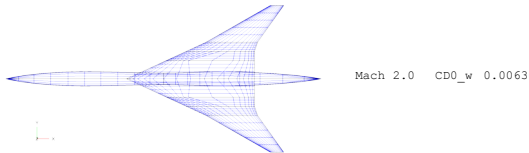
**SST WING LOCATION**

20 METERS (ORIGINAL LOCATION)



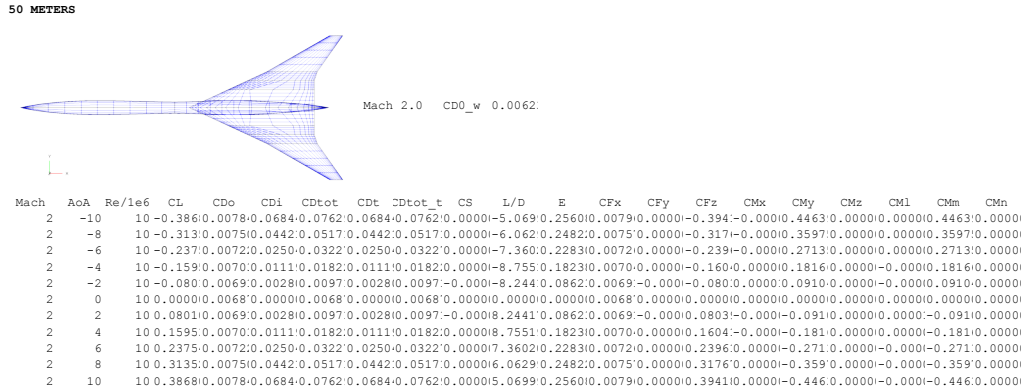
Mach	AoA	Re/1e6	CL	CDo	CDi	CDtot	CDt	CDtot_t	CS	L/D	E	CFx	CFy	CFz	CMx	CMy	CMz	CMl	CMm	CMn
2	-10	10	-0.3860	0.0078	0.0683	0.0762	0.0683	0.0762	0.0000	-5.0710	0.2559	0.0079	0.0000	-0.3930	0.0001	0.0527	0.0000	-0.0000	0.0527	-0.0000
2	-8	10	-0.3130	0.0074	0.0441	0.0516	0.0441	0.0516	0.0000	-6.0660	0.2480	0.0075	0.0000	-0.3170	0.0001	0.0425	0.0000	-0.0000	0.0425	-0.0000
2	-6	10	-0.2370	0.0072	0.0250	0.0322	0.0250	0.0322	0.0000	-7.3590	0.2282	0.0072	0.0000	-0.2390	0.0000	0.0321	0.0000	-0.0000	0.0321	-0.0000
2	-4	10	-0.1590	0.0070	0.0111	0.0182	0.0111	0.0182	0.0000	-8.7560	0.1822	0.0070	0.0000	-0.1600	0.0000	0.0214	0.0000	-0.0000	0.0214	-0.0000
2	-2	10	-0.0800	0.0069	0.0028	0.0097	0.0028	0.0097	0.0000	-8.2430	0.0862	0.0069	0.0000	-0.0800	0.0000	0.0107	0.0000	-0.0000	0.0107	-0.0000
2	0	10	0.0000	0.0068	0.0000	0.0068	0.0000	0.0068	0.0000	0.0000	0.0000	0.0068	0.0000	0.0000	0.0000	0.0000	0.0000	0.0000	0.0000	0.0000
2	2	10	0.0800	0.0069	0.0028	0.0097	0.0028	0.0097	0.0000	8.2430	0.0862	0.0069	0.0000	0.0800	0.0000	0.0107	0.0000	-0.0000	0.0107	-0.0000
2	4	10	0.1590	0.0070	0.0111	0.0182	0.0111	0.0182	0.0000	8.7560	0.1822	0.0070	0.0000	0.1600	0.0000	0.0214	0.0000	-0.0000	0.0214	-0.0000
2	6	10	0.2370	0.0072	0.0250	0.0322	0.0250	0.0322	0.0000	7.3590	0.2282	0.0072	0.0000	0.2390	0.0000	0.0321	0.0000	-0.0000	0.0321	-0.0000
2	8	10	0.3130	0.0074	0.0441	0.0516	0.0441	0.0516	0.0000	6.0660	0.2480	0.0075	0.0000	0.3170	0.0000	0.0425	0.0000	-0.0000	0.0425	-0.0000
2	10	10	0.3860	0.0078	0.0683	0.0762	0.0683	0.0762	0.0000	5.0710	0.2559	0.0079	0.0000	0.3930	0.0000	0.0527	0.0000	-0.0000	0.0527	-0.0000

35 METERS

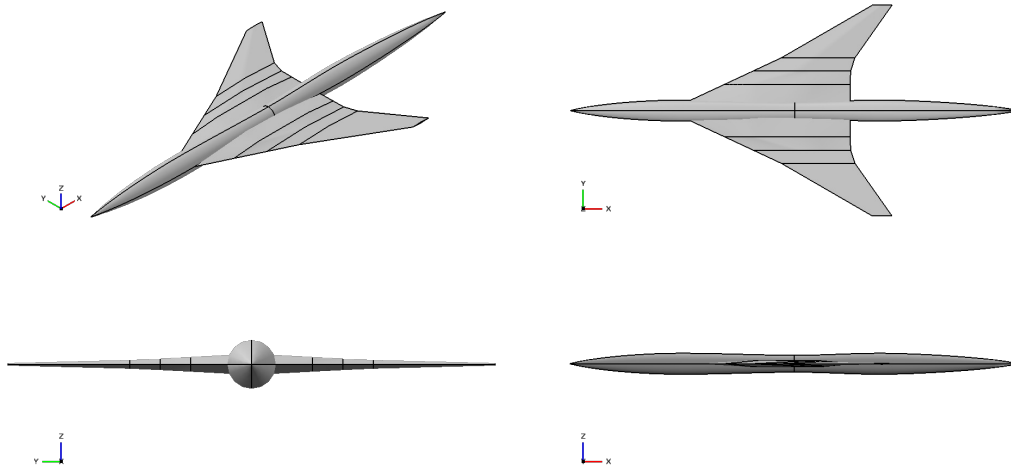


Mach	AoA	Re/1e6	CL	CDo	CDi	CDtot	CDt	CDtot_t	CS	L/D	E	CFx	CFy	CFz	CMx	CMy	CMz	CMl	CMm	CMn
2	-10	10	-0.3860	0.0078	0.0683	0.0761	0.0683	0.0761	0.0000	-5.0690	0.2555	0.0079	0.0000	-0.3930	0.0000	0.0527	0.0000	-0.0000	0.0527	-0.0000
2	-8	10	-0.3120	0.0074	0.0441	0.0516	0.0441	0.0516	0.0000	-6.0620	0.2477	0.0075	0.0000	-0.3170	0.0000	0.0425	0.0000	-0.0000	0.0425	-0.0000
2	-6	10	-0.2360	0.0072	0.0249	0.0321	0.0249	0.0321	0.0000	-7.3600	0.2276	0.0072	0.0000	-0.2380	0.0000	0.0321	0.0000	-0.0000	0.0321	-0.0000
2	-4	10	-0.1590	0.0070	0.0111	0.0181	0.0111	0.0181	0.0000	-8.7500	0.1819	0.0070	0.0000	-0.1600	0.0000	0.0214	0.0000	-0.0000	0.0214	-0.0000
2	-2	10	-0.0790	0.0069	0.0028	0.0097	0.0028	0.0097	0.0000	-8.2330	0.0859	0.0069	0.0000	-0.0800	0.0000	0.0107	0.0000	-0.0000	0.0107	-0.0000
2	0	10	0.0000	0.0068	0.0000	0.0068	0.0000	0.0068	0.0000	0.0000	0.0000	0.0068	0.0000	0.0000	0.0000	0.0000	0.0000	0.0000	0.0000	0.0000
2	2	10	0.0790	0.0069	0.0028	0.0097	0.0028	0.0097	0.0000	8.2330	0.0859	0.0069	0.0000	0.0800	0.0000	0.0107	0.0000	-0.0000	0.0107	-0.0000
2	4	10	0.1590	0.0070	0.0111	0.0181	0.0111	0.0181	0.0000	8.7500	0.1819	0.0070	0.0000	0.1600	0.0000	0.0214	0.0000	-0.0000	0.0214	-0.0000
2	6	10	0.2360	0.0072	0.0249	0.0321	0.0249	0.0321	0.0000	7.3600	0.2276	0.0072	0.0000	0.2380	0.0000	0.0321	0.0000	-0.0000	0.0321	-0.0000
2	8	10	0.3120	0.0074	0.0441	0.0516	0.0441	0.0516	0.0000	6.0620	0.2477	0.0075	0.0000	0.3170	0.0000	0.0425	0.0000	-0.0000	0.0425	-0.0000
2	10	10	0.3860	0.0078	0.0683	0.0761	0.0683	0.0761	0.0000	5.0690	0.2555	0.0079	0.0000	0.3930	0.0000	0.0527	0.0000	-0.0000	0.0527	-0.0000

# EFFECT OF WING LOCATION ON THE AERODYNAMIC PROFILE OF A SUPERSONIC AIRCRAFT USING ANSYS FLUENT



## .1.3 SST OpenVSP Model Four View



## .2 ANSYS Fluent Results

### .2.1 Aerodynamic Coefficients of wing location at 20 m

Outline of All Parameters				
	A	B	C	D
1	ID	Parameter Name	Value	Unit
2	⊕ Input Parameters			
4	⊖ Output Parameters			
5	⊖  Fluent (with Fluent Meshing) (B1)			
6	 P1	drag-coeff-op	0.03201	
7	 P2	lift-coeff-op	0.22936	
8	 P3	moment-coeff-op	5.8436	
9	 P4	momcoef1-op	0.63319	
10	 P5	momcoeff2-op	-3.954	
*	 New output parameter		New expression	
12	Charts			

### .2.2 Aerodynamic Coefficients of wing location at 35 m

Outline of All Parameters				
	A	B	C	D
1	ID	Parameter Name	Value	Unit
2	⊕ Input Parameters			
4	⊖ Output Parameters			
5	⊖  Fluent (with Fluent Meshing) (B1)			
6	 P1	drag-coeff-op	0.031785	
7	 P2	lift-coeff-op	0.22617	
8	 P3	moment-coeff-op	0.014199	
9	 P4	moment-coefficient-op	8.9957	
10	 P5	momentcoeffcg-op	2.3765	
*	 New output parameter		New expression	
12	Charts			

## **Turnitin Report**

# EFFECT OF WING LOCATION ON THE AERODYNAMIC PROFILE OF A SUPERSONIC AIRCRAFT USING ANSYS FLUENT

## ORIGINALITY REPORT

8%

SIMILARITY INDEX

7%

INTERNET SOURCES

4%

PUBLICATIONS

4%

STUDENT PAPERS

## PRIMARY SOURCES

1

[vdoc.pub](#)

Internet Source

1%

2

[onlinelibrary.wiley.com](#)

Internet Source

1%

3

[archive.org](#)

Internet Source

<1%

4

Submitted to Georgia Institute of Technology

Main Campus

Student Paper

<1%

5

Submitted to Cranfield University

Student Paper

<1%

6

[www.ijrte.org](#)

Internet Source

<1%

7

[core.ac.uk](#)

Internet Source

<1%

8

Submitted to College of Science and

Technology, Bhutan

Student Paper

<1%

9	Submitted to University of Dayton Student Paper	<1 %
10	Submitted to Universiti Malaysia Pahang Student Paper	<1 %
11	Mohammad H. Sadraey. "Aircraft Performance - An Engineering Approach", CRC Press, 2023 Publication	<1 %
12	Submitted to Kingston University Student Paper	<1 %
13	Submitted to University of Salford Student Paper	<1 %
14	Dipan Deb, Abdelrahman A. Elmaradny, Kevin Huang, Moatasem Fouda, Haithem E. Taha. "Enhancing Lift and Reducing Wingtip Vortices Using a Passive Rotor on Finite-Span Wings", Aerospace Science and Technology, 2024 Publication	<1 %
15	Submitted to Richard Taunton Sixth Form Student Paper	<1 %
16	<a href="http://www.coursehero.com">www.coursehero.com</a> Internet Source	<1 %
17	<a href="http://www.scribd.com">www.scribd.com</a> Internet Source	<1 %

18 Kenji Yoshida. "Supersonic drag reduction technology in the scaled supersonic experimental airplane project by JAXA", *Progress in Aerospace Sciences*, 2009  
Publication <1 %

---

19 Submitted to Sheffield Hallam University  
Student Paper <1 %

---

20 András Sóbester, Alexander I J Forrester. "Aircraft Aerodynamic Design", Wiley, 2014  
Publication <1 %

---

21 Submitted to University of Sheffield  
Student Paper <1 %

---

22 Submitted to University of Surrey  
Student Paper <1 %

---

23 Submitted to University of Witwatersrand  
Student Paper <1 %

---

24 Xu Wang, Weiqi Qian, Tun Zhao, Hai Chen, Lei He, Haisheng Sun, Yuan Tian. "A generative design method of airfoil based on conditional variational autoencoder", *Engineering Applications of Artificial Intelligence*, 2025  
Publication <1 %

---

25 [ia601505.us.archive.org](http://ia601505.us.archive.org)  
Internet Source <1 %

---

26 Submitted to Technological University Dublin  
Student Paper <1 %

---

27	"Aerodynamics", Elsevier BV, 2012 Publication	<1 %
28	dalspace.library.dal.ca Internet Source	<1 %
29	Submitted to Aston University Student Paper	<1 %
30	Mădălin-Dorin Feraru, Daniel Măriuța, Marius Stoia-Djeska, Lucian-Teodor Grigorie. "Numerical Investigation of an NACA 13112 Morphing Airfoil", Biomimetics, 2024 Publication	<1 %
31	Submitted to University of Bradford Student Paper	<1 %
32	Submitted to Universitas Diponegoro Student Paper	<1 %
33	lib.buet.ac.bd:8080 Internet Source	<1 %
34	www.cray.com Internet Source	<1 %
35	eprints.soton.ac.uk Internet Source	<1 %
36	etd.aau.edu.et Internet Source	<1 %
37	cgspace.cgiar.org Internet Source	<1 %

38	<a href="http://etheses.whiterose.ac.uk">etheses.whiterose.ac.uk</a> Internet Source	<1 %
39	<a href="http://www.macnaughtongroup.com">www.macnaughtongroup.com</a> Internet Source	<1 %
40	Submitted to International Islamic University Malaysia Student Paper	<1 %
41	<a href="http://eprints.qut.edu.au">eprints.qut.edu.au</a> Internet Source	<1 %
42	<a href="http://www.hindawi.com">www.hindawi.com</a> Internet Source	<1 %
43	<a href="http://www.mrs.org">www.mrs.org</a> Internet Source	<1 %
44	F. Gao, L. Zhao, M.C. Boufadel, T. King, B. Robinson, R. Conmy, R. Miller. "Hydrodynamics of oil jets without and with dispersant: Experimental and numerical characterization", Applied Ocean Research, 2017 Publication	<1 %
45	<a href="http://ir.library.osaka-u.ac.jp">ir.library.osaka-u.ac.jp</a> Internet Source	<1 %
46	<a href="http://pdfslide.net">pdfslide.net</a> Internet Source	<1 %
47	<a href="http://repository.charlotte.edu">repository.charlotte.edu</a> Internet Source	<1 %

<1 %

---

48 repository.lcu.edu.ng  
Internet Source

<1 %

---

49 w3.uwyo.edu  
Internet Source

<1 %

---

50 www.iare.ac.in  
Internet Source

<1 %

---

51 mdpi-res.com  
Internet Source

<1 %

---

Exclude quotes Off

Exclude matches Off

Exclude bibliography On

## Curriculum Vitae



---

### Basic Information

---

Name	Kevin Rahangiar
Place of Birth	Aberdeen, Scotland, United Kingdom
Date of Birth	16, 03, 2003
Address	The Green Clus. Vineyard DB 1/5, Kota Tangerang Selatan, Indonesia

---

Year	Education
------	-----------

---

2021 - present	International University Liaison Indonesia (IULI)
2016 - 2021	Saint John's Catholic School
2015 - 2016	Garden International School
2011 - 2015	Sekolah Pelita Harapan

---

Year	Courses
------	---------

---

2024	Exchange Program in Taiwan at National Formosa University
2024	2kg W-wing EVTOL UAV Project Work at National Formosa University

---

Year	Seminars & Workshops
------	----------------------

---

2022	Onshape Workshop
2023	Basic Aircraft Maintenance at UNSURYA
2024	AIAA Design Competition

---